

**NEUTRAL AND CHARGED RECEPTORS AS VOLTAMMETRIC
SENSORS FOR IONS**

A
Thesis submitted in
fulfillment of the requirement of the degree of

Doctor of Philosophy

Submitted by
Karamjeet Kaur
(900909005)

Under the Supervision
Of

Dr. Susheel Mittal
Senior Professor
Thapar University, Patiala



Dr. Ashok Kumar SK
Assistant Professor
VIT, Vellore

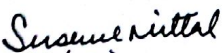
School of Chemistry & Biochemistry

Thapar University
Patiala-147004, India


July, 2013

Certificate

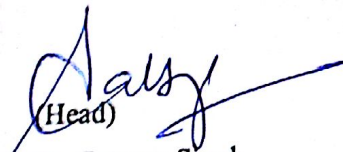
Certified that the thesis entitled "**Neutral and Charged Receptors As Voltammetric Sensors For Ions**" which is submitted by Mrs. Karamjeet Kaur in fulfillment of the requirement for the award of the Degree of Doctor of Philosophy in the School of Chemistry and Biochemistry, Thapar University, Patiala, is a record of candidate's own independent and original research work carried out by her under our supervision and guidance. The material embodied in this thesis has not been submitted in part or full to any other University or Institute for the award of any degree.


(Supervisor)

Dr. Susheel Mittal
Senior Professor
School of Chemistry and Biochemistry
Thapar University, Patiala-147004


(Supervisor)

Dr Ashok Kumar SK
Assistant professor (Senior)
School of Advanced Sciences
VIT University, Vellore


(Head)


Dr. Satnam Singh
Associate Professor
School of Chemistry and Biochemistry
Thapar University, Patiala-147004, Punjab (INDIA)

Candidate's Declaration

I, hereby declare that the work presented in the thesis entitled "**Neutral and charged receptors as voltammetric sensors for ions**" in fulfillment of the requirement for the award of the Degree of Doctor of Philosophy, School of Chemistry and Biochemistry, Thapar University, Patiala, is an authentic record of my own work carried out under the joint supervision of Dr. Susheel Mittal, Senior Professor, School of Chemistry & Biochemistry, Thapar University, Patiala, India and Dr Ashok Kumar SK, Assistant Professor (Senior), School of Advanced Sciences, VIT University, Vellore (TN), India. The matter embodied in this thesis has not been submitted in part or full to any other university or institute for the award of any degree in India or Abroad.

Place: Patiala

Date: June 21, 2013



Karamjeet Kaur

900909005

Acknowledgement

Apart from the efforts of oneself, the success of any project depends largely on the encouragement and guidelines of many others. In my journey to the completion of Ph.D. thesis there are many who walked along and beside me to help support and motivate me all these years.

I take this opportunity to gratefully acknowledge the enthusiastic supervision of Dr. Susheel Mittal, Senior Professor, School of Chemistry & Biochemistry, Thapar University, Patiala and Dr. Ashok Kumar SK, Assistant Professor, VIT, Vellore, for having faith in me and entrusting me with this opportunity to work under their guidance and supervision, providing all kinds of support and inspiration, wise counsel, constant encouragement, valuable suggestions and comments, expertise and fruitful advice throughout this exploration and preparation of the thesis. It's a great privilege to experience a sustained enthusiastic, involved interest, constructive criticism, tremendous enthusiasm and careful supervision from their side throughout the period of my work.

I express my gratitude to Director, Thapar University, Patiala and Dr. Satnam Singh, Head, School of Chemistry and Biochemistry, for all the facilities which have been immensely helpful for the completion of my work.

I express my deep gratitude to Dr. Subodh Kumar, GNDU, Amritsar, his students, Ashwani Kumar and Sandeep Kumar for providing the molecules to carry out the studies and providing guidance from time to time. I am extremely thankful to Dr. C.E. Banks, Associate Professor, MM University, Manchester (UK), in helping us to add new dimension to our research and timely guidance, coordination and support.

I express my regards to Dr. Raj Kumar Gupta and Dr. Ranjana Prakash (Doctoral committee members) for suggestions and taking interest in the progress of work along with laboratory facilities.

I extend my thanks to all the faculty members of School of Chemistry and Biochemistry, Thapar University, Patiala for providing necessary guidance during my research work. I am thankful to Mr. Chandar Thakur and other non-teaching staff, School of Chemistry and Biochemistry for the constant official help and cooperation.

I owe a debt of gratitude and heartfelt thanks to my big brother, labmate, senior and colleague - Mr. Jasminder Singh, my best companions throughout Ms. Nidhi Gupta, Ms Maitri Bhutani and Dr. Satnam Singh Aulakh (Big B) for their kind concern, critical observations in planning experiments and above all their support, which always helped me endure hard times and to accomplish all my goals. I extend my thanks to my seniors Dr. Nirankar Singh and Mr. Pawan Kumar for their timely advice and support, which helped me throughout my endeavor.

I take this opportunity to thank Ms. Harpreet Kaur, Ms. Tajbir Kaur, Ms. Mandeep Kaur Chahal, Ms. Gurvinder Kaur Waraich, Ms. Kiran Sandhu, Mrs. Anupam Dhiman, Mrs. Preeti Tatra, Mr. Ankush Kanwar, Mr. Anirudh Sharma, Mr. Sumit Jaiswal, Ms. Manisha Pabbi, Mr. Sanjeev Kumar and Ms. Rashmi Sharma, Ms. Mandeep Kaur, Ms. Pankil Singla and Ms. Poonam Bhatia for fruitful discussions and support. I owe a word of thanks to all research scholars at the School of Chemistry and Biochemistry for providing constant support, encouragement and a good working atmosphere.

I am thankful to all the students who worked with me and people, who taught me various lessons of life and helped me in polishing my skills of both personal and professional arena.

I feel deeply indebted and sense of gratitude for my parents, who despite of all the difficulties, made me what I am today, my siblings (Taranjit Kaur, Shehbaz Dosanjh), my maternal uncle and aunty (Gurjit Singh Dosanjh and Kulwinder Kaur Dosanjh), my maternal grandparents (Lt. Sohan Singh Dosanjh and Gurmit Kaur Dosanjh), for their blessings and belief in me, who have always showered unconditional love on me, encouraged and supported me in every aspect. I am extremely thankful to my in-laws, my sister-in-law Mrs. Sarbjeet Kaur, my husband Arvinder Singh Sidhu, for his support and the time he gave me throughout this journey. They formed a part of my vision and taught me the good things that really matter in life.

Above all, I'm grateful to Almighty God for blessing me to complete this work successfully.

Karamjeet Kaur

List of Contents

S.No	Contents	Page No.
	List of Figures	x-xv
	List of Tables	xvi
	Abstract	xvii-xviii
	Chapter 1 Introduction	1-15
1.1	Chemical Sensing	
1.1.1	Chemical Sensors	3-3
1.1.2	Methods of Chemical Sensing	3-5
1.1.3	Sensing by electrochemical methods	5-6
1.2	Voltammetric ion sensing	6-7
1.3	Electrode modification	7-8
1.3.1	Polymer film coating	8-10
1.4	Applications of chemically modified electrodes	10-10
1.5	References	11-15
	Chapter 2 Review of Literature	16-37
2.1	Cation sensing	16-16
2.1.1	Electrochemically active receptors (using unmodified electrodes)	16-18
2.1.2	Modified electrodes	18-23
2.2	Anion sensing	23-27
2.2.1	Modified electrode	27-28
2.3	References	29-37
	Chapter 3 Materials and Methods	38-48
3.1	Introduction	38-38
3.2	Chemicals	38-38

3.3	Molecules studied	38-39
3.4	Instrumentation	39-40
3.5	Techniques used	
	3.5.1 Voltammetry	40-40
	3.5.2 Cyclic voltammetry	40-43
	3.5.3 Differential pulse voltammetry	43-43
	3.5.4 Chronopotentiometry	43-43
	3.5.5 Chronoamperometry	43-44
3.6	Limit of detection determination	44-44
3.7	Scanning electron microscopy (SEM)	44-45
3.8	Atomic absorption spectroscopy	45-45
3.9	Theoretical study	45-45
3.10	Experimental Procedures	
	3.10.1 CV conditions for voltammetric study of molecules	45-46
	3.10.2 DPV conditions for voltammetric study	46-46
	3.10.3 Cation and anion detection	46-46
	3.10.4 Interference studies	46-47
	3.10.5 Real life sampling	47-47
3.11	Electrode preparation	
	3.11.1 Screen printed electrode	47-47
	3.11.2 Polyaniline modified electrode	47-48
3.12	References	48-48
Chapter 4 Anion Selective Anthrone Derivatives		49-67
4.1	Results and Discussion	50-51
4.2	Mechanism	52-52
4.3	Theoretical study	52-55
4.4	Effect of scan rate	55-56
4.5	Solvent effect	56-57
4.6	Anion selectivity	

4.6.1	Colorimetric study	58-58
4.6.2	Analytical study	58-61
4.6.3	Calibration curve for cyanide ion	61-63
4.7	Interference of ions	63-64
4.8	Conclusions	64-64
4.9	References	65-67
Chapter 5 Cation Sensitive Anthrone Derivatives		68-92
5.1	Results and Discussion	
5.1.1	Electrochemical behavior of anthrone 1, 2 and 3	69-71
5.1.2	Mechanism of electrochemical process	71-73
5.1.3	Influence of scan rate	73-75
5.1.4	Effect of concentration of the electroactive compound	76-76
5.1.5	Effect of change in concentration of supporting electrolyte	76-77
5.1.6	Effect of solvent	77-79
5.1.7	Electrochemical recognition of cation by anthrone 1, 2 and 3	79-88
5.1.8	Anthrone3 in ACN: Water system	88-89
5.1.9	Interefernce study	90-90
5.2	Conclusions	90-90
5.3	References	91-92
Chapter 6 Chemical Sensors Based on Imidazole Derivatives		93-107
6.1	Results and discussion	
6.1.1	Electrochemical behavior of the molecules	94-96
6.1.2	Effect of scan rate	96-97
6.1.3	Solvent effect	97-99
6.1.4	Cation interaction	99-102
6.1.5	Differential pulse voltammetry – a quantitative study	102-104
6.1.6	Interference study	104-105
6.1.7	Sensitivity (LOD and LOQ)	106-106
6.2	Conclusions	106-106

6.3	References	107-107
Chapter 7 Chemical Sensing With Electrode Modification		108-135
7.1	Anthrone modified screen printed electrode (SPE-A)	
7.1.1	Voltammetric study of anthrone ³ using glassy carbon electrode and screen printed electrode modified with anthrone ³	109-111
7.1.2	Solvent effect	111-114
7.1.3	Effect of scan rate	114-115
7.1.4	Cation selectivity behaviour	115-118
7.1.5	Interference of ions	118-119
7.1.6	Sensitivity (LOD and LOQ)	119-120
7.1.7	Regeneration of screen printed electrodes	120-122
7.1.8	SEM images of EDTA-treated and non-treated SPE-A electrodes	122-123
7.1.9	Validation of mercury determination using SPE-A with AAS	124-124
7.2	Polyaniline modified electrode	
7.2.1	Electrode modification	124-125
7.2.2	Electrochemistry of PANI in acetonitrile	125-126
7.2.3	Permeability of PANI coating on working electrode	126-127
7.2.4	Application of PANI modified electrode	127-129
7.2.5	Real samples	129-132
7.3	Conclusions	132-132
7.4	References	133-134
7.5	List of publications	135-135

List of Figures

- Fig 1.1** Generalized form of polyaniline where $n+m = 1$, $x =$ degree of polymerization.
- Fig. 4.1** Cyclic voltammograms of *1* and *2* in acetonitrile (ACN) medium using 0.1M TBAP supporting electrolyte (GC working electrode, scan rate 20 mVs^{-1} E vs Ag/Ag^+)
- Scheme 1** Resonance stabilisation of viologen substituted anthrone molecules *1* and *2* through conjugation of lone pairs on $-\text{NH}$ group with bipyridyl substituent
- Fig. 4.2** Optimized geometries of *1* (2-1) and *2* (2-2) at B3LYP/6-311++G** level acetonitrile with serial number of atoms using Guassian 03W software
- Fig. 4.3** Electronic density distribution in HOMO, LUMO and LUMO+1 states of *1* and *2* computed by the B3LYP/6-311++G** (ACN as solvent) method using Guassian 03W software
- Fig. 4.4** Cyclic voltammograms of *1* and *2* in acetonitrile (ACN) at different scan rates 20, 40, 60, 80, 100 mVs^{-1} using 0.1M TBAP as supporting electrolyte and GC as working electrode
- Fig. 4.5** Cyclic voltammograms of 10^{-4} M solution of a) *1* and b) *2* in different solvents using 0.1M TBAP as supporting electrolyte (GC working electrode, scan rate 20 mVs^{-1} E vs Ag/Ag^+)
- Fig. 4.6** Color changes on treatment of *1* and *2* with 2equivalents of different anions as their tetrabutyl ammonium (TBA) salts in acetonitrile
- Fig. 4.7** Cyclic voltammograms of *1* a) and *2* b) (10^{-4} M) with 2 equivalents of different anions using 0.1M TBAP as supporting electrolyte (GC working electrode, scan rate 20 mVs^{-1} E vs Ag/Ag^+)
- Fig. 4.8** Calibration plots between concentration of cyanide and current in acetonitrile medium using 0.1M TBAP as supporting electrolyte (GC working electrode, scan rate 20 mVs^{-1} E vs Ag/Ag^+)

- Fig. 4.9** Cyclic voltammogram of *I* showing interference of ions using TBAP as supporting electrolyte (GC working electrode, scan rate 20 mVs⁻¹ E vs Ag/Ag⁺)
- Fig. 5.1** Cyclic voltammograms of anthrone1, anthrone2 and anthrone3 (10⁻⁴M) in ACN using 0.1M TBAP as supporting electrolyte, GC working electrode, scan rate 20mVs⁻¹ E vs Ag/Ag⁺
- Fig. 5.2** Cyclic voltammograms showing the effect of scan rate in ACN. From inner to outer the scan rates are (20, 40, 60, 80, 100, 200, 400, 600, 800, 1000 mVs⁻¹), 0.1M TBAP, GC as working electrode. (Plots show non-linear relation between *i*_{pa} and *v*^{1/2})
- Fig. 5.3** Cyclic voltammograms of anthrone1 at GC electrode, 0.1M TBAP as supporting electrolyte and scan rate 20mVs⁻¹ at different concentrations
- Fig. 5.4** Cyclic voltammograms curves of anthrone1 (10⁻⁴M) with different electrolyte (TBAP) concentrations in ACN (GC working electrode, scan rate 20mVs⁻¹ E vs Ag/Ag⁺)
- Fig. 5.5** Cyclic voltammograms of (a) anthrone1, (b) anthrone2 and c) anthrone 3 (10⁻⁴M) in different solvents using 0.1M TBAP as supporting electrolyte (GC working electrode, scan rate 20 mVs⁻¹ E vs Ag/Ag⁺)
- Fig. 5.6** Cyclic voltammograms of anthrone1 with different equivalents of a) Hg²⁺ and b) Cu²⁺ ion in ACN with 0.1M TBAP supporting electrolyte (GC working electrode, scan rate 20 mVs⁻¹ E vs Ag/Ag⁺)
- Fig. 5.7** Cyclic voltammograms of anthrone2 with different equivalents of a) Hg²⁺ ion and b) Cu²⁺ in ACN with 0.1M TBAP supporting electrolyte (GC working electrode, scan rate 20 mVs⁻¹ and E vs Ag/Ag⁺)
- Fig. 5.8** Cyclic voltammograms of anthrone3 with different concentrations of Cu²⁺ a) and b) Hg²⁺ ion, in ACN with 0.1M TBAP supporting electrolyte (GC working electrode, scan rate 20mVs⁻¹ and E vs Ag/Ag⁺)
- Fig. 5.9** Cyclic voltammograms of anthrone1 with 1 equivalent of different metal ions in ACN with 0.1M TBAP supporting electrolyte, GC working electrode (scan rate 20 mVs⁻¹ and E vs Ag/Ag⁺).

- Fig. 5.10** Cyclic voltammograms of anthrone2 with 1 equivalent of different metal ions in ACN with 0.1M TBAP supporting electrolyte (GC working electrode, scan rate 20 mVs^{-1} and E vs Ag/Ag^+)
- Fig. 5.11** Cyclic voltammograms of anthrone3 with 1 equivalent of different metal ions in ACN with 0.1M TBAP supporting electrolyte, (GC working electrode, scan rate 20 mVs^{-1} and E vs Ag/Ag^+)
- Fig. 5.12** Cyclic voltammograms of anthrone3 10^{-4}M in 1:1 water : ACN with 0.1M HEPES buffer/KCl (pH-7) supporting electrolyte (GC working electrode, scan rate 20 mVs^{-1} and E vs Ag/AgCl)
- Fig. 5.13** Cyclic voltammograms of anthrone3 with 2 equivalents of different metal ions in 1:1 water : ACN with 0.1M HEPES buffer/KCl (pH-7) supporting electrolyte (GC working electrode, scan rate 20 mVs^{-1} and E vs Ag/AgCl)
- Fig. 6.1** Cyclic voltammograms of TPAN and TPF (10^{-4} M) in acetonitrile (ACN) medium using 0.1M TBAP supporting electrolyte (GC working electrode, scan rate 20 mVs^{-1} E vs Ag/Ag^+)
- Fig. 6.2** Cyclic voltammograms of TPIAM and TPIM (10^{-4} M) in acetonitrile (ACN) medium using 0.1M TBAP supporting electrolyte (GC working electrode, scan rate 20 mVs^{-1} E vs Ag/Ag^+)
- Fig. 6.3** Cyclic voltammograms of TPAN and TPF in acetonitrile (ACN) at different scan rates (10 to 100 mVs^{-1}), using 0.1M TBAP as supporting electrolyte and GC as working electrode
- Fig. 6.4** Cyclic voltammograms of 10^{-4} M solution of a) TPAN, b) TPF, c) TPIM and d) TPIAM in different solvents using 0.1M TBAP as supporting electrolyte (GC working electrode, scan rate 20 mVs^{-1} E vs Ag/Ag^+)
- Fig. 6.5** Cyclic voltammograms of a) TPIM and b) TPIAM (10^{-4}M) with different concentrations of Hg^{2+} and Cu^{2+} ions in acetonitrile and in inset- CVs with other metal ions at scan rate 0.02Vs^{-1} , 0.1M TBAP, GC as working electrode.

- Fig. 6.6** Differential pulse voltammograms of TPAN and TPF (10^{-4}M) with different concentrations of Hg^{2+} and Cu^{2+} ions in acetonitrile and corresponding CV studies (in inset)
- Fig. 6.7** Plots of current vs L/M ratio for TPAN and TPF with Hg^{2+} and Cu^{2+} ions
- Fig. 6.8** Differential pulse voltammograms of TPAN and TPF (10^{-4}M) in presence of different metal ions, at amplitude 25mV, scan rate 0.02Vs^{-1}
- Fig. 7.1** Cyclic voltammogram of anthrone3 (solution phase) with GC as working electrode and SPE-A, in 1:1 Water- ACN solvent system, scan rate: 0.02Vs^{-1} ; supporting electrolyte: 0.1M KCl, pH 7, E vs Ag/AgCl)
- Fig. 7.2** Effect of solvent system on anthrone3 modified screen printed electrode (scan rate 0.02Vs^{-1} , supporting electrolyte 0.1M KCl, pH 7, E vs Ag/AgCl)
- Fig. 7.3** Effect of solvent system on anthrone3 (solution phase) with GC as working electrode (scan rate 0.02V s^{-1} , supporting electrolyte 0.1M KCl, pH 7, E vs Ag/AgCl)
- Fig. 7.4** Cyclic voltammogram of anthrone3 in acetonitrile solvent, with 0.1M TBAP as supporting electrolyte (GC working electrode, scan rate 20 mVs^{-1} E vs Ag/Ag⁺)
- Fig. 7.5** Cyclic voltammograms of SPE-A (4a) and anthrone3 (4b) in 1:1 water-ACN at different scan rates (supporting electrolyte 0.1M KCl, pH 7, E vs Ag/AgCl)
- Fig. 7.6** Cyclic voltammograms of SPE-A with different equivalents of Hg^{2+} ions in 1:1 water- ACN (scan rate 0.02V s^{-1} , supporting electrolyte 0.1M KCl, pH 7, E vs Ag/AgCl)
- Fig. 7.7** Cyclic voltammograms of anthrone3 (solution phase) with different equivalents of Cu^{2+} ions in 1:1 water-ACN (scan rate 0.02V s^{-1} , supporting electrolyte 0.1M KCl, pH 7, E vs Ag/AgCl)
- Fig. 7.8** Interference study of a) Anthrone3 in solution phase and b) SPE-A with different metal ions in 1:1 water-ACN (scan rate 0.02Vs^{-1} , supporting electrolyte 0.1M KCl, pH 7, E vs Ag/AgCl)

- Fig. 7.9** Cyclic voltammograms of SPE-A after treating it with Cu^{2+} ions and EDTA in 1:1 water- ACN (scan rate 0.02V s^{-1} , supporting electrolyte 0.1M KCl, pH 7, E vs Ag/AgCl)
- Fig. 7.10** Cyclic voltammograms of SPE-A after treating it with Hg^{2+} ions and EDTA in 1:1 water-ACN (scan rate 0.02V s^{-1} , supporting electrolyte 0.1M KCl, pH 7, E vs Ag/AgCl)
- Fig. 7.11** Cyclic voltammograms of anthrone3 after addition of Hg^{2+} ions and EDTA in 1:1 water-ACN (scan rate 0.02V s^{-1} , supporting electrolyte 0.1M KCl, pH 7, E vs Ag/AgCl)
- Fig. 7.12** Cyclic voltammograms of anthrone3 after addition of Cu^{2+} ions and EDTA in 1:1 water-ACN (scan rate 0.02V s^{-1} , supporting electrolyte 0.1M KCl, pH 7, E vs Ag/AgCl)
- Fig. 7.13** SEM image of anthrone3 modified screen printed electrode
- Fig. 7.14** SEM images of anthrone3 modified screen printed electrode a) after treatment with Hg^{2+} b) Hg^{2+} treated electrode after treatment with EDTA solution, c) after treatment with Cu^{2+} , d) Cu^{2+} treated electrode after treatment with EDTA solution
- Fig.7.2.1** Chronoamperometric deposition of PANI on glassy carbon electrode in acetonitrile containing 0.1M CF_3COOH , 0.1M TBAP, as supporting electrolyte, time varying from 100 to 300 s, Inset contains CVs corresponding to PANI formed, E vs Ag/Ag⁺)
- Fig. 7.2.2** Cyclic voltammogram of PANI coated on glassy carbon electrode in acetonitrile containing 0.1M TBAP as supporting electrolyte, scan rate 0.02Vs^{-1} , E vs Ag/Ag⁺)
- Fig. 7.2.3** Cyclic voltammogram of PANI coated and Bare glassy carbon electrode with 0.01M ferrocene in acetonitrile containing 0.1M TBAP as supporting electrolyte, scan rate 0.02Vs^{-1} , E vs Ag/Ag⁺)
- Fig. 7.2.4** SEM images of a) porous morphology of polyaniline after chronopotentiometric treatment b) ionophore coated polyaniline

- Fig. 7.2.5** Cyclic voltammogram of a) TPAN/PANI coated glassy carbon electrode, b) TPF/PANI coated glassy carbon electrode, in acetonitrile containing 0.1M TBAP as supporting electrolyte, scan rate 0.02Vs^{-1} , E vs Ag/Ag⁺)
- Fig. 7.2.6** DPVs of TPAN and TPF coated PANI/GC modified electrode in 0.2M HNO₃ aqueous solution, conditioning potential -0.3 V for 60s at amplitude 25 mV.
- Fig. 7.2.7** Differential pulse voltammograms of soil sample with ionophore/PANI/GC electrode from main dump site and after spiking the sample with Cu²⁺ and Hg²⁺ solution(0.01M) at pH 3, scan rate 0.02Vs^{-1} , E vs Ag/AgCl)
- Fig. 7.2.8** Differential pulse voltammograms of soil sample with ionophore/PANI/GC electrode collected from some distance from main dump site and after spiking the sample with Cu²⁺ and Hg²⁺ solution(0.01M) at pH 3, scan rate 0.02Vs^{-1} , E vs Ag/AgCl)
- Scheme 4.1** Mechanism scheme for the formation of radical cations for anthrone1 and anthrone3
- Scheme 7.1** Resonance stabilisation of substituted anthrone3 through conjugation of lone pairs on Oxygen of -CO group.

List of Tables

- Table 4.1** Energies of HOMO and LUMO for molecules *1* and *2* measured using Gaussian software
- Table 4.2** Cathodic shift in peak potential (with binding constants) of *1* and *2* on interaction with different anions
- Table 4.3** Concentration measurement of cyanide samples using proposed voltammetric method compared with spectrophotometric method
- Table 4.4** Comparison of lower detection limits and interferences for anion detection for the reported methods with the proposed method
- Table 5.1** Peak potentials (V) and peak currents (μA) values for different substrates
- Table 5.2** Peak potentials of oxidation peaks of anthrone derivatives in different solvents
- Table 5.3** Peak potential (V) values for of anthrone1 alone and with different metal ions
- Table 5.4** Peak potential (V) values for anthrone2 alone and with different metal ions
- Table 5.5** Peak potential (V) values of anthrone3 alone and with different equivalents of Cu^{2+} ion
- Table 5.6** Peak potential (V) values for anthrone3 alone and with different metal ions
- Table 7.1** Voltammetric data of SPE-A (SPE-Anthrone3) with different metal ions
- Table 7.2** Real time sample analysis of laboratory tap water and its verification with atomic absorption spectroscopy for Hg^{2+} ions
- Table 7.2.1** Real time sample analysis of soil samples from CFL dump site and their verification with atomic absorption spectroscopy for Hg^{2+} and Cu^{2+} ions.

Abstract

Electrochemical studies for all the molecules were carried out using cyclic voltammetry. Neutral anthrone derivatives- anthrone1, anthrone2 and anthrone3 were studied electrochemically for sensing cations at galssy carbon electrodes. On the basis of the results obtained mechanism of metal ligand complexation on the electrode is proposed to explain the preferential oxidation at the electrode. Anthrone derivatives showed selectivity toward copper and mercury ions even in the presence of other metal ions. Electrochemical reaction of anthrone3 was identified as a kinetically controlled process rather than a diffusion-controlled process based on different scan rates. Influence of polarity of the solvent on the shape and peak position is also studied.

Electrochemical behavior of positively charged anthrone derivatives BPODS and BPMS, functionalized with viologen group were inspected extensively using cyclic voltammetry, taking clue from colorimetric studies of these molecules indicating their selectivity towards anions like cyanide, acetate and fluoride. Cation selectivity of anthrone derivative changed to anions because of the viologen group. Anthrone derivative stabilizes viologen through conjugation, reducing one of its two redox couples which are characteristics of viologen group for molecule *1*. Mechanisms were proposed duly supported by density functional theory calculation based theoretical studies carried out using Guassian 03W for the electrochemical behaviour of the compounds *1* and *2*. Voltammograms of dicationic viologen derivative *1* showed near quenching of anodic peaks (a decrease of almost 90% of current) as well as cathodic peaks (a decrease of almost 100% current) in presence of 1 equivalent of cyanide ions. The monocationic viologen derivative *2* also showed quenching of the cathodic peak while anodic peak survives in presence of the anions, cyanide, acetate and fluoride. The proposed electrochemical sensors were selective for CN^- , OAc^- and F^- based on binding constants which are much larger than for anions like Cl^- , Br^- , I^- , HSO_4^- and have also been used for determination of unknown samples of cyanide ions.

Neutral imidazole based molecules TPAN, TPF, TPIM and TPIAM showed irreversible electrochemical nature as only oxidation peaks were obtained. All the four molecules as a sensor gave selective and distinguishable signals on interaction with Cu^{2+} and Hg^{2+} ions

with no interference from other potentially interfering ions like Zn^{2+} , Pb^{2+} , Co^{2+} , Ni^{2+} . Differential pulse voltammetry studies of TPAN and TPF with metal ions showed that both the molecules interact differently with Hg^{2+} and Cu^{2+} ion.

Two types of electrode modifications were done: one anthrone³ modified screen printed electrode and second is polyaniline modified glassy carbon electrode with ionophore (TPAN and TPF) drop coated on the surface. The voltammetric study of anthrone³ conducted in 1:1 water-acetonitrile solvent system was compared with modified screen printed electrode (SPE-A) and anthrone³ in solution phase. Anthrone³ displayed an electrochemically quasi-reversible nature in voltammograms with both the systems and is presented as a novel disposable voltammetric sensor for mercury ions. Upon interaction with cations, both the electrode systems showed sensitivity towards Hg^{2+} ions with a lower detection limit of $0.61\mu M$. The magnitude of the voltammetric current with the SPE-A exhibited three times the current obtained with a bare glassy carbon electrode (GC).

Polyaniline modified gave better results than unmodified GC electrode. As tested with ferrocene it was found to be highly permeable. Results obtained after modifying the electrode with ionophores TPAN and TPF were better than bare GC electrode results in terms of peak current intensity. On the basis of selectivity shown by TPAN and TPF toward ions Hg^{2+} and Cu^{2+} ions, ionophore/PANI/GC modified electrode was also used to sense these ions and for their determination in soil sample of CFL dump site.

Chapter 1

Introduction

Science is helping us to gain knowledge about everything which is happening in and around us. With every bit of knowledge that man is gaining, he is trying to get independence from nature but becoming more and more dependent on technology and science. This awareness is no doubt helping us to make our lives easy and comfortable. Any kind of deficiency related to minerals or vitamins can be overcome by taking supplements externally. Food can be saved for days with the help of preservatives. Fertilizers, pesticides, insecticides, high yielding seeds with superior genetics, all are marvels of science only. Means of transportation are improving day by day. In our daily life, from toothpaste, dental fillings, cosmetics, medicines, food, to paper, clothing, thermometer, cellphones, transportation etc., almost everything involves science and makes us realize how much dependent we have become on it.

All these things along with comforts are also bringing some serious danger in our lives. Most of the things that are used every day include application of many dangerous elements in their manufacturing and processing. Some of these hazardous things are organic compounds like formaldehyde in paints, volatile organic compounds (VOCs) are in all petroleum products like flooring adhesives, paint, wall materials and cleaning products. Others are inorganic like chloride, fluoride, sulphates, heavy metal ions like mercury, lead, chromium, copper, zinc etc. Human exposure to these is through the food chain, air, water chain, industry products and also through occupational exposure. The poisoning effects of heavy metals are due to their interference with the normal body biochemistry in the normal metabolic processes. Everyday exposure to these toxins is leading to their accumulation in our body which is leading to serious health problems.

Some heavy metals like iron (hemoglobin, myoglobin), cobalt (coenzyme), copper (co-factor in enzymes), zinc (in enzymes), chromium (Cr^{3+} in enzymes) have essential physiological roles in human body at trace concentration levels. Copper and iron are

essential elements, necessary for life, they are very toxic above but the recommended level. Excess of iron can cause hemochromatosis (Bacon 2011), which leads to failure of liver, heart and pancreas. Diseases of aging such as alzheimer, other neurodegenerative diseases, arteriosclerosis, diabetes mellitus, and others may all be contributed to by excess copper and iron (Brewer, 2010).

The processes which cause heavy metals reaching to toxic and carcinogenic amounts in soil and water resources following their increase in the atmosphere depending on climate conditions are industrial flue gases, local and intercity vehicle traffic, fossil fuels, mines, agricultural irrigation made with domestic and industrial wastewaters. Contamination with fertilizers, pesticides, leaking waters from solid waste storing areas, forestry activities etc. are other few factors leading to their relative accessibility (Deveci and Ekmekyapar, 2008)

Like cations, anions also play a vital role in our daily life. Some anions like cyanide (Authman et al, 2013) can be lethal for us but have industrial scale applications in the manufacturing of daily need goods. Cyanide is mainly produced for the mining of gold and silver. It helps dissolve these metals and their ores. Fluoride is often added to drinking water and toothpaste because of its beneficial effects in dental health. It is also administered in the treatment of osteoporosis (Aaseth et al, 2004). Polytetrafluoro ethylene (Teflon), is an example of more complex compound of fluorine, which is used in both industrial and household environments. While the beneficial effects of fluoride are well documented, chronic exposure to high levels of this anion can lead to dental or even skeletal fluorosis (Wade, 2010). Chloride is needed to keep the proper balance of body fluids. On the other hand excess of chloride in the body can increase blood pressure and cause hyperchloremia (Berend et al, 2012).

Even some of the bromine compounds like methyl bromide used as pesticide are outdated and banned. Unlike bromine, iodine has biological purpose. It is widely used as antiseptic and disinfectant. But iodine in larger amounts can cause metallic taste, soreness of teeth and gums, burning in mouth and throat, increased saliva, throat inflammation, stomach upset, diarrhea, depression, skin problems, and many other side effects (Wexler et al,

1998). Taking into account the adverse effects of these ions, a great deal of attention is required for new and improvised analytical methods for the detection of these ions.

1.1 Chemical Sensing

1.1.1 Chemical Sensors

According to IUPAC definition “a chemical sensor is a device that transforms chemical information, ranging from the concentration of a specific sample component to total composition analysis, into an analytically useful signal. The chemical information mentioned above, may originate from a chemical reaction of the analyte or from a physical property of the system investigated (Hulanicki et al, 1991). This whole procedure leads to chemical sensing. Receptor and transducer parts are two basic units of chemical sensors. The receptor part transforms the chemical information into a form of energy which may be measured by the transducer which further transforms the information into a useful analytical signal. Important parameters for an effective sensor are sensitivity, selectivity, specificity, resolution, reversibility and durability. Sensitivity is a measure of the amount of change to the output signal produced in response to a given concentration of a chemical. Selectivity characterizes the degree to which a sensor distinguishes one chemical from another. Specificity refers to the number of chemicals that a sensor detects or can differentiate between. Resolution is a measure of the minimum change of input quantity to which they can respond. Reversibility relates to how well the device recovers to a neutral state (Ballantine et al, 1997).

1.1.2 Methods of Chemical Sensing

The development of instrumentation and techniques makes it possible to design appropriate chemical sensors utilizing most of the known chemical, physical and biological principles for effective chemical sensing based on following categories:

- a) Receptor unit based classification
 - b) Transducer based classification
- a) Receptor unit based classification of chemical sensors**

Chemical sensing of a guest by a receptor requires an appropriate guest binding site in that receptor. It can be a neutral, positively charged or negatively charged unit of receptor depending on which it can sense cations, anions or gases through different types of interactions (Beer et al, 1999). Charged species have the advantage of higher solubility in polar media including water and electrostatic interaction is very strong when compared to hydrogen bonding. It is composed of species which employ electrostatic cation-anion interactions as the main driving force for the binding. Receptors containing positively charged groups like guanidium (Schmuck, 2006), imidazolium (Thomas et al, 2000), ammonium (Llinares et al, 2003, Mateus et al, 2010), pyridinium (Wenzel et al, 2012), organometallic metallocenes (Beer et al, 1996, Beer, 1998) etc. are most commonly studied receptors for anion sensing. There are hardly any reports of receptors with negatively charged units for cation sensing. The binding of ions to neutral receptors is of special significance since it avoids the competing counter ion complexes present if ionic hosts are used and improves selectivity due to the dominance of directional interactions (Garau et al, 2005) which explains the high specificity of neutral anion binding proteins. Neutral receptors with units like imidazole (Wagner-Wysiecka et al, 2007, Li et al, 2008), ferrocene (Zapata et al, 2008, Alfonso et al, 2011), calixarenes (Beer et al, 1999), crown ethers (Bernhardt *et al*, 2002, Kim et al, 2008), quinolone (Cheng et al, 2006, Mittal *et al*, 2007) etc., are used for cation sensing. Urea, thiourea, amide, pyrrole, imidazole (Cametti et al, 2009, Francisco et al, 2009, Wenzel et al, 2012) based neutral receptors are reported for anion sensing too.

b) Transducer based classification of chemical sensor

There are more than half a dozen types of chemical sensors that are classified according to the operating principle of the transducer. Most common are optical devices, electrochemical devices, thermometric devices, electrical devices, mass sensitive devices and magnetic devices.

1. Optical devices transform changes of optical phenomena, which are the result of an interaction of the analyte with the receptor part. This group may be further subdivided according to the type of optical properties which have been applied in chemical sensors like absorbance (Beer et al, 1999, Kaur et al, 2010, Yang et al, 2011), reflectance, luminescence (Patra et al, 2010), fluorescence (Martinez-Manez, et al, 2003, Nui et al, 2008), refractive index, optothermal effect.

2. Electrochemical devices transform the effect of the electrochemical interaction between analyte and electrode into a useful signal. Such effects may be stimulated electrically or may result in a spontaneous interaction at the zero-current condition. The following subgroups may be distinguished.

- a) Voltammetric sensors
- b) Potentiometric sensors
- c) Chemically sensitized field effect transistor (CHEMFET)
- d) Potentiometric solid electrolyte gas sensors

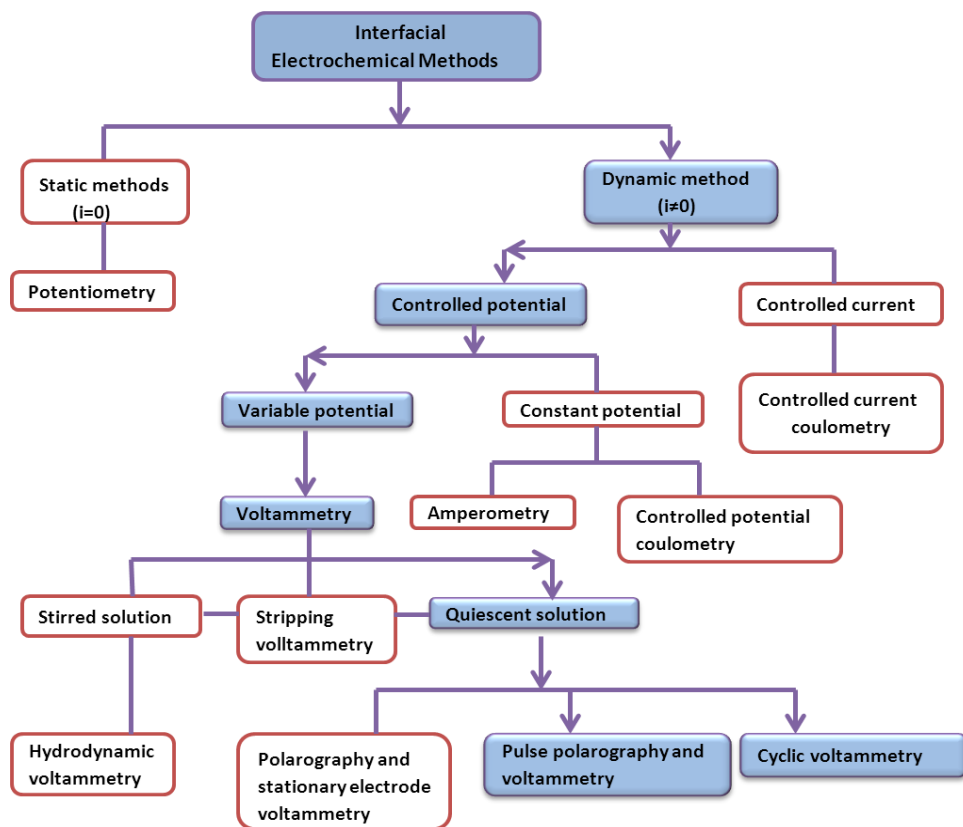
1.1.3 Sensing by electrochemical methods

These are the analytical methods in which a measurement of potential, current, or charge in an electrochemical cell serves as the analytical signal (Harvey, 1999)

The simplest division is between

1. Bulk methods, which measure properties of the whole solution. The measurement of conductivity of a solution, which is proportional to the total concentration of dissolved ions, is one example of a bulk electrochemical method.
2. Interfacial methods, in which the signal is a function of the phenomena occurring at the interface between an electrode and the solution in contact with the electrode. Determination of pH using the glass electrode is one example of an interfacial electrochemical method.

Interfacial methods are further categorized into potentiometry, conductometry, coulometry, and voltammetry depending on which aspects of the cell are controlled and which are measured.



Interfacial electrochemical methods

Voltammetry applies a constant or varying potential at the surface of an electrode and measures the resulting current with a three electrode system. It can reveal the reduction/oxidation potential of an analyte and its electrochemical reactivity.

1.2 Voltammetric ion sensing

Voltammetry is widely used by analytical, inorganic, physical, and biological chemists for fundamental studies. The analytical advantages of various voltammetric techniques include rapid location of redox potentials of the electroactive species, quantitative and qualitative determination of organic and inorganic compounds in aqueous and non-aqueous solutions, number of electrons involved in each step of the process, adsorption processes on surfaces, a wide range of temperatures, rapid analysis time (seconds), simultaneous determination of several analytes, the ability to determine kinetic and mechanistic

parameters, a well-developed theory and thus the ability to reasonably estimate the values of unknown parameters (Kounaves, 1997).

Cyclic voltammetry (CV) is one of the most versatile techniques performed in electrochemistry and is used extensively in organic chemistry, biochemistry, and inorganic chemistry (Kissinger, 2000, Speiser, 1999, Neol et al, 1990). The study of the electrochemical properties of supramolecular systems capable of sensing charged or neutral substrates and reporting their presence by means of an electrochemical response (Boulas et al, 1998) is an area of intense interest (Beer, 1992) for the last two decades. Redox-active receptors containing redox active units like ferrocene (Bui et al, 2008) or quinone, anthraquinone, calix[n]arenes (Schuhle et al, 2011) and nitroaromatic containing species are selective for cations. In all these cases, an anodic shift of the redox-process is expected to be observed as the positively charged cation–receptor complex will be difficult to oxidize (or more easy to reduce) than the neutral receptor alone. Electrochemical receptors for anions are expected to show cathodic shifts in their redox-process when complexed to an anion as they are either easier to oxidize or hard to reduce than the free redox-active receptor. Most of these receptors are either based on positively charged species like imidazolium, guanidinium (Beer and Schmidt, 1999), protonated cryptands, based or neutral receptors like benzimidazole (Joo et al, 2007), amide, pyrrole (Gale et al, 2007), urea and thiourea (Cametti *et al*, 2009) or metal based receptors (Beer, 1998).

1.3 Electrode modification

The need for modification of electrodes arose to acquire knowledge with more profundity by surpassing the limitations of bare electrodes in the field of electrochemical science. Chemically modified electrodes (CMEs) have a molecular monolayers or micrometer thick layers of film made from a certain compound coated on the surface of the electrode. CMEs have not only the surface properties changed as per the target function but also to increase factors like selectivity, sensitivity and response (Alkire et al, 2009).

CMEs and electrodes in general greatly depend on electron transport i.e., electrochemical processes where the charge transports through the chemical films to the electrode surface. Atoms, molecules, and nano-particles are attached to the surface of materials to modify

their electronic and structural properties, leading to change in their functionality. There are four ways to chemically modify the surface of electrodes (Durst et al, 1997, Zen et al, 2003):

- 1) **Chemisorption-adsorption-** In this monolayer structures of chemical compounds are formed using the physical and chemical interactions. This method gives easy surface modification with chemical film strongly and irreversibly adsorbed (chemisorbed) onto the electrode surface like self assembled monolayers (SAMs).
- 2) **Covalent bonding-** Functional groups such as organosilanes or $>C=O$, are used to covalently attach monomolecular layers of the chemical modifier to the electrode surface.
- 3) **Polymer film coating-** The polymer film prepared is less vulnerable than layers prepared by chemisorption and covalent bonding. Multilayer films are easy to prepare, chemically stable, highly conductive and can incorporate any desired electroactive chemical functionality.
- 4) **Composite-** The chemical modifier is simply mixed with an electrode matrix material, as in the case of an electron-transfer mediator (electrocatalyst) combined with the carbon particles (plus binder) of a carbon paste electrode.

1.3.1 Polymer film coating

Perspectives of using polymers as plastic materials changed rapidly after the discovery of a new class of polymers known as intrinsically conductive polymers or electroactive polymers in 1977 (Shirakawa et al, 1977). Different groups working under A. J. Heeger, A. G. MacDiarmid, and H. Shirakawa have shown that the electrical conductivity of polyacetylene can be increased by 13 orders of magnitude upon doping with electron acceptors and electron-donors (Chiang et al, 1978), and this spurred the development of new field of conducting polymers. The achievement of conductivity in polyacetylene as high as that of copper metal by H. Naarmann and coworkers (1982), was a milestone discovery. But its poor stability and processability lead to the development of new conductive polymers such as polyaniline, polypyrrole, polythiophene, poly(p-phenylene), poly(p-phenylenesulphide). Out of these polyaniline is economical, has high thermal

stability, easy processing and synthesis (Bhadra et al, 2009). The main characteristic of a conducting polymer is a conjugated backbone that can be subjected to oxidation or reduction by electron acceptors or donors. The most common type of polymer film coating is done by using polyaniline, polypyrrole, polythiophenes, poly(acetylene)s, poly(phenylene)s etc. Polyaniline being most stable and easily processable is used commonly.

The base form of polyanilines has the generalized formula as shown in Fig. 1.1, where some of the C_6H_4 rings are in the benzoid form while others in the quinonoid form.

Polyaniline (PANI) can be prepared by either chemical or electrochemical oxidation of aniline under acidic conditions (Genies *et al*, 1990).

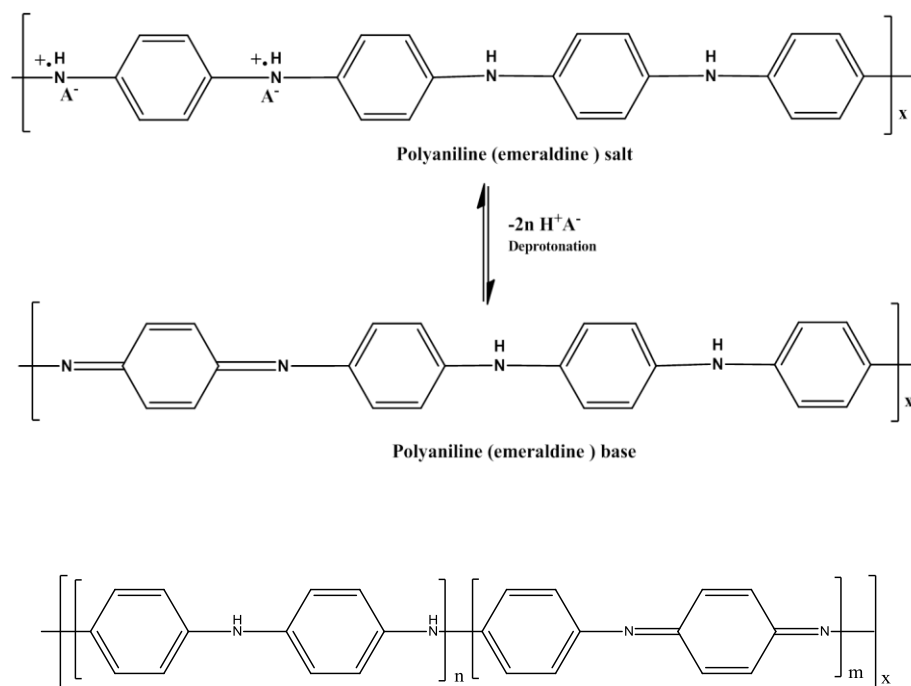


Fig 1.1 Generalized form of polyaniline where $n+m = 1$, $x =$ degree of polymerization.

The most common green protonated emeraldine has conductivity on a semiconductor level of the order of $10 S cm^{-1}$, many orders of magnitude higher than that of common polymers ($<10^{-9} S cm^{-1}$) but lower than that of typical metals ($>10^4 S cm^{-1}$). Protonated PANI, (e.g., PANI hydrochloride) converts to a non-conducting blue emeraldine base when treated with

a base like ammonium hydroxide (Stejskal, 2002). The efficient polymerization of aniline is achieved only in an acidic medium, where aniline exists as an anilinium cation.

1.4 Applications of chemically modified electrodes

Since the first report of a chemically grafted group to a platinum electrode surface [Moses et al, 1975] chemically modified electrodes by single and multiple molecular layers have been extensively studied. The applications involving modified electrodes are multiple and widespread: chemical sensing, energy conversion and storage, and electrochromic displays, etc. In addition, modified electrodes have always been used as a tool in fundamental scientific investigations. The main focus of this work is ion sensing with chemically modified electrodes. Huge amount of literature is available reporting ions sensing by different types of CMEs like carbon paste electrodes (Svancara et al, 2008, Vytras et al, 2009,), electrodes modified with conducting polymer, self-assembled monolayers etc. CMEs modified with conducting polymers shows sensing toward inorganic ions (MuthuKumar et al, 2007, Evtugyn et al, 2007), organic molecules and gases as well (Xu *et al*, 2007, Lange *et al*, 2008). Further, the responses of these are improvised by modification with carbon nanotubes (Konyushenko et al, 2006), copolymerization, nanoscale polymers (Li et al, 2009, Tran et al, 2011), by making derivatives with electroactive species like ferrocene, tetrathiafulvalene etc. These modified electrodes are characterized using techniques like scanning electron microscopy (SEM) (Tran et al, 2011), tunneling electron microscopy (TEM) (Hu et al, 2012), atomic force microscopy (AFM) (Evtugyn et al, 2007), voltammetry like cyclic voltammetry, differential pulse voltammetry, square wave voltammetry (Zangneh et al, 2007, 2008) etc.

1.5 References

Alfonso, M., Espinosa, A., Tarraga, A., Molina, P., 2011, A simple but effective dual redox and fluorescent ion pair receptor based on a ferrocene-imidazopyrene dyad, *Organic Letters*, 13, 8, 2078-2081.

Alkire, R.C., Kolb, D.M., Lipkowski, J., Ross, P., (eds.) 2009, Advances in Electrochemical Science and Engineering, Vol. 11. Chemically Modified Electrodes. Wiley-VCH, Weinheim, Germany.

Authman, M.M.N., Abbas Wafaa T., Abumourad, I.M.K., Kenawy, A.M., 2013, Effects of illegal cyanide fishing on vitellogenin in the freshwater African catfish, *Clarias gariepinus* (Burchell, 1822) *Ecotoxicology and Environmental Safety*, 91, 61-70.

Bacon, B.R., 2011, Iron overload (hemochromatosis) In: Goldman L, Ausiello D, eds. *Cecil Medicine*. 24th ed. Philadelphia, Pa: Saunders Elsevier;:ch- 219.

Ballantine, D.S., White, R.M., Martin, S.J., Ricco, A.J., Zellers, E.T., Fry, G.C., Wohltjen, H., 1997, Acoustic Wave Sensors Theory, Design, and Physico-Chemical Applications. San Diego: Academic Press, pp. 435.

Bhadra, S., Khastgir, D., Singhaa, N.K., Hee Lee, J., 2009, Progress in preparation, processing and applications of polyaniline, *Progress in Polymer Science*, 34, 783–810.

Beer, P.D., 1992, Transition metal and organic redox-active macrocycles designed to electrochemically recognize charged and neutral guest species, *Advances in Inorganic Chemistry*, 39, 79-157.

Beer, P.D., 1998, Transition-Metal receptor systems for the selective recognition and sensing of anionic guest species, *Accounts of Chemical Research*, 31, 71-80.

Beer, P.D., Cadman, J., 1999, Electrochemical and optical sensing of anions by transition metal based receptors, *Coordination Chemistry Reviews*, 205, 131–155.

Beer, P.D., Gale, P.A., Chen, G.Z., 1999, Mechanisms of electrochemical recognition of cations, anions and neutral guest species by redox-active receptor molecules, *Coordination Chemistry Reviews*, 185–186, 3–36.

Beer, P.D. and Schmitt P., 1999 Molecular recognition of anions by synthetic receptors, *Current Biology in Chemical Biology*, 1, 475-462.

Beer, P.D., Fletcher N.C., Grieve A., Wheeler J.W., Moore C.P., Wear T., 1996, Halide anion recognition by new acyclic quaternary polybipyridinium and polypyridinium receptors. *Journal of Chemical Society, Perkin transactions*, 2, 1545-1551.

Beer, P.D., Drew, M.G.B., Graydon, A.R., 1996, Chloride- and dihydrogenphosphate-selective anion recognition by new acyclic mono-, bis- and his-cobaltocenium receptors, *Journal of Chemical Society. Dalton Transactions*, 4129-4134.

Berend, K., Hendrik L., Hulsteijn V., GansRijk O. B., 2012, Chloride: The queen of electrolytes? *European Journal of Internal Medicine*, 23, 3, 203-211.

- Bernhardt**, P.V., Hayes, E. J., **2002**, Crown ether appended cyclam receptors for cationic guests, *Inorganic Chemistry*, 41, 2892-2902
- Boulas**, P.L., Gomez-Kaifer, M., L. Echegoyen, *1998*, Electrochemistry of Supramolecular Systems, *Angewandte Chemie International Edition (English)*, 37, 216-247.
- Brewer**, G.J., *2010*, Risks of copper and iron toxicity during aging in humans, *Chemical Research in Toxicology*., 23, 319–326.
- Bui**, N., Hong J., Mho S., Jang H., *2008*, A ferrocene derivative redox sensor for mercuric ion: synthesis and electrochemical study, *Bulletin of Korean Chemical Society*, 29, 7, 1395-1398.
- Cametti**, M., Rissanen, K., *2009*, Recognition and sensing of fluoride anion, *Chemical Communications*., 2809–2829.
- Cheng**, Y., Zhao, D., Zhang, M., Liu, Z., Zhou, Y., Shu, T., Li, F., Yi, T., Huang, C., *2006*, Azo 8-hydroxyquinoline benzoate as selective chromogenic chemosensor for Hg²⁺ and Cu²⁺, *Tetrahedron Letters* 47, 6413–6416.
- Deveci**, M., Ekmekyapar, F., *2008*, Environmental problems induced by pollutants in air, soil and water resources, *Enviornmental technologies* edited by E. BurcuÖzkaraovaGüngör, Published by I-Tech Education and Publishing, Austria, Ch-3, 41-54.
- Durst**, R.A., Baumner, A. J., Murray, R.W., Buck, R.P., Andrieux, C.P., *1997*, Chemically modified electrodes: recommended terminology and definitions, *Pure & Applied Chemistry*, 69, 6, 1317-1323.
- Evtugyn**, G.A., Stoikov, I. I., Beljyakova, S.V., Shamagsumova, R.V., Stoikova, E. E., Zhukov, A.Yu., Antipin, I.S., Budnikov, H. C., *2007*, Ag selective electrode based on glassy carbon electrode covered with polyaniline and thiacalix[4]arene as neutral carrier, *Talanta*, 71, 1720–1727.
- Gale**, P.A., Garcí'a-Garrido, S.E., Garric, J., *2008*, Anion receptors based on organic frameworks: highlights from 2005 and 2006, *Chemical Society Reviews*, 37, 151–190.
- Garau**, C., Frontera, A., Ballester, P., Quinonero, D., Costa, A., Deya, P. M., *2005*, *European Journal of Organic Chemistry*, 179-183,
- Harvey**, D., *1999*, Modern analytical chemistry, McGraw-hill, 1st ed., Ch-11, 461-541.
- Hu**, F., Chen, S., Wang, C., Yuan, R., Xiang, Y., Wang, C., *2012*, Multi-wall carbon nanotube-polyaniline biosensor based on lectin–carbohydrate affinity for ultrasensitive detection of Con A, *Biosensors and Bioelectronics*, 34, 202- 207.
- Hulanicki**, A., Geab, S., Ingman, F., *1991*, Chemical sensors definitions and classifications, *Pure & Applied Chemistry*, 63, 9, 1247-1250.
- Joo**, T.Y., Singh, N., Lee, G.W., Jang, D.O., *2007*, Benzimidazole-based ratiometric fluorescent receptor for selective recognition of acetate, *Tetrahedron Letters*, 48, 8846–8850.

- Kaur, V.**, Malik, A.K., Verma, N., 2010, Simultaneous determination of Cu(II) and Pd(II) as 4- phenylpiperazinecarbodithioate complex using H-point standard addition method and derivative spectrophotometry, *Turkish Journal of Chemistry*, 34, 295-305.
- Kim. T.H.**, Kim, J.S., Kim, H., 2008, Voltammetric studies for cation recognition with thiocalix[4]crown-6s, *Journal of Electroanalytical Chemistry*, 615, 103-109.
- Kissinger P.T.**, 2000, Electrochemical biosensors - Promise vs. reality, *Quimica Analitica*, 19, 5-7.
- Konyushenko, E.N.**, Stejskal, J., Trchovaa, M., Hradil, J., Kovarova, J., Prokes, J., Cieslar, M., Hwang, J., Chen, K., Sapurina, I., 2006, Multi-wall carbon nanotubes coated with polyaniline, *Polymer*, 47, 5715-5723.
- Kounaves, S.P.**, Voltammetric Techniques, Handbook of Instrumental Techniques for Analytical Chemistry, 1/e Frank A. Settle, National Science Foundation, Arlington, Virginia Published June, 1997 by Prentice Hall PTR (ECS Professional).
- Lange, U.**, Roznyatovskaya, N.V., Mirsky, V.M., 2008, Conducting polymers in chemical sensors and arrays, *Analytica Chimica Acta*, 614, 1, 1–26.
- Lee, M.H.**, Lee, S.J., Jung, J.H., Lima, H., Kim, J.S., 2007, Luminophore-immobilized mesoporous silica for selective Hg²⁺ sensing, *Tetrahedron* 63, 12087–12092.
- Li, Z.**, Lou, X., Yu, H., Li, Z., Qin, J., 2008, An imidazole-functionalized polyfluorene derivative as sensitive fluorescent probe for metal ions and cyanide, *Macromolecules*, 41, 7433-7439.
- Li, C.**, Bai, H., Shi, G., 2009, Conducting polymer nanomaterials: electrosynthesis and applications, *Chemical Society Reviews*, 38, 2397–2409.
- Llinares, J.M.**, Powell D., Bowman-James, K., 2003, Ammonium based anion receptors, *Coordination Chemistry Reviews*, 240, 57-75.
- Mateusa, P.**, Berniera, N., Delgado R., 2010, Recognition of anions by polyammonium macrocyclic and cryptand receptors: Influence of the dimensionality on the binding behavior, *Coordination Chemistry Reviews*, 254, 1726-1747.
- Martínez-Mañez, R.**, Sancenó, F., 2003, Fluorogenic and Chromogenic Chemosensors and Reagents for Anions, *Chemical Reviews*, 103, 4419-4476.
- Mersal, G.A.M.**, 2009, Electrochemical Sensor for Voltammetric Determination of Catechol Based on Screen Printed Graphite Electrode, *International Journal of Electrochemical Science*, 4, 1167 – 1177.
- Mittal, S.K.**, Kumar A. S.K., Gupta, N., Kaur, S., Kumar, S., 2007, 8-Hydroxyquinoline based neutral tripodal ionophore as a copper (II) selective electrode and the effect of remote substituents on electrode properties, *Analytica Chimica Acta*, 585, 161–170.
- Moses, P. R.**, Wier, L., Murray, R. W., 1975, Superficially Mixed Metal Oxide Electrodes *Analytical Chemistry*, 47, 1882.

- Muthukumar**, C., Kesarkar, S. D., Srivastava, D. N., 2007, Conductometric mercury [II] sensor based on polyaniline–cryptand-222 hybrid, *Journal of Electroanalytical Chemistry*, 602, 172–180.
- Noel**, M., Vasu, K. I., 1990, Cyclic Voltammetry and the frontiers of electrochemistry: oxford and IBH Publishing Co.: New Delhi.
- Niu**, H., Yin, Z., Su, D., Niu, D., He, J., Cheng, J., 2008, Imidazolium-based macrocycles as multisignaling chemosensors for anions, *Dalton Transactions*, 28, 3994-3700.
- Oton**, F., Espinosa, A., Tarraga, A., Ratera, I., Wurst, K., Veciana, J., 2009, Molina, P., Mononuclear ferrocenophane structural motifs with two thiourea arms acting as a dual binding site for anions and cations, *Inorganic Chemistry*, 48, 1566-1576.
- Patra**, S., Boricha, V.P., Sreenidhi, K.R., Suresh, E., Paul, P., 2010, Luminescent metalloreceptors with pendant macrocyclic ionophore: Synthesis, characterization, electrochemistry and ion-binding study, *Inorganica Chimica Acta* 363, 1639–1648.
- Rosette**, M. Roat-Malone, A John Wiley & Sons, Inc., Publication, *Bioinorganic Chemistry*, Edn Ch-1 , 1-23.
- Schmuck**, C., 2006, How to improve guanidinium cations for oxoanion binding in aqueous solution? The design of artificial peptide receptors, *Coordination Chemistry Reviews*, 250, 3053–3067.
- Schühle**, D.T., Petersa, J.A., Schatzb, J., 2011, Metal binding calixarenes with potential biomimetic and biomedical applications, *Coordination Chemistry Reviews*, 255, 23-24, 2727-2745.
- Speiser** B., 1999, From cyclic voltammetry to scanning electron microscopy: modern Electroanalytical methods to study organic compounds, materials and reactions, *Current Organic Chemistry*, 3,171-191.
- Stejskal**, J., 2002, Polyaniline: Preparation of a conducting polymer (IUPAC Technical Report), *Pure Applied Chemistry*, 74, 5, 857–867.
- Svancara**, I., Vytrasa, K., Kalcher, K., Walcarius, A., Wang, J., 2009, Carbon paste electrodes in facts, numbers, and notes: a review on the occasion of the 50-years jubilee of carbon paste in electrochemistry and electroanalysis, *Electroanalysis*, 21, 1, 7-28.
- Thomas**, J., Howarth, J., Hanlon, K., McGuirk, D., 2000, Ferrocenyl imidazolium salts as a new class of anion receptors with C–H...X⁻ hydrogen bonding, *Tetrahedron Letters*, 41, 413–416.
- Tran**, H.D., D’Arcy, J.M., Wang, Y., Beltramo, P.J., Strong, V.A., Kaner, R.B., 2011, The oxidation of aniline to produce “polyaniline”: a process yielding many different nanoscale structures, *Journal of Materials Chemistry*, 21, 3534–3550.
- Vytras**, K., Svancara, I., Metelka, R., 2009 Carbon paste electrodes in electroanalytical chemistry, *Journal of Serbian Chemical Society*, 74, 10, 1021–1033.

- Wackett**, L.P., Orme-Johnson, W.H., Walsh, C.T., 1989, Transition metal enzymes in bacterial metabolism. In: Beveridge, T.J., Doyle R.J. (eds) Metal ions and bacteria. Wiley, New York, pp 165-206.
- Wade**, C.R., Broomsgrrove, A.E.J., Aldridge, S., Gabba, F.P., 2010, Fluoride ion complexation and sensing using organoboron compounds, *Chemical Reviews*, 110, 3958–3984.
- Wagner-Wysiecka**, E., Jamrogiewicz, M., Fonarib, M.S., Biernat, J.F., 2007, Azomacrocyclic derivatives of imidazole: synthesis, structure, and metal ion complexation properties, *Tetrahedron*, 63, 4414-4421.
- Wenzel**, M., Hiscock, J.R., Gale, P.A., 2012, Anion receptor chemistry: highlights from 2010, *Chemical Society Reviews*, 41, 480–520.
- Wexler**, P., Gad, S.C., Hartung, R., Henderson, R.F., Krenzelok, E.P., Locey, B.J., Mehendale H.M., Plaa, G.L., Pope, C., Witschi H., 1998. Encyclopedia of Toxicology, Vol. 2. San Diego: Academic Press. Pp. 186–187.
- Xu**, K., Zhu, L., Zhang, A., Jiang, G., Tang, H., 2007, A peculiar cyclic voltammetric behavior of polyaniline in acetonitrile and its application in ammonia vapor sensor, *Journal of Electroanalytical Chemistry*, 608, 141–147.
- Yanga**, Y., Gaoa, W., Shengb, R., Wang, W., Liua, H., Yangc, W., Zhanga, T., Zhanga, X., 2011, Rhodamine-based derivatives for Cu²⁺ sensing: spectroscopic studies, structure-recognition relationships and its test strips, *Spectrochimica Acta Part A*, 81, 14– 20.
- Young**, J.T., Singh, N., Lee, G.W., Jang, D.O., 2007, Benzimidazole-based ratiometric fluorescent receptor for selective recognition of acetate, *Tetrahedron Letters*, 48, 8846–8850.
- Zanganeh**, A.R., Amini, M.K., 2007, A potentiometric and voltammetric sensor based on polypyrrole film with electrochemically induced recognition sites for detection of silver ion, *Electrochimica Acta*, 52, 3822–3830.
- Zanganeh**, A.R., Amini, M.K., 2008, Polypyrrole-modified electrodes with induced recognition sites for potentiometric and voltammetric detection of copper(II) ion, *Sensors and Actuators B* 135, 358–365.
- Zapata**, F., Caballero, A., Espinosa, A., Tarraga, A., Molina P., 2008, Triple channel sensing of Pb(II) ions by a simple multiresponsive ferrocene receptor having a 1-Deazapurine backbone, *Organic Letters*, 10, 1, 41-44.

Chapter 2

Review of Literature

Electro-analytical chemistry has a long history of development of analytical methods based upon the electrical properties of the solution of the analyte, when it is made part of an electrochemical cell. In order to ascertain the current state of knowledge, publications from technical journal articles since 2003 to 2013 are included in this chapter. In this review of literature, the articles related only to electrochemical sensing of ions by modified or unmodified electrodes are included.

2.1 Cation sensing

Importance of cation sensing is very well known because of the harmful effects they can cause, if present in excess. Cation sensing can be categorized on the basis of molecules, methods or technique used for sensing. Most popular techniques for cation sensing are spectrophotometry, spectrofluorimetry, ion selective electrodes, potentiometry, colorimetry, atomic absorption spectroscopy (AAS), inductively coupled plasma mass spectroscopy (ICP-MS) etc. These are well established methods used for cation sensing. Another upcoming field for cation sensing is voltammetry.

2.1.1 Electrochemically active receptors (using unmodified electrodes)

Redox-active receptors for cations can be either oxidizable (and hence form less stable complexes with cations), e.g. ferrocene containing receptors, or reducible (and hence form more stable complexes with cations), e.g. quinone, anthraquinone and nitroaromatic, calixarenes, crown ethers, lariat ethers, containing species. Molecules like crown ethers and calixarenes are very commonly used for metal ion sensing and extraction because of the CH- π or π - π interactions and the molecular design which are used to vary their binding properties. Oueslati (2007), published a review of calix(aza)crowns on their synthesis, recognition and coordination chemistry with cations ranging from alkaline earth metals to heavy metal ions. Detection of uranium (VI) in aqueous solution has been reported to be improved with calixarene modified gold electrode by Becker et al (2008). The cone

structure of the calix[6]arene containing six phenol units lead to the host guest interactions between calix[6]arene and uranyl ion. Lyskawa et al (2010) reported calix[4]arene substituted with four redox active tetrathiafulvalene(TTF) moieties selective for sodium ion. They utilized the redox active property and high π donating ability of TTF along with the binding property of calix[4]arene for electrochemical detection of metal ion. Bingol et al (2011), synthesized a novel azacalix[4]arene derivative as a highly selective electrochemical sensor for Cr^{3+} ion with no interference from other heavy metal ions.

Ferrocene based molecules is a very popular category of electrochemically active receptors as they show redox active behavior on its inclusion and show electrochemical sensing toward cations by analyzing the change in oxidation potential of ferrocene. Huang et al (2003) reported ferrocenyl based cyclopeptides selective for Ca^{2+} and K^+ . Cyclopeptides are well known for their ability to complex and release metal ions. This property along with incorporating of ferrocene group was used to make a redox switchable receptor for metal ion sensing. Oton et al (2007) reported ferrocenophanes with guanidine bridging units based receptors for cation, anions and amino acids. Bui et al (2008) synthesized 2-(ethylthiomethyl)-N-ferrocenylmethyl aniline for electrochemically sensing of Hg^{2+} ions. Nitrogen and sulphur present in the molecule helped in binding of mercuric ion which lead to anodic shift in potential of Fc/Fc^+ redox couple. Shi et al (2011) synthesized a multichannel sensor based on 8-hydroxyquinoline ferrocenoate for Hg^{2+} ion sensing. For real life sampling screen printed carbon electrode modified with compound was used as a sensor. Alfonso et al (2011) synthesized a Bisferrocene-Benzimidazole based triad as a redox active multichannel sensor for HSO_4^- and Hg^{2+} ions in acetonitrile as a solvent. Alfonso et al (2011), synthesized another redox active ferrocene-imidazopyrene based site for sensing cations and anions in order $\text{Pb}^{2+} > \text{Hg}^{2+} > \text{Zn}^{2+}$ and $\text{H}_2\text{PO}_4^- > \text{AcO}^-$, respectively.

A huge literature is available on neutral molecules containing subunits like urea, thiourea, rhodamine, quinones, pyrroles, tetrathiafulvalenes etc., reported as colorimetric, luminescent or fluorescent sensors or probes for cation sensing. But for electrochemical

sensors most of reports are on modified electrodes, ion selective electrodes or carbon paste electrodes.

2.1.2 Modified electrodes

i) Modification with polymeric membranes - Ion selective electrodes (ISEs)

Potentiometric determination using ion selective electrode is one of the popular field for ion sensing because of the advantages like selectivity, sensitivity, precision and low cost. Kuswandi et al (2007) prepared an ion selective optode using Hg^{2+} ion selective neutral ionophore, trityl-picolinamide. Its application potential was studied using water samples from different rivers. Gupta et al (2007) used neutral carriers i.e., 2-amino-6-purinethiol and 5-amino-1, 3,4-thiadiazole-2-thiol to prepare ion selective electrode for potentiometric determination of Hg^{2+} ions. The ability of S or P atoms to acts as exclusive donor atoms on coordination with soft metal ions such as Ag (I) and Hg (II) (these are large and often poorly solvated) was used to prepare the sensor. Mittal et al (2007) used 2-aminothiophenol based dipodal ionophore for the potentiometric determination of Ag^+ ion with further application to determine SCN^- , CN^- , S^{2-} and I^- ions as silver ion forms stable complexes with these ions. Gupta et al (2008) prepared cobalt selective potentiometric sensor using bridge modified 4-tert-butylthiacalix[4]arene in a polymeric membrane with detection limit of 0.30 ppm. Calix[4]arene based derivatives containing N, S, and O as binding sites have been reported as ion selective sensors for mercury(II) ions by Mahajan et al (2008). Chen et al (2010) studied the electrochemical and ion sensing properties of various calix[4]arene derivatives. Ion selective electrodes prepared from these derivatives containing monophenolic, p-bromodienone and monoquinone group, were found to be selective for cesium ion even in the presence of other potentially interfering ions. Yuan et al (2012) prepared a Schiff base complex $[\text{Co}(\text{L})_2](\text{ClO}_4) \cdot (\text{C}_3\text{H}_6\text{O}) \cdot (\text{H}_2\text{O})$ [$\text{L} = 2-((\text{E})-(3\text{-aminopyridin-4-ylimino)methyl})\text{-phenol}$ and $\text{C}_3\text{H}_6\text{O} = \text{acetone}$] and used it as an ionophore for Pb(II) selective ion selective electrode.

ii) Modification with self-assembled membranes

The application of self-assembled monolayers (SAMs) is increasing due to simplicity of preparation, versatility, stability and reproducibility (Freire et al (2004), Medard et al (2009), Civit et al (2010)). Huan et al (2004) used self-assembled membrane imprinting for metal ion detection, which were found to be selective for Hg^{2+} and Cu^{2+} ions even in presence of other interfering metal ions. The ion imprinted SAMs were prepared by mixing two monomers, o-amino thiophenol and dodecyl mercaptan. Recognition sites were prepared using o-amino thiophenol while dodecyl mercaptan blocked the unassembled gold surface. The assembling process was directed by the coordinate bond formed between copper ions and amino groups. Han et al (2009) used ferrocene-labeled DNA to form self-assembled layer through S–Au bonding on a polycrystalline gold electrode surface and used 3-mercapto-1-propanol to block the surface and form a mixed monolayer. The prepared sensor was used for electrochemical sensing of Hg^{2+} ions on the basis of Hg^{2+} -induced conformational changes. Oztekin et al (2011) prepared a 4-amino-6-hydroxy-2-mercaptopyrimidine monohydrate (AHMP)-based self-assembled monolayer (SAM) on the gold electrode surface to make a highly selective electrochemical Cu^{2+} ion sensor.

iii) Modification with carbon nanotubes

Carbon nanotubes have large surface to volume ratio, high surface reaction activity, conductivity and adsorption ability. These properties are very useful for increasing the sensitivity and selectivity of a sensor. Abbaspour et al (2007) prepared a platinum electrode modified with multi walled carbon nanotube composite coated containing polyvinylchloride (MWNT-PVC) based on 1,5-diphenylcarbazine as an ionophore for detection of Cr^{3+} ions. Kempegowda et al (2012) determined mercury at picomolar level by covalently modifying multiwalled carbon nanotubes with Fast Violet B salt. The nitrogen and oxygen atoms of the modifying molecules helped in binding and sensing Hg^{2+} ions. Morton et al (2009) used carbon nanotubes modified with cysteine (contains amino acid with high affinities towards heavy metals) for modification of electrode for sensing Pb^{2+} and Cu^{2+} ions through differential pulse voltammetry. Mohadesi et al (2010), modified multiwalled carbon nanotubes with a ligand, 1-(2-pyridylazo)-2-naphthol (PAN), and used

it to prepare a selective modified glassy carbon electrode for determination of Pb (II) by stripping voltammetry.

Nguyen et al (2011) used a modified inter-digitated array by electropolymerizing poly(1,8-diaminonaphthalene)/carbon nanotubes composite on to a silicon chip for selective voltammetric detection of mercury(II) ions. While Ouyang et al (2011), prepared a modified glassy carbon electrode using bimetallic Hg–Bi/single-walled carbon nanotubes (SWNTs) composite for simultaneous determination of Zn, Cd and Pb in aqueous solutions by stripping voltammetry. Hg and Bi provided large activated surface while SWNTs provided high conductivity for the effective electrochemical detection. Ashkenani et al (2012) used a Cu(II) imprinted polymer using 1-(2-pyridylazo)-2-naphthol carbon nanotubes modified carbon paste electrode as a Cu(II) selective voltammetric sensor. Aragay and Merkoci (2012) reported a review on usage of nanomaterials like CNTs, graphene, nanoparticles etc., as electrochemical sensors for heavy metal ions over a period of time. Guo et al (2011) prepared a novel sensor for lead determination using multiwalled carbon nanotubes grafted onto 2-aminothiophenol. Carbon paste electrode was prepared with this modified ionophore and was used for the potentiometric determination of Pb²⁺ ions in environmental samples. Wanekaya (2011), gave a review based on carbon nanomaterials used for sensing heavy metal ions

iv) Modification of electrode with conducting polymers

Electrode modification with conducting polymer films is another attractive approach to prepare electrochemical sensor as it yields large amounts of ligand at the electrode surface and allows large amounts of metal ion accumulation. Heitzmann et al (2005) modified the carbon electrode by oxidative electropolymerisation of (3-pyrrol-1-ylpropyl)malonic acid monomer to make sensor for electroanalysis of Cu(II), Pb(II), Cd(II) and Hg(II) ions using anodic stripping voltammetry. In another publication Heitzmann et al (2007) used electrode modified with complexing polymer containing malonic acid group which showed complexation with Cu²⁺ and Pb²⁺ ions and characterized it using anodic stripping voltammetry. Malonic acid was used to elaborate the ligating polymer like other commonly used material, amines, carboxylic acids, urea thiourea etc. Heitzmann et al (2007) reported

another *N,N'*-ethylenebis[*N*-[(3-(pyrrole-1-yl)propyl) carbamoyl) methyl]-glycine] complexing polymer modified electrode for electrochemical detection of Cu^{2+} , Pb^{2+} and Cd^{2+} ions through stripping them anodically.

Zangneh et al (2007) developed polypyrrole film based potentiometric and voltammetric sensor for silver ion sensing using the doping property of conducting polymers. The electropolymerisation of the polymer was done potentiostatically at a constant potential of 0.75V for fixed period of time. Algi et al (2008) prepared a thiophene, benzo-15-crown-5 (SNS-Crown) and pyrrole based polymer for voltammetric sensing of alkali metal ions in aqueous medium. It was found to be selective for Li^+ , Na^+ and K^+ ions. Evtugyn et al (2007) reported glassy carbon electrode modification using polyaniline and thiacalix[4]arene for selective determination of Ag^+ ions. The reported potentiometric sensor showed a response time of 12s. Masking agent NaF was used to avoid the interference of Hg^{2+} and Fe^{3+} ions. Thiacalix[4]arene was drop coated onto the PANI coated electrode which resulted in improved analytical performance of the sensor.

There is a report of conductometric determination (Muthukumar et al, 2007) of Hg^{2+} ions by a polyaniline-cryptand-222 based conductometric sensor. Sensing of ions was based on protonation of cryptand-222, acquiring H^+ from the polyaniline followed by deprotonation after binding with Hg^{2+} which changes the conductance of polyaniline. Zanganeh et al (2008), modified the glassy carbon electrode by electropolymerization of pyrrole in the presence of an anionic complexing ligand, Eriochrome Blue-black B which was templated with respect to copper ions to be used for its potentiometric and voltammetric detection. The potentiometric results showed the detection limit to be 10^{-8}M . Hu et al (2009) prepared a well-defined polyaniline/polyacrylic acid (PANI/PAA) nanocomposite film by alternatively dipping the electrode depositing nanostructured PANI and PAA via layer by layer (LBL) self-assembly technique. Buica et al in 2009 reported modification of electrode by oxidatively electropolymerising ethylenediamine tetra-*N*-(3-pyrrole-1-yl) propylacetamide for voltammetric sensing of mercury and copper cations. The four pyrrole groups present on EDTA skeleton were used for electrochemical detection of cations. Lin et al (2009) used copolymer film comprising 3-methyl thiophene (3MT) and 3-thiophene

acetic acid (3TA) to form a conducting copolymer modified electrode for electrochemical sensing of trace level copper ions. Carboxylic groups of the copolymer were modified to produce iminodiacetic acid which leads to the detection of copper ions. Oztekin et al (2010) did electrochemical modification of electrode for sensing Cu^{2+} ions. Poly-4-nitroaniline was electrochemically reduced in a non-aqueous system for modifying the glassy carbon electrode.

Electrode modification with nanomaterials synthesized from conducting polymers is another emerging area in the field of sensor preparation. Lin et al (2010) utilized the properties of polypyrrole and conducting polymer nanomaterials to prepare polypyrrole nanowire electrode. Sensor fabrication was based on Gly-Gly-His (GGH) tripeptide attached covalently onto overoxidised polypyrrole nanowires for determination of Cu^{2+} ions at very low concentration levels. Polyaniline has generally been used in the field of biosensing (Ben-valid et al (2010), Dhand et al (2011), Hu et al (2012)) or gas sensing (Stasyuk et al (2012))

v) Modification using carbon paste electrodes (CPEs)

Like ion selective electrodes, carbon paste electrodes too possess numerous properties such as low background current, chemical inertness, low cost, non-toxicity, stability in various solvents, wide potential range, easy fabrication and renewal. Mashhadizadeh et al (2006) prepared a carbon paste electrode and coated wire electrode by using a Schiff base [bis 5-(4-nitrophenyl azo)salicylaldehyde] 1,8-diamino, 3,6-dioxo octan (BNSAO) for potentiometric sensing of silver ions. Abu-shawish et al (2008) prepared a salicylidine-functionalized polysiloxane carbon paste electrode for selective potentiometric sensing of Cu^{2+} ions. Tonle et al (2010) prepared a thiol functionalized Kaolinite (clay) based carbon paste electrode for voltammetric determination of Pb^{2+} ions. Wang et al (2013) prepared a carbon paste electrode modified with a metal-organic framework of $\text{Zn}_4\text{O}(\text{BDC})_3$ (MOF^{-5} ; $\text{BDC}^{2-} = 1,4\text{-benzenedicarboxylate}$) for electrochemical detection of lead ions using differential pulse voltammetry.

vi) Modification with screen printed electrodes (SPEs)

Recent trends in field of sensor leading to their miniaturization as a solution to their lack of commercial viability. Miniature and disposable electrodes help in avoiding pre-treatment/polishing of electrode (Kadara et al (2009) and are easy for electrochemical applications. Honeychurch et al (2003) utilised thin film mercury coated screen printed electrodes for electroanalytical sensing and monitoring metal ion pollutants in biological, environmental and industrial samples. Khaled et al (2010) prepared a chitosan modified screen printed electrode for electrochemical analysis of heavy metal ions like Pb(II), Cu(II), Cd(II) and Hg(II). The property of Chitosan being one of the most abundant natural polymers which form stable chelates with many transition metal ions through the hydroxyl and amino groups present was used to make a sensor. Injang et al (2010), did trace level simultaneous determination of heavy metal ions Pb(II), Cd(II), and Zn(II) in herbs with screen printed carbon nanotube electrodes using sequential injection analysis-anodic stripping voltammetry (SIA-ASV).

Sanchez et al (2010), modified a screen-printed carbon electrode with functionalized mesoporous silica nanoparticles (MTTZMSU-2) for trace level sensing of Pb(II) ions by anodic stripping square wave voltammetry in natural waters samples. Hallam et al (2010) used graphite screen printed electrode for Cr⁶⁺ ion detection in real life samples. Aragay et al (2011) modified the screen printed electrode with heated graphite nanoparticles for multidetection of heavy metal ions like Cd²⁺, Pb²⁺, Cu²⁺ and Hg²⁺ ions and studied the effect of temperature. The modified nanoparticle based electrode showed better results on increase in temperature as it lead to the higher available surface area and number of edge planes, which allowed a higher electron transfer. Lezi et al (2012) used five bismuth precursor compounds (bismuth citrate, bismuth titanate, bismuth oxide, bismuth aluminate and bismuth zirconate) for preparing a disposable screen printed electrode modified with them to detect Pb²⁺ and Cd²⁺ ions.

2.2 Anion sensing

Electrochemical anion sensing by artificial receptors is quite an old field of research because of the important roles these anions play in our daily life (Schmidtchen et al (1997), Snowden et al (1999), Reynes et al (2001), Peso et al (2002). Pratt and Beer, 2003 reported

mono- and bis-urea substituted ferrocene receptors electrochemically active for H_2PO_4^- and Cl^- and AcO^- anions. In 2003, Coles et al (synthesized mono- and bis-ferrocene 2,5-diamidopyrrole clefts which were found to be electrochemically selective for dihydrogenphosphate. In 2005, Rynes et al (studied electrochemical sensing of anions like HSO_4^- , H_2PO_4^- , F^- and NO_3^- by electroactive receptors based on ferrocenyl cyclam framework and were found to be selective for HSO_4^- ion in non- aqueous system. Brooks et al (2005), studied a anthraquinone based receptor 1,3-diphenylcarboxamidoanthraquinone (AAR) for electrochemical sensing of F^- ion. Electrochemical signals obtained were based on the change caused by interaction of anions with the hydrogen bond donor groups rather than quinone oxygen atoms which further removed the H- bonding interaction with the redox-active quinone centre of the receptor. Beer et al (2005 gave a review based on metal based receptors used for anion sensing. Literature was reviewed on the basis of organometallic anion receptors, complexes of transition metals and mixed metal receptors

Tan et al (2007 studied ferrocene derivative for electrochemical ion sensing prepared through reaction of ferrocene carbonate acid and epoxy rosin E-51. Ferrocene derivative showed sensing toward dihydrogenphosphate. Gu et al (2007 prepared a ferrocene-based 1,3-alternate thiacalix[4]arene ditopic receptor containing ferrocene amide terminated four identical polyether arms. The receptor was studied for both cation and anion sensing and was found to be selective for europium and dihydrogen phosphate ions, respectively. Schumacher et al (2007) reported an electrochemically fluoride anion selective oxoporphyrinogen, N_{21} , N_{23} -dibenzyl-5,10,15,20-(3,5-di-t-butyl-4-oxo-cyclohexa-2,5-dienylidene)porphyrinogen, receptor in o-dichlorobenzene. The receptor was also found to be chemically responsive towards CH_3COO^- , H_2PO_4^- , ClO_4^- and NO_3^- ions. Cookson et al (2008) synthesized amide functionalised ruthenium (II) bis-bipyridyl dithiocarbamate receptor electrochemically selective for dihydrogenphosphate. The potential electrochemical sensing of receptor toward anions was evaluated on the basis of cathodic shifts obtained in the ruthenium (II/III) redox couple upon addition of five equivalents of anion guests. Niu et al (2008) prepared ferrocene-based imidazolium receptors electrochemically selective for AcO^- and HSO_4^- ions. Yang et al (2008) synthesized

calix[4]pyrrole based receptors containing ferrocene amide group electrochemically selective for dihydrogenphosphate in acetonitrile medium.

Lorenzo et al (2009) synthesized bisferrocenyl-substituted urea and thiourea and trisferrocenyl-substituted guanidine. All the derivatives showed electrochemical selectivity towards dihydrogen phosphate anion with a cathodic shift of 100-170 mV upon its addition. Kivlehan et al (2009) carried out voltammetric, spectrometric and potentiometric study of urea-functionalized calix[4]arene ionophore with various anions. All the three studies showed good selectivity for HPO_4^- over other anions. Cao et al (2012) synthesized a cleft form receptor for electrochemical anion sensing. The receptor contained amide and triazole donor groups which through N-H... anion and C-H...anion interactions showed a anodic shift for H_2PO_4^- and F^- anions which were further supported by theoretical studies.

Amendola et al (2009) reported a review on anion receptors with metals as structural units. Report included receptors with iron, cobalt, copper and ruthenium as metal centres. Ma et al (2009) reported ferrocene-based compounds glycidyl ester of ferrocene carboxylate (GEFC) and 1,3-diferrocenecarboxylic acid diacylglycerol (DFCDG) used for electrochemical sensing of anions. Both the molecules showed selective recognition toward dihydrogen phosphate in dichloromethane solvent. Ma and Dasgupta (2010) reviewed developments in the field of cyanide detection. The review included reports based on optical, fluorometry, chemiluminescence, atomic absorption spectrometry, potentionmetry, amperometry, mass spectrometry etc., used in the recent years for detection of cyanide ion. Bejger et al (2010) synthesized a receptor tetrathiafulvalene diindolylquinoxaline using an organic redox active TTF unit and dihydrogen phosphate sensitive diindolylquinoxaline to prepare optical- electrochemical chemosensor for H_2PO_4^- ion. Lee et al (2011) utilised the electrochemical properties of tetrathiafulvalene and synthesized two cone- and 1,3-alternate-calix[4]arenes bearing four modified TTF groups on the upper rim and tested their binding ability for various anions. The receptors were found to be most selective for $\text{HP}_2\text{O}_7^{3-}$ ion. Xu et al (2010) gave a review based on imidazolium based receptors used between years 2006-2009 for anion sensing. The review included reports based on cage type imidazoliums, imidazolium calixarenes, ferrocenyl imidazolium, cyclophane based

imidazoliums, chiral imidazolium, bile, tripodal system based imidazoliums etc. with only two reports of electrochemically active imidazolium derivatives.

Rivadehi et al (2012) prepared dipyrrolyl-tetrathiafulvalene based chromophore evaluated as both optical and electrochemical sensor for various anions in dichloromethane. Studies conducted with various anions showed the receptor to be highly selective toward fluoride ion. Sathayaraj et al (2012) synthesized two chemosensors containing imidazolyl and phenol moieties as linkers and ferrocene as redox active unit. Both spectral and electrochemical studies were conducted for sensing anions as well as cations. The imidazolephenol unit interacted efficiently with cations like Fe^{2+} , Cd^{2+} , Co^{2+} , Cu^{2+} , Ni^{2+} and Pb^{2+} as well as anions like HSO_4^- , F^- , B^- , I^- , OAc^- and OH^- .

Theoretical studies by density functional theory (DFT) method at B3LYP/LANL2DZ level of theory were conducted with Guassion 03W for geometry optimization and finding HOMO –LUMO orbitals. Jia et al (2012) prepared a receptor tetrathiafulvalene donor annulated to 2,3-di(1H-2-pyrrolyl)quinoxaline and found it to be electrochemically active for fluoride anion in dichloromethane. Corry et al (2012) synthesized N-(ferrocenyl)₂ and N-(ferrocenoyl)₂ cystine dimethyl ester derivatives and found them to be voltammetrically selective for dihydrogen phosphate ions. The recognition process was a result of electrostatic interactions between the ferricenium cation and the anion, and hydrogen bonding interactions between the peptide amide bonds and the anion.

Thakur et al (2013) recently prepared a triazole based triferrocene derivative as a multiresponsive chemosensor. Its optical and electrochemical studies on interaction with cations and anions showed it to be selective for Hg^{2+} and H_2PO_4^- ions, respectively. Xiong et al (2013) prepared modified dye 2,4-dinitrophenylhydrazine with tetrathiafulvalene attached to its one end making it electrochemically active and selective for F^- ion in dichloromethane. Kong et al (2013) prepared a ferrocene based methylimidazolium receptors to study their electrochemical behaviours and responses toward anions in acetonitrile medium. Ion pairing between anions and oxidized ligands caused negative shift in the potential of ligands. All the receptors were found to be selective for F^- ions. Madhu et al (2013) carried out spectrometric and voltammetric study of selective detection of

cyanide ion by 3,5-Diformyl-borondipyrromethene. Cyanide ion attacks the carbonyl groups of the receptor leading to generation of cyanohydrin which resulted in distinctive changes while carrying absorption, emission and electrochemical studies.

2.2.1 Modified electrode

Aoki et al (2003) used self-assembled membranes of bis thiourea to modify gold electrode for sensing phosphate through ion channel sensing. The response was based on the changes in response of $[\text{Fe}(\text{CN})_6]^{4-/3-}$ marker, before and after binding of phosphate to the receptor on the electrode surface. Abbaspour et al (2005) prepared a modified carbon paste electrode for potentiometric sensing of free cyanide ion. The electrode was chemically modified with 3,4-tetra pyridinoporphyrazinatocobalt(II) (Co(3,4 tppa) and was selective for CN^- ion only even in the presence of other interfering ions. Lindsay and O'Hare, (2006) prepared a Nafion coated gold electrode for amperometric determination of free cyanide at physiological pH. Zhang et al (2006) prepared self-assembled monolayers of Tetra-amide Calix[6]arene for modification gold surface. The SAM-modified gold electrodes were used for anion interaction studies and were found to be electrochemically responsive toward F^- and AcO^- anions. Szyman'ska et al (2006) prepared a carbon paste electrode and ion selective electrode using redox active ferrocene functionalized calix[4]pyrrole receptor for ion sensing in water. Osteryoung square wave voltammetry was conducted to study receptor-anion interactions. On the basis of decrease in current vs. concentration of anionic species, the sensitivity was proposed to be $\text{H}_2\text{PO}_4^- \geq \text{F}^- \geq \text{Br}^- \geq \text{Cl}^-$. Gonz'alez-Bellavista et al (2007) prepared an ion selective electrode with a conducting polymer (Sulfonated poly(ether ether ketone) (SPEEK)), to build an anion selective electrode. The modified electrode was found to be selective for nitrate ion. Mahajan et al (2007) prepared a potentiometric sensor with a Zn(II) complexes coordinated by tetradentate ligands. The modified electrode was used for anion sensing and showed high selectivity for nitrate ions than perchlorate and thiocyanate ions.

Gupta et al (2009) prepared a potentiometric sensor based on 2-(1-H-imidazo [4,5-f][1,10] phenanthroline-2-yl)-6methoxyphenol (HIPM) as a hydrogen bonding anion receptor and was found to be chloride selective. Taheri et al (2009) prepared a modified gold electrode

with self-assembled silica gel layer and silver nanoparticles for the electrochemical detection of cyanide ions. Li et al (2009) used Zn–Al LDH (Layered double hydroxides) to modified gold electrode and used it for amperometric detection of Iodate ions. Doménech et al (2010) prepared an electrode chemically modified with Au(I)–Cu(I) heterotrimetallic alkynyl cluster complexes containing ferrocenyl groups. The electrode showed distinctive responses towards fluoride, chloride, bromide, perchlorate, bicarbonate, carbonate, phosphate, hydrogen phosphate, dihydrogen phosphate, and nitrate anions. Kang et al (2010) utilised scandium(III) octaethylporphyrin to prepare an ion selective electrode using polymer membrane for sensing fluoride ion. Zhang et al (2010) reported voltammetric ion selective electrode for anion and cation sensing. Polymeric solution containing ionophores were drop coated on to the glassy carbon electrode for its modification. Khairy et al (2010) prepared screen printed microelectrodes for electroanalytical sensing of nitrite ions. Lou et al (2013) prepared a conducting polymer film modified electrodes integrated on paper-based chips for electrochemical sensing of chloride ions. The polypyrrole film doped with chloride was electrochemically polymerized onto the paper based chips.

2.3 References

- Abu-Shawish**, H.M., Saadeh, S.M., Hussien, A.R., 2008, Enhanced sensitivity for Cu(II) by a salicylidine-functionalized polysiloxane carbon paste electrode, *Talanta* 76, 941–948.
- Abbaspour**, A., Asadi, M., Ghaffarinejad, A., Safaei, E., 2005, A selective modified carbon paste electrode for determination of cyanide using tetra-3,4-pyridinoporphyrazinatocobalt(II), *Talanta*, 66, 931–936.
- Alfonso**, M., Tarraga, A., Molina, P., 2011, A Bisferrocene-Benzobisimidazole triad as a multichannel ditopic receptor for selective sensing of hydrogen sulfate and mercury ions, *Organic Letters*, 13, 24, 6432-6435.
- Algi**, F., Cihaner, A., 2008, An electroactive polymeric material and its voltammetric response towards alkali metal cations in neat water, *Tetrahedron Letters*, 49, 3530–3533.
- Amendola** V., Luigi, F., 2009, Anion receptors that contain metals as structural units, *Chemical Communication*, 5, 513–531.
- Aoki**, H., Hasegawa, K., Tohda, K., Umezawa, Y., 2003, Voltammetric detection of inorganic phosphate using ion-channel sensing with self-assembled monolayers of a hydrogen bond-forming receptor, *Biosensors and Bioelectronics*, 18, 261-267.
- Ashkenani**, H., Taher, M.A., 2012, Selective voltammetric determination of Cu(II) based on multiwalled carbon nanotube and nano-porous Cu-ion imprinted polymer, *Journal of Electroanalytical Chemistry*, 683, 80–87.
- Aragay**, G., Pons, J., Merkoç, A., 2011, Enhanced electrochemical detection of heavy metals at heated graphite nanoparticle-based screen-printed electrodes, *Journal of Materials Chemistry*, 21, 4326–4331.
- Aragay**, G., Merkoçi, A., 2012, Nanomaterials application in electrochemical detection of heavy metals, *Electrochimica Acta*, 84, 49– 61.
- Becker**, A., Tobias, H., Porat, Z., Mandler, D., 2008, Detection of uranium (VI) in aqueous solution by a calix[6]arene modified electrode, *Journal of Electroanalytical Chemistry*, 621, 214–221.
- Beer**, P.D., Bayly, S.R., 2005, Anion sensing by metal-based receptors, *Topics in Current Chemistry*, 255, 125–162.
- Bejger**, C., Park, J.S., Silvera, E.S., Sessler, J.L., 2010, Tetrathiafulvalene diindolylquinoxaline: a dual signaling anion receptor with phosphate selectivity, *Chemical Communication*, 46, 7745–7747.
- Ben-Valid**, S., Dumortier, H., Decossas, M., Sfez, R., Meneghetti, M., Bianco, A., Yitzchaik, S., 2010, Polyaniline-coated single-walled carbon nanotubes: synthesis, characterization and impact on primary immune cells, *Journal of Materials Chemistry*, 20, 2408–2417.

- Bingol**, H., Kocabas, E., Zor, E., Coskun, A., 2011, Spectrophotometric and electrochemical behavior of a novel azocalix[4]arene derivative as a highly selective chromogenic chemosensor for Cr⁺³, *Electrochimica Acta*, 56, 2057–2061.
- Brooks**, S.J., Birkin, P.R., Gale, P.A., 2005, Electrochemical measurement of switchable hydrogen bonding in an anthraquinone-based anion receptor, *Electrochemistry Communications*, 7, 1351–1356.
- Bui**, N.N., Hong, J., Mho, S., Jang, H., 2008, A ferrocene derivative redox sensor for mercuric ion: synthesis and electrochemical study, *Bulletin of Korean Chemical Society*, 29, 7, 1395–1398.
- Buica**, G.O., Bucher, C., Moutet, J., Royal, G., Saint-Aman, E., Ungureanua, E.M., 2009, Voltammetric sensing of mercury and copper cations at poly(EDTA-like) film modified electrode, *Electroanalysis*, 21, 1, 77 – 86.
- Cao**, Q., Pradhan, T., Lee, M.H., Choi, D. H., Kim, J. S., 2012, Cleft-form electrochemical anion chemosensor with amide and triazole donor groups, *Tetrahedron Letters*, 53, 4917–4920.
- Chen**, S., Webster, R.D., Talotta, C., Troisi, F., Gaeta, C., Neri, P., 2010, Electrochemistry and ion-sensing properties of calix[4]arene derivatives, *Electrochimica Acta*, 55, 7036–7043.
- Civit**, L., Frago, A., O’Sullivan, C.K., 2010, Thermal stability of diazonium derived and thiol-derived layers on gold for application in genosensors, *Electrochemical Communications*, 12, 1045–1048.
- Corry**, A.J., Goel, A., Kenny, P.T.M., 2012, The synthesis and structural characterization of N-(ferrocenyl)₂ and N-(ferrocenoyl)₂ cystine dimethyl ester derivatives: Potential anion sensing agents, *Inorganica Chimica Acta*, 384, 293–301.
- Coles**, S.J., Denuault, G., Gale, P.A., Horton, P.N., Hursthouse, M.B., Light, M.E., Warriner, C.N., 2003, Mono- and bis-ferrocene 2,5-diamidopyrrole clefts: solid-state assembly, anion binding and electrochemical properties, *Polyhedron*, 22, 699–709.
- Cookson**, J., Vickers, M.S. Paul, R.L., Cowley, A.R., Beer, P.D., 2008, Amide functionalised dithiocarbamate ruthenium(II) bis-bipyridyl receptors: A new class of redox-responsive anion sensor, *Inorganica Chimica Acta*, 361, 1689–1698.
- Dhand**, C., Dasa, M., Datta, M., Malhotra, B.D., 2011, Recent advances in polyaniline based biosensors, *Biosensors and Bioelectronics*, 26, 2811–2821.
- Doménech**, A., Koshevoy, I.O., Montoya, N., Pakkanen, T.A., 2010, Electrochemical anion sensing using electrodes chemically modified with Au(I)–Cu(I) heterotrimetallic alkynyl cluster complexes containing ferrocenyl groups, *Analytical and Bioanalytical Chemistry*, 397, 2013–2022.
- Evtugyn**, G.A., Stoikov, I.I., Beljyakova, S.V., Shamagsumova, R.V., Stoikova, E.E., Zhukov, A.Yu., Antipin, I.S., Budnikov, H.C., 2007, Ag selective electrode based on

glassy carbon electrode covered with polyaniline and thiacalix[4]arene as neutral carrier, *Talanta*, 71, 1720–1727.

Freire, R.S., Kubota, L.T., 2004, Application of self-assembled monolayer-based electrode for voltammetric determination of copper, *Electrochimica Acta*, 49, 3795–3800.

González-Bellavista, A., Macanás, J., Muñoz, M., Fabregas, E., 2007, Sulfonated poly(ether ether ketone), an ion conducting polymer, as alternative polymeric membrane for the construction of anion-selective electrodes, *Sensors and Actuators B*, 125, 100–105.

Gupta, V.K., Singh, A.K., Khayat, M. A., Gupta, B., 2007, Neutral carriers based polymeric membrane electrodes for selective determination of mercury (II), *Analytica Chimica Acta*, 590, 81–90.

Gupta, V.K., Jain, A.K., Khayat, M.A., Bhargava, S.K., Raison, J.R., 2008, Electroanalytical studies on cobalt(II) selective potentiometric sensor based on bridge modified calixarene in poly(vinyl chloride), *Electrochimica Acta*, 53, 5409–5414.

Gupta, V.K., Goyal, R.N., Sharma, R.A., 2009, Chloride selective potentiometric sensor based on a newly synthesized hydrogen bonding anion receptor, *Electrochimica Acta*, 54, 4216–4222.

Guo, D., Liu, Z., Ma, J., Huang, R., 2007, A novel ferrocene-based thiacalix[4]arene ditopic receptor for electrochemical sensing of europium(III) and dihydrogen phosphate ions, *Tetrahedron Letters*, 48, 1221–1224.

Guo, J., Chai, Y., Yuan, R., Song, Z., Zou, Z., 2011, Lead (II) carbon paste electrode based on derivatized multi-walled carbon nanotubes: Application to lead content determination in environmental samples, *Sensors and Actuators B*, 155, 639–645.

Hallam, P.M., Kampouris, D.K., Kadara, R.O., Banks, C.E., 2010, Graphite screen printed electrodes for the electrochemical sensing of chromium (VI), *Analyst*, 135, 1947–1952.

Han, D., Kim, Y., Oh, J., Kim, T.H., Mahajan, R.K., Kim, J. S., Kim, H., 2009, A regenerative electrochemical sensor based on oligonucleotide for the selective determination of mercury(II), *Analyst*, 134, 1857–1862.

Heitzmann, M., Basaez, L., Brovelli, F., Bucher, C., Limosin, D., Pereira, E., Rivas, B.L., Royal, G., Saint-Aman, E., Moutet, J., 2005, Voltammetric sensing of trace metals at a poly(pyrrole-malonic acid) film modified carbon electrode, *Electroanalysis* 17, 21, 1970 – 1976.

Heitzmann, M., C., Bucher, J., Moutet, J., Pereira, E., Rivas, B.L., Royal, G., Saint-Aman, E., 2007, Characterization of metal cations-complexing polymer films interactions followed with anodic stripping voltammetry, *Journal of Electroanalytical Chemistry*, 610, 147–153.

Heitzmann, M., Bucher, C., Moutet, J., Pereira, E., Rivas, B.L., Royal, G., Saint-Aman, E., 2007, Complexation of poly(pyrrole-EDTA like) film modified electrodes: Application to metal cations electroanalysis, *Electrochimica Acta*, 52, 3082–3087.

- Honeychurch**, K.C., J.P., 2003, Hart Screen-printed electrochemical sensors for monitoring metal pollutants, *Trends in Analytical Chemistry*, 22, 7-8, 456-469.
- Hu**, F., Chen, S., Wang, C., Yuan, R., Xiang, Y., Wang, C., 2012, Multi-wall carbon nanotube-polyaniline biosensor based on lectin-carbohydrate affinity for ultrasensitive detection of Con A, *Biosensors and Bioelectronics*, 34, 202–207.
- Huang**, H., Mu, L., He, J., Cheng, J., 2003, Ferrocenyl-Bearing Cyclopeptide as Redox-Switchable Cation Receptors, *Journal of Organic Chemistry*, 68, 7605-7611.
- Huan**, S., Jiao, C., Shen, Q., Jiang, J., Zeng, G., Huang, G., Shen, G., Yu, R., 2004, Determination of heavy metal ions in mixed solution by imprinted SAMs, *Electrochimica Acta*, 49, 4273–4280.
- Injang**, U., Noyrod, P., Siangproh, W., Dungchai, W., Motomizu, S., Chailapakul, O., 2010, Determination of trace heavy metals in herbs by sequential injection analysis-anodic stripping voltammetry using screen-printed carbon nanotubes electrodes, *Analytica Chimica Acta*, 668, 54–60.
- Jia**, H., Forgie, J.C., Liu, S., Sanguinet, L., Levillain, E., Derf, F.L., Salle, M., Neels, A., Skabara, P.J., Decurtins, S., 2012, Tetrathiafulvalene-annulated dipyrrolylquinoxaline: the effect of fluoride on its optical and electrochemical behaviors, *Tetrahedron*, 68, 1590-1594.
- Jose**, D.A., Singh, A., Das, A., Ganguly B., 2007, A density functional study towards the preferential binding of anions to urea and thiourea, *Tetrahedron Letters*, 48, 3695–3698.
- Kadara**, R.O., Jenkinson, N., Banks, C.E., 2009, Characterization and fabrication of disposable screen printed microelectrodes, *Electrochemistry Communications*, 11, 1377–1380.
- Kang**, Y., Lutz, C., Hong, S.A., Sung, D., Lee, J.S., Shin, J.H., Nam, H., Cha, G.S., Meyerhoff, M.E., 2010, Development of a fluoride-selective electrode based on scandium(III) octaethylporphyrin in a plasticized polymeric membrane, *Bulletin of Korean Chemical Society*, 31, 6, 1601-1608.
- Kempegowda**, R.G., Malingappa, P., 2012, Covalently modified multiwalled carbon nanotubes as a new voltammetric interface for the determination of mercury at picomolar level, *Electrochemistry Communications*, 25, 83–86.
- Khairy, M., Kadara, R.O., Banks, C.E., 2010, Electroanalytical sensing of nitrite at shallow recessed screen printed microelectrode arrays, *Analytical Methods*, 2, 851–854.
- Khaled**, E., Hassan, H.N.A., Habib, I.H.I., Metelka, R., 2010, Chitosan modified screen-printed carbon electrode for sensitive analysis of heavy metals, *International Journal of Electrochemical Science*, 5, 158 – 167.
- Kivlehan**, F., Mace, W.J., Moynihan, H.A., Arrigan, D.W.M., 2009, Study of electrochemical phosphate sensing systems: Spectrometric, potentiometric and voltammetric evaluation, *Electrochimica Acta*, 54, 1919–1924.

- Kong, D.**, Weng, T., He, W., Liu, B., Jin, S., Hao, X., Liu, S., 2013, Synthesis, characterization, and electrochemical properties of ferrocenylimidazolium, *Journal of Organometallic Chemistry*, 727, 19-27.
- Kuswandi, B.**, Nuriman, Dam, H.H., Reinhoudt, D.N., Verboom, W., 2007, Development of a disposable mercury ion-selective optode based on trityl-picolinamide as ionophore, *Analytica Chimica Acta*, 591, 208–213.
- Lee, M.H.**, Cao, Q., S.K., Kim, Sessler, J.L., Kim, J.S., 2011, Anion responsive TTF-appended calix[4]arenes. Synthesis and study of two different conformers, *Journal of Organic Chemistry*, 76, 870–874
- Lezi, N.**, Economou, A., Dimovasilis, P.A., Trikalitis, P.N., Prodromidis, M.I., 2012, Disposable screen-printed sensors modified with bismuth precursor compounds for the rapid voltammetric screening of trace Pb(II) and Cd(II), *Analytica Chimica Acta*, 728, 1–8.
- Li, M.**, Ni, F., Wang, Y., Xu, S., Zhang, D., Wang, L., 2009, LDH modified electrode for sensitive and facile determination of iodate, *Applied Clay Science*, 46, 4, 396-400.
- Lin, M.**, Cho, M., Choe, W., Son, Y., Lee, Y., 2009, Electrochemical detection of copper ion using a modified copolythiophene electrode, *Electrochimica Acta*, 54, 7012–7017.
- Lin, M.**, Cho, M., Choe, W., Yoo, J., Lee, Y., 2010, Polypyrrole nanowire modified with Gly-Gly-His tripeptide for electrochemical detection of copper ion, *Biosensors and Bioelectronics*, 26, 940–945.
- Lorenzo, A.**, Aller, E., Molina, P., 2009, Iminophosphorane-based synthesis of multinuclear ferrocenyl urea, thiourea and guanidine derivatives and exploration of their anion sensing properties, *Tetrahedron*, 65, 1397–1401.
- Lou, B.**, Chen, C., Zhou, Z., Zhang, L., Wang, E., Dong, S., 2013, A novel electrochemical sensing platform for anions based on conducting polymer film modified electrodes integrated on paper-based chips, *Talanta*, 105, 40–45.
- Lyskawa J.**, Canevet, D., Allain, M., M., Sallé, 2010, An electron-rich three dimensional receptor based on a calixarene-tetrathiafulvalene assembly, *Tetrahedron Letters*, 51, 5868–5872.
- Ma, L.**, Wang, L., Tan, Q., Yu, H., Huo, J., Ma, Z., Hu, H., Chen, Z., 2009, Study on synthesis and electrochemical properties of novel ferrocene-based compounds and their applications in anion recognition, *Electrochimica Acta* 54, 5413–5420.
- Ma, J.**, Dasgupta, P.K., 2010, Recent developments in cyanide detection: A review, *Analytica Chimica Acta*, 673, 117–125.
- Madhu, S.**, Basu, S.K., Jadhav S., Ravikanth, M., 2013, 3,5-Diformylborondipyromethene for selective detection of cyanide anion, *Analyst*, 138, 299–306.
- Mahajan, R.K.**, Kaur, R., Miyake, H., Tsukube, H., 2007, Zn(II) complex-based potentiometric sensors for selective determination of nitrate anion, *Analytica Chimica Acta*, 584, 89–94.

- Mahajan** R. K., Kaur, R., Bhalla, V., Kumar, M., Hattori, T., Miyano, S., Mercury (II) sensors based on calix[4]arene derivatives as receptor molecules, *Sensors and Actuators B* 130 (2008) 290–294.
- Mashhadizadeh**, M.H., Mostafavi, A., Allah-Abadi, H., Sheikhshoai, I., 2006, New Schiff base modified carbon paste and coated wire PVC membrane electrode for silver ion, *Sensors and Actuators B*, 113, 930–936.
- Medard**, C., Morin, M., 2009, Chemisorption of aromatic thiols onto a glassy carbon surface, *Journal of Electroanalytical Chemistry*, 632, 120–126.
- Mittal**, S. K., Kumar, A.S.K., Kaur, S., Kumar, S., 2007, Potentiometric performance of 2-aminothiophenol based dipodal ionophore as a silver sensing material, *Sensors and Actuators B*, 121, 386–395.
- Mohadesi**, A., Motallebi, Z., Salmanipour, A., 2010, Multiwalled carbon nanotube modified with 1-(2-pyridylazo)-2-naphthol for stripping voltammetric determination of Pb(II), *Analyst*, 135, 1686–1690.
- Morton**, J., Havens, N., Mugweru, A., Wanekaya, A.K., 2009, Detection of trace heavy metal ions using carbon nanotube-modified electrodes, *Electroanalysis*, 21, 14, 1597 – 1603.
- Muthukumar**, C., Kesarkar, S.D., Srivastava, D.N., 2007, Conductometric mercury [II] sensor based on polyaniline–cryptand-222 hybrid, *Journal of Electroanalytical Chemistry*, 602, 172–180.
- Nguyen**, D.T., Tran, L.D., Nguyen, H.L., Nguyen, B.H., Nguyen, V.H., 2011, Modified interdigitated arrays by novel poly(1,8-diaminonaphthalene)/carbon nanotubes composite for selective detection of mercury(II), *Talanta*, 85, 2445– 2450.
- Niu**, H., Yin, Z., Su, D., Niu, D., Ao, Y., He, J., Cheng, J., 2008, Ferrocene-based imidazolium receptors for anions, *Tetrahedron*, 64, 6300–6306.
- Oton**, F., Espinosa A., Tarraga, A., de Arellano, C. R., Molina, P., 2007, Ferrocenophanes with guanidine bridging units as multisignalling receptor molecules for selective recognition of anions, cations, and amino acids, *Chemistry A European Journal*, 13, 5742 – 5752.
- Ouyang**, R., Zhu, Z., Tatum, C.E., Chambers, J.Q., Xue, Z., 2011, Simultaneous stripping detection of Zn(II), Cd(II) and Pb(II) using a bimetallic Hg–Bi/single-walled carbon nanotubes composite electrode, *Journal of Electroanalytical Chemistry*, 656, 78–84.
- Oueslati**, I., 2007, Calix(aza)crowns: synthesis, recognition, and coordination. A mini review, *Tetrahedron*, 63, 10840–10851.
- Oztekin**, Y., Tok, M., Nalvuran, H., Kiyak, S., Gover, T., Yazicigil, Z., Ramanaviciene, A., Ramanavicius, A., 2010, Electrochemical modification of glassy carbon electrode by poly-4-nitroaniline and its application for determination of copper (II), *Electrochimica Acta*, 56, 387–395.

- Oztekin**, Y., Ramanaviciene, A., Ramanavicius, A., 2011, Electrochemical copper (II) sensor based on self-assembled 4-amino-6-hydroxy-2-mercaptopyrimidine monohydrate, *Sensors and Actuators B*, 155, 612–617.
- Peso**, I., Alonso, B., Lobete, F., Casado, C.M., Cuadrado, I., Barrio, J. L., 2002, A polymerizable pyrrole–cobaltocenium receptor for the electrochemical recognition of anions in solution and immobilised onto electrode surfaces, *Inorganic Chemistry Communications*, 5, 288–291.
- Pratt**, M.D., Beer, P.D., 2003, Anion recognition and sensing by mono- and bis-urea substituted ferrocene receptors, *Polyhedron*, 22, 649–653.
- Reynes**, O., Maillard, F., Moutet, J., Royal, G., Saint-Aman, E., Stanciu, G., Dutasta, J., Gosse, I., Mulatier, J., 2001, Complexation and electrochemical sensing of anions by amide-substituted ferrocenyl ligands, *Journal of Organometallic Chemistry*, 637–639, 356–363.
- Reynes**, O., Gulon, T., Moutet, J., Royal, G., Saint-Aman, E., 2002, Amplification upon polymerization of the electrochemical anion sensing properties of an amidoferrocene monoreceptor molecule, *Journal of Organometallic Chemistry*, 656, 116–119.
- Reynes**, O., Bucher, C., Moutet, J., Royal, G., Saint-Aman, E., Ungureanu, E., 2005, Electrochemical sensing of anions by redox-active receptors built on the ferrocenyl cyclam framework, *Journal of Electroanalytical Chemistry*, 580, 291–299.
- Rivadehi**, S., Reid, E.F., Hogan, C.F., Bhosale, S.V., Langford, S.J., 2012, Fluoride-selective optical sensor based on the dipyrrolyl-tetrathiafulvalene chromophore, *Organic and Biomolecular Chemistry*, 10, 705–709.
- Sánchez**, A., Morante-Zarcelero, S., Pérez-Quintanilla, D., Sierra, I., Hierro, I., 2010, Development of screen-printed carbon electrodes modified with functionalized mesoporous silica nanoparticles: Application to voltammetric stripping determination of Pb(II) in non-pretreated natural waters, *Electrochimica Acta*, 55, 6983–6990.
- Sathyaraj**, G., Muthamilselvan, D., Kiruthika, M., Weyhermüller, T., Nair, B.U., 2012, Ferrocene conjugated imidazolephenols as multichannel ditopic chemosensor for biologically active cations and anions, *Journal of Organometallic Chemistry*, 716, 150–158.
- Schmidtchen**, F.P., Berger, M., 1997, Artificial organic host molecules for anions. *Chemical Reviews*, 97, 1609–1646.
- Schumacher**, A.L., Hill, J.P., Ariga, K., D'Souza, F., 2007, Highly effective electrochemical anion sensing based on oxoporphyrinogen, *Electrochemistry Communications*, 9, 2751–2754.
- Shi**, L., Song, W., Li, Y., Li, D., Swanick, K.N., Ding, Z., Long, Y., 2011, A multi-channel sensor based on 8-hydroxyquinoline ferrocenoate for probing Hg(II) ion, *Talanta*, 84, 900–904.

- Snowden**, T.S., Anslyn, E.V., 1999, Anion recognition: synthetic receptors for anions and their application in sensors, *Current Opinion in Chemical Biology*, 3, 6, 740–746.
- Stasyuk**, N., Smutok, O., Gayda, G., Vus, B., Koval'chuk, Y., Gonchar, M., 2012, Bi-enzyme L-arginine-selective amperometric biosensor based on ammonium-sensing polyaniline-modified electrode, *Biosensors and Bioelectronics*, 37, 46–52.
- Szyman'iska**, I., Radecka, H., Radecki, J., Gale, P.A., Warriner, C.N., 2006, Ferrocene-substituted calix[4]pyrrole modified carbon paste electrodes for anion detection in water, *Journal of Electroanalytical Chemistry*, 591, 223–228.
- Tan**, Q., Wang, L., Yu, H., Deng, L., 2007, Study on synthesis and electrochemical properties of a novel ferrocene-based compound and its application in anion recognition, *Journal of Physical Chemistry B*, 111, 3904–3909.
- Taheri**, A., Noroozifar, M., Khorasani-Motlagh, M., 2009, Investigation of a new electrochemical cyanide sensor based on Ag nanoparticles embedded in a three-dimensional sol–gel, *Journal of Electroanalytical Chemistry*, 628, 48–54.
- Thakur**, A., Mandal, D., Ghosh, S., 2013, A triazole based triferrocene derivative as a multiresponsive chemosensor for Hg(II) ion and a redox chemosensor for H₂PO₄⁻ ion, *Journal of Organometallic Chemistry*, 726, 71–78.
- Tonle**, I.K., Letaief, S., Ngameni, E., Walcarius, A., Detellier, C., 2011, Square wave voltammetric determination of lead(II) ions using a carbon paste electrode modified by a thiol-functionalized kaolinite, *Electroanalysis*, 23, 1, 245 – 252.
- Wanekaya**, A.K., 2011, Applications of nanoscale carbon-based materials in heavy metal sensing and detection, *Analyst*, 136, 4383–4391.
- Wang**, Y., Wu, Y., Xie, J., Hu, X., 2013, Metal–organic framework modified carbon paste electrode for lead sensor, *Sensors and Actuators B*, 177, 1161– 1166.
- Xiong**, J., Cui, L., Liu, W., Beves, J.E., Li, Y., Zuo, J., 2013, Large and selective electrochemical response to fluoride by a tetrathiafulvalene-based sensor, *Tetrahedron Letters*, 54, 1998–2000.
- Yang**, W., Yin, Z., Wang, C., Huang, C., He, J., Zhu, X., Cheng, J., 2008, New redox anion receptors based on calix[4]pyrrole bearing ferrocene amide, *Tetrahedron*, 64, 9244–9252.
- Yuan**, X., Wang, R., Mao, C., Wu, L., Chu, C., Yao, R., Gao, Z., Wu, B., Zhang, H., 2012, New Pb(II)-selective membrane electrode based on a new Schiff base complex, *Inorganic Chemistry Communications*, 15, 29–32.
- Zhang**, S., Palkar, A., Echegoyen, L., 2006, Selective anion sensing based on tetra-amide calix[6]arene derivatives in solution and immobilized on gold surfaces via self-assembled monolayers, *Langmuir*, 22, 10732–10738.
- Zhang**, J., A.R., Harris, R.W., Cattrall, A.M., Bond, 2010, Voltammetric ion-selective electrodes for the selective determination of cations and anions, *Analytical Chemistry*, 82, 1624–1633.

Zanganeh, A.R., M.K., Amini, 2007, A potentiometric and voltammetric sensor based on polypyrrole film with electrochemically induced recognition sites for detection of silver ion, *Electrochimica Acta*, 52, 3822–3830.

Zanganeh, A.R., Amini, M.K., 2008, Polypyrrole-modified electrodes with induced recognition sites for potentiometric and voltammetric detection of copper(II) ion, *Sensors and Actuators B*, 135, 358–365.

3.1 Introduction

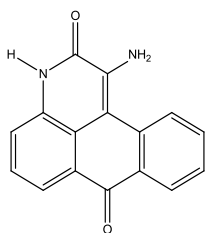
This chapter reports the materials and methods used to know about the nature of the molecules with voltammetry and theoretical study, their ability to sense cations and anions voltammetrically, modification of electrode and their application. Cyclic voltammetry, differential pulse voltammetry, chronopotentiometry, chronoamperometry, scanning electron microscopy were the techniques used throughout to carry out the experiments and characterization studies. Experimental details of the methods and techniques are mentioned in this chapter in detail.

3.2 Chemicals

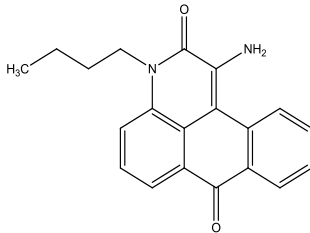
Perchlorate salts of mercury, lead, zinc, copper, nickel, cobalt and tetrabutyl ammonium salts of cyanide, acetate, hydrogen sulphate, fluoride, chloride, bromide, iodide perchlorate were obtained from Sigma Aldrich and used as received. HPLC grade solvents like acetonitrile, dimethyl sulphoxide (DMSO), tetrahydrofuran(THF), dichloromethane(DCM), N,N' dimethylformamide(DMF) were obtained from Merck and used as received. Potassium chloride and silver nitrate of analytical reagent (AR) grade were obtained from Loba Chemie, India. HEPES buffer of AR grade from Loba chemie, India, was used to maintain pH. Stock solutions of compounds and salts were prepared in above mentioned solvents as per requirements. All the glassware were cleaned with HNO₃ and rinsed thoroughly with distilled water before use. Inert environment in the test solution used for voltammetric studies was created by purging the solution with nitrogen gas of 99.9% purity.

3.3 Molecules studied

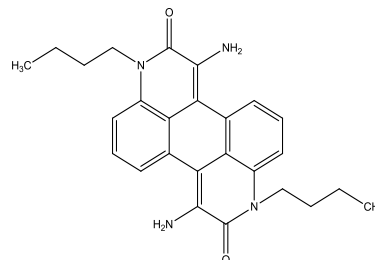
Anthrone and imidazole based derivatives were used for the voltammetric studies. These molecules were obtained from our collaborator Dr. Subodh's lab, Guru Nanak Dev University, Amritsar. Molecules used for the study are as follows.



1-amino-2H-naphtho[1,2,3-de]quinoline-2,7(3H)-dione



1-amino-3-butyl-2H-naphtho[1,2,3-de]quinoline-2,7(3H)-dione

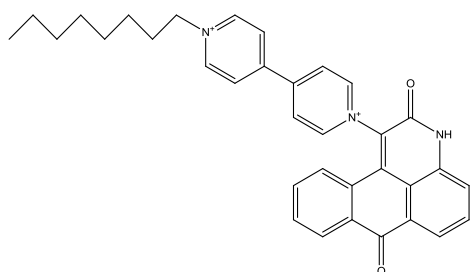


1,7-diamino-3,9-dibutylbenzo[1,2,3-de:4,5,6-d'e']diquinoline-2,8(3H,9H)-dione

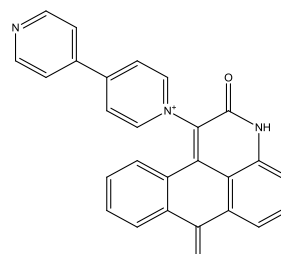
Anthrone 1

Anthrone 2

Anthrone 3



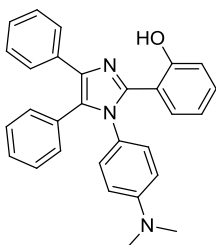
1-(2,7-dioxo-3,7-dihydro-2H-naphtho[1,2,3-de]quinolin-1-yl)-1'-octyl-[4,4'-bipyridine]-1,1'-diium



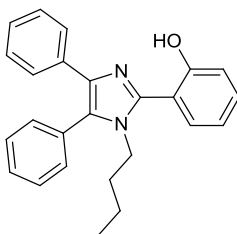
1-(2,7-dioxo-3,7-dihydro-2H-naphtho[1,2,3-de]quinolin-1-yl)-[4,4'-bipyridin]-1-ium

BPODS

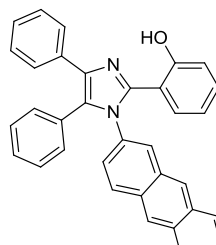
BPMS



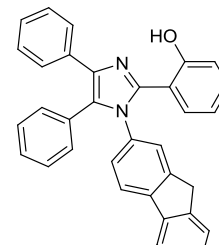
2-(1-(4-(dimethylamino)phenyl)-4,5-diphenyl-1H-imidazol-2-yl)phenol



2-(1-butyl-4,5-diphenyl-1H-imidazol-2-yl)phenol



2-(1-(anthracen-2-yl)-4,5-diphenyl-1H-imidazol-2-yl)phenol



2-(1-(9H-fluoren-2-yl)-4,5-diphenyl-1H-imidazol-2-yl)phenol

TPIAM

TPIM

TPAN

TPF

3.4 Instrumentation

All voltammetric studies were recorded with a three-electrode system immersed in a solution of the analyte species and the supporting electrolyte on an Autolab Potentiostat/Galvanostat model PGSTAT12 (ECO Chemie, The Netherlands). Glassy carbon (GC) electrode (CH Instruments, USA, 3mm diameter) was used as working

electrode and platinum wire was used as a counter electrode. For non-aqueous medium all the potentials were taken against Ag/Ag^+ reference electrode. The Ag/Ag^+ electrode contained an internal solution of 0.01M AgNO_3 and 0.1M TBAP in solvents like acetonitrile (ACN), dimethyl formamide (DMF) and dichloromethane (DCM). For aqueous system all the potentials were recorded against Ag/AgCl reference electrode containing 1 M KCl solution. The working GC electrode was polished with alumina followed by washing with water and solvent before each experiment. The electrochemical measurements were carried out at a temperature of $25.0 \pm 0.1^\circ\text{C}$. In all experiments, the test solutions were deaerated by a stream of N_2 gas purging through the solution for at least 4-5 minutes.

3.5 Techniques used

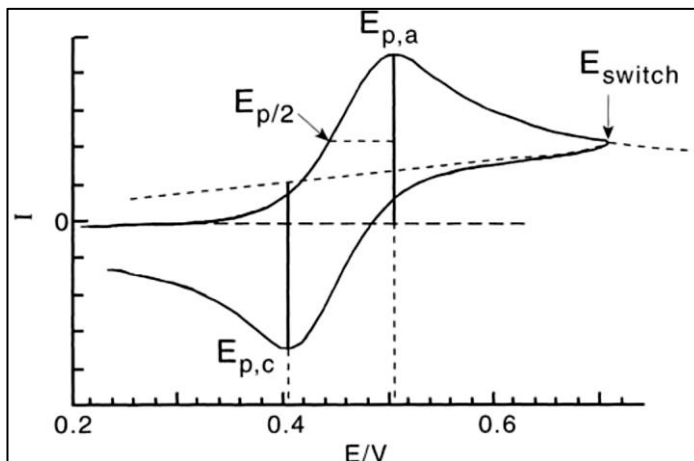
3.5.1 Voltammetry

Voltammetry comprises of group of electroanalytical methods in which information about analyte is obtained from the measurement of current as a function of applied potential. Some of the basic applications include studies of oxidation – reduction process, adsorption process on surface, electron transfer mechanisms at chemically modified electrode surfaces. Voltammetry is divided into four categories: linear sweep voltammetry (LSW), differential pulse voltammetry (DPV), square wave voltammetry (SWV) and cyclic voltammetry (CV). Since CV and DPV were the techniques used for study, they are discussed in detail.

3.5.2 Cyclic voltammetry

Cyclic voltammetry is an important technique to study electrochemical behaviour of system under various conditions. In typical cyclic voltammetry, a solution component is electrolyzed (oxidized or reduced) by placing the solution in contact with an electrode surface, and then making that surface sufficiently positive or negative in voltage to force electron transfer. The potential first varies linearly in one direction, whereupon the direction is reversed to return to the original potential value. The rate at which the potential is swept between the potential range is called scan rate i.e., V/s or mV/s. Important parameters of CV are cathodic peak potential anodic (E_{pc}), peak potential (E_{pa}), cathodic

peak current (I_{pc}) and anodic peak current (I_{pa}). For a reversible electrochemical reaction the CV recorded has certain well defined characteristics (Wang (2004), Bard (2000), Scholz, (2010)).



I) The voltage separation between the current peaks is

$$\Delta E = E_p^a - E_p^c = (59/n) \text{ mV} \quad (1)$$

II) The positions of peak voltage do not alter as a function of voltage scan rate

III) The ratio of the peak currents is equal to one

$$\left| \frac{i_p^a}{i_p^c} \right| = 1 \quad (2)$$

IV) The peak currents are proportional to the square root of the scan rate

The expression of the peak current (A) for the forward sweep in a reversible system at 298 K is given by the Randles–Sevcik equation:

$$i_p = (2.69 \times 10^5) ACD^{1/2}n^{3/2}v^{1/2} \quad (3)$$

where n is the number of electron equivalent exchanged during the redox process, A (cm^2) the active area of the working electrode, D ($\text{cm}^2 \text{ s}^{-1}$) and C (mol cm^{-3}) the diffusion coefficient and the bulk concentration of the electroactive species; v is the voltage scan rate (V s^{-1}).

For irreversible processes (slow electron exchange), the peaks are reduced in size and widely separated. The Randles–Ševcik expression for the irreversible electrochemical

response is different to the reversible case by a factor of $0.496(\alpha)$ taking account of the change in wave shape.

$$i_p = (2.99 \times 10^5)n(\alpha n')^{1/2}ACD^{1/2}\nu^{1/2} \quad (5)$$

In this expression, n' denotes the number of electrons transferred in the rate determining reaction step, whereas n denotes the overall numbers of transferred electrons per molecule diffusing to the electrode surface, A (cm^2) the active area of the working electrode, D ($\text{cm}^2 \text{s}^{-1}$) and C (molcm^{-3}) the diffusion coefficient and the bulk concentration of the electroactive species; ν is the voltage scan rate (V s^{-1}).

Totally irreversible systems are characterized by a shift of the peak potential with the scan rate.

$$E_p = E^\circ - \frac{RT}{\alpha nF} \left[0.78 - \ln \left(\frac{k^\circ}{D^{1/2}} \right) + \ln \left(\frac{\alpha nF}{RT} \right)^{1/2} \right] \quad (4)$$

Where α is the transfer coefficient and n is the number of electrons involved in the charge-transfer step. Thus, E_p occurs at potentials higher than E° , with the overpotential related to k° and α . Independent of the value k° , such peak displacement can be compensated by an appropriate change of the scan rate. The peak potential and the half-peak potential (at 25°C) will differ by $48/\alpha n$ mV. Hence, the voltammogram becomes more drawn-out as αn decreases. The peak current, given by:

The transfer coefficient can be determined from the electrochemical peak characteristics (peak width, $E_p - E_{p/2}$), or from the slope of the E_p vs $\log(\nu)$ plot.

$$\alpha = -\frac{RT}{2F} \left(\frac{\partial E_p}{\partial \log(\nu)} \right)^{-1} = -29.6 \left(\frac{\partial E_p}{\partial \log(\nu)} \right)^{-1} \quad (6)$$

$$\alpha = \frac{RT}{F} \left(\frac{1.85}{E_{p/2} - E_p} \right) = 47.7 \frac{1}{E_{p/2} - E_p} \quad (7)$$

E_p is the peak potential and $E_{p/2}$ is the half peak potential

3.5.3 Differential pulse voltammetry

The importance of DPV in chemical analysis is based on its superior elimination of the capacitive/background current. This is achieved by sampling the current twice: once before pulse application and then at the end of the pulse. The output from the potentiostat/voltammograph is equal to the difference in the two current values. Current sampling allows the analyst to detect the analytes present in the solution at a concentration as low as 0.05 μM . Another consequence of double sampling is that the differential pulse voltammograms are peak-shaped. The width of the peak (at half height) is related to the electron stoichiometry. (Scholz, 2010)

$$W_{1/2} = \frac{3.52RT}{nF} \quad (9)$$

Where, R is gas constant, T (K) is temperature, n is no of electrons transferred and F is faraday's constant.

3.5.4 Chronopotentiometry

In this technique the current flowing in the cell is instantaneously stepped from zero to some finite value i.e., potential is measured as a function of time at constant applied current. The solution is not stirred and a large excess of supporting electrolyte is present in the solution; diffusion is the only mass transfer process to be considered.

3.5.5 Chronoamperometry

Chronoamperometry involves stepping the potential of the working electrode from a value at which no current flows, i.e., the oxidation or reduction of the electrochemically active species does not take place, to E_2 where the current belongs to the electrode reaction and is limited by diffusion in an unstirred solution with stationary working electrodes. The resulting current-time dependence is monitored. The current flow at any time after application of the potential step will obey the Cottrell equation (Equation 10) i.e., the current will decay with time

$$i(t) = \frac{nFACD^{\frac{1}{2}}}{\pi^{\frac{1}{2}}t^{\frac{1}{2}}} = kt^{-1/2} \quad (10)$$

$i(t)$ is current at any time t (in seconds), A is area of electrode in cm^2 , D , the diffusion coefficient in $\text{m}^2 \text{s}^{-1}$, k is rate constant, n is the number of electrons transferred per molecule diffusing to the electrode, $F = 96485 \text{Cmol}^{-1}$ the Faraday constant, and v the scan rate in V s^{-1}

3.6 Limit of detection determination

The limit of detection (LOD) was found on the basis of standard deviation of the response and the slope using 3sigma method.

The detection limit (DL) may be expressed as:

$$DL = \frac{3.3\sigma}{S} \quad (11)$$

Where σ = the standard deviation of the response, S = the slope of the calibration curve

The slope S may be estimated from the calibration curve of the analyte. The estimate may be carried out in a variety of ways, for example:

a) Based on the standard deviation of the blank

Measurement of the magnitude of analytical background response is performed by analysing an appropriate number of blank samples and calculating the standard deviation of these responses.

b) Based on the calibration curve

A specific calibration curve should be studied using samples containing an analyte in the range of DL. The residual standard deviation of a regression line or the standard deviation of y-intercepts of regression lines may be used as the standard deviation.

3.7 Scanning electron microscopy (SEM)

Scanning electron microscopy was used to obtain information about the external morphology of the modified electrodes. The SEM images depend on the electron interactions at the surface rather than on transmissions so it can produce images that are good representation of 3D structure of the sample. Scanning electron microscopy was

conducted by using SEM JEOL JSM-6610LV Scanning Electron Microscope (SEM). Samples were placed on a specimen stub which were lined with double side adhesive, conducting tape and was then coated with a thin layer of gold in order to reduce sample charging. SEM analysis was done from Sophisticated Analysis Instrumentation Laboratory, Thapar University, Patiala, India and Indian Institute of Technology, Ropar, India.

3.8 Atomic absorption spectroscopy

Atomic absorption spectroscopy (AAS) is a spectroanalytical method used for the quantitative determination of chemical elements like metals employing the absorption of optical radiation (light) by free atoms in the gaseous state. Atomic absorption is so sensitive that it can measure down to parts per billion of a gram ($\mu\text{g dm}^{-3}$) in a sample. AAS analysis of the real samples was done from Sophisticated Analysis Instrumentation Laboratory, Thapar University, Patiala, India.

3.9 Theoretical study

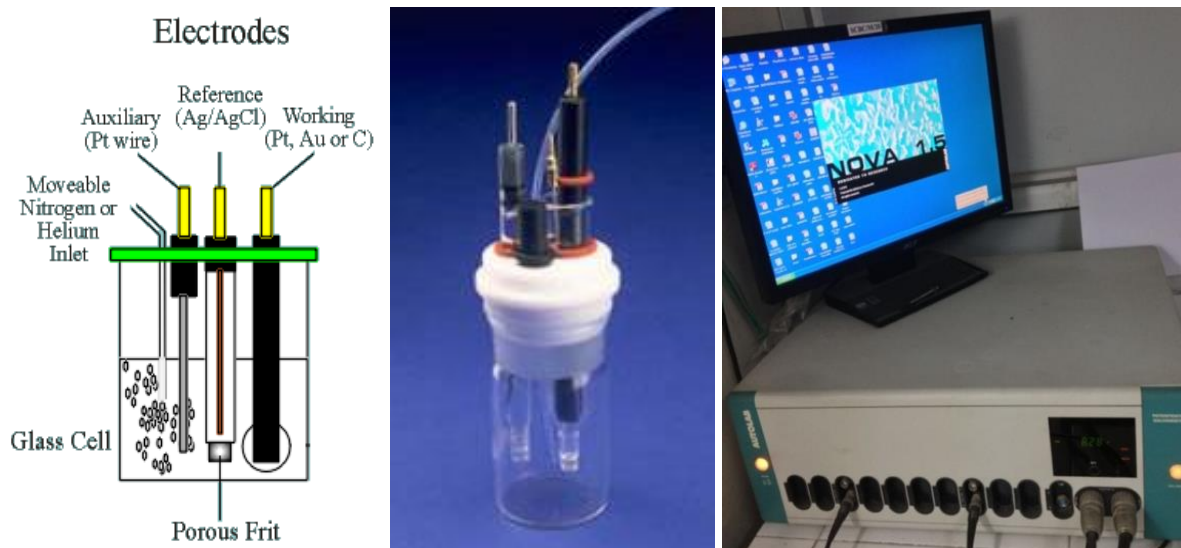
Theoretical studies of anthrone derivatives were done using DFT (density functional theory) (Riahi et al (2008), Sharma et al (2013), Mohammad-Shiri et al (2011)) calculations using B3LYP/6-311+G** level of theory with the GAUSSIAN 03 package of programs implemented on computer with an intel (R) 2.4 GHz processor. Optimization of structures in acetonitrile solvent was done using self-consistent reaction field (SCRF) methods with the conductor-like polarizable continuum model (CPCM). HOMO–LUMO orbitals of the optimized structure were located to find the electron density in molecules. Mechanisms of the electrochemical behaviour of molecules are proposed and cross verified with these theoretical studies.

3.10 Experimental Procedures

3.10.1 CV conditions for voltammetric study of molecules

Stock solutions of the anthrone derivatives of concentration 5×10^{-3} M were prepared in DMSO as per their solubility. Potential cycling window for anthrone1, anthrone2 and anthrone3 was found to be 0 to 1.1V. For BPMS it was -1.0 to 1.0V while for BPODS it was found to be 0 to -0.8V. Stock solutions of imidazole based derivatives were made in THF of concentration 5×10^{-3} M. For these derivatives the potential cycling window was in

the range 0 to 1.2V. Solutions of particular concentration of these molecules were made from stock solutions, in different solvents to carry out further studies. CV studies were done at different scan rates ranging from 20mV s^{-1} to 1000mV s^{-1} to study the nature of the molecules.



3.10.2 DPV conditions for voltammetric study

Differential pulse voltammetry was done at pulse amplitude of 50 mV and scan rate 20mVs^{-1} . For anodic stripping of metal ions conditioning potential was 1.2V, conditioning time 60 -120s, deposition potential -0.6V, deposition time 300s and equilibration time 10s.

3.10.3 Cation and anion detection

For cation interaction studies, perchlorate salts of different metal (Co, Ni, Cu, Zn, Hg and Pb) were used by preparing stock solution of concentration 10^{-2} M in acetonitrile and in water separately. Similarly stock solutions were prepared for tetrabutylammonium salts of anions like CN^- , CH_3COO^- , F^- , Cl^- , Br^- , I^- and HSO_4^- ions in acetonitrile and in water separately.

3.10.4 Interference studies

Studies for interference were carried out by adding 10 times the concentration i.e. 1×10^{-3} M of metal ions like Cu^{2+} , Ni^{2+} , Zn^{2+} , Co^{2+} and Pb^{2+} to that of primary ions (10^{-4} M) and the same procedure was followed for anions.

3.10.5 Real life sampling

Real life sampling for mercury was done by collecting soil samples from condensed fluorescent lamps (CFL) tubes dump yard and other surrounding areas in Thapar University. Two samples were collected from each site and one from a nearby park as a reference in order to confirm the leaching of mercury from CFL tubes to the soil. 2g each of the soil samples were air dried and finely powdered for metal extraction, done by acid digestion using nitric acid and perchloric acid. The final extract obtained was made upto 100 mL and analysed using atomic absorption spectroscopy (AAS) and differential pulse voltammetry (DPV).

3.11 Electrode preparation

3.11.1 Screen printed electrode

Screen printed carbon electrodes were got fabricated from the MMU laboratory UK on request. It was done with appropriate stencil designs using a microdek 1760RS screen printing machine (DEK, UK). The multistage printing process involved the sequential deposition of carbongraphite, silver–silver chloride and dielectric inks (obtained from Gwent, Pontypool, UK) onto a polyester substrate material. Further modification of the working surface was carried out by mixing together anthrone³ within the carbon-graphite ink and placed into a fan oven for 15 min at 40 °C to dry. A three electrode connector was used to efficiently connect the SPE with the potentiostat. When the screen printed electrodes were used with the screen printed silver–silver chloride reference electrode to conduct measurements, 40 μ L of the desired buffer solution was applied on to the electrode surface with the aid of a micropipette.

3.11.2 Polyaniline modified electrode

The polymer film was electrochemically deposited on glassy carbon electrode from a non-aqueous solution (acetonitrile) containing aniline (0.5M), 0.1 M tetrabutylammonium

perchlorate (Bu_4NClO_4) and 0.1 M trifluoroacetic acid. The electropolymerization was performed galvanostatically on an Autolab Potentiostat/Galvanostat model PGSTAT12 (ECO Chemie, Netherlands) at 1 mAcm^{-2} . The film was then washed in monomer free ACN solution containing only TBAP and trifluoroacetic acid in order to remove soluble species from the film by cycling between potential -0.2 to 0.9V for 10 scans. After drying the electrode at room temperature, 40 μL of the ionophore solution (in THF) was drop coated onto the electrode and left for drying for 2 hours.

3.12 References

Bard, A.J., Faulkner L.R., *Electrochemical Methods: Fundamentals and Applications*, A John Wiley & Sons INC., Publications, 2nd edition (2000).

Mohammad-Shiri, H., Ghaemi, M., Riahi, S., Akbari-Sehat, A., 2011, Computational and electrochemical studies on the redox reaction of dopamine in aqueous solution, *International Journal of Electrochemical Science*, 6, 317 – 336.

Scholz, F., *Electroanalytical Methods: Guide to Experiments and Applications*, Springer, 2nd revised edition, (2010).

Sharma, D., Bera, R.K., Sahoo S.K., 2013, Naphthalene based colorimetric sensor for bioactive anions: Experimental and DFT study, *Spectrochimica Acta Part A: Molecular and Biomolecular Spectroscopy*, 105, 477–482.

Riahi, S., Ganjali, M.R., Moghaddam, A.B., Norouzi, P., 2008, Molecular geometry, vibrations and electrode potentials of 2-(4,5-dihydroxy-2-methylphenyl)-2-phenyl-2H-indene-1,3-dione; experimental and theoretical attempts, *Journal of Molecular Modelling*, 14, 325–333.

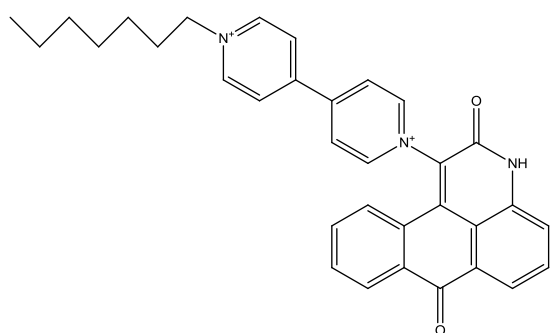
Wang, J., *Analytical electrochemistry*, A John Wiley & Sons INC., Publications, 2nd edition (2004).

Biological and environmental importance of anions is very well known. But some of these like cyanide and fluoride can be hazardous. So, their selective determination and sensing holds great importance (Bianchi et al, 1997, Sessler et al, 2006, Isaada et al, 2011, Kim et al, 2012). Anion sensing poses a greater difficulty as compared to cations, because of their bigger size and ionic strength. Various methods of selective determination of anions have been reported in literature, but their electrochemical recognition by artificial molecular hosts has got greater attention in recent times (Beer et al, 2001, Lindsay et al, 2006, Gale et al 2006, Gale et al, 2008, Caltagirone et al, 2009). Various anions like cyanide, fluoride, acetate etc. have been used in large quantities in various industries like electroplating, metallurgy, organic chemicals production, plastic, etc. and other applications like fumigation and mining (Zang et al, 2012). Cyanide has high lethal characteristics while fluoride causes diseases like dental fluorosis (yellowing of teeth), skeletal fluorosis, renal osteodystrophy (Kirk et al, 1991, Cametti et al, 2009) etc. Acetate, although being used as a critical component of numerous metabolic processes, production and oxidation rates of the acetate anion have been frequently used as an indicator of organic decomposition in marine sediments. It is yet very harmful as it causes a great effect on plant growth. Hence, their selective determination becomes quite critical. Various methods for detection of anions like fluorimetry, chemiluminescence, colorimetry, voltammetry and spectrophotometry are reported in literature (Ma et al, 2010). But reports on the voltammetric study of cyanide using ionophores/ artificial receptors are very rare.

Ferrocene (Kong et al, 2013), tetrathiafulvalene (Jia et al, 2012, Xiong et al, 2013), urea, thiourea (Lorenzo et al, 2009) etc based receptors show efficient anion binding capabilities and transducing these processes electrochemically. Viologens (1,1'-disubstituted-4,4'-bipyridinium derivatives) (Reynes et al, 2004) are one of the potential molecules which can be used in contemporary field of voltammetric determination of anions. Viologens mainly exist in three oxidation states:

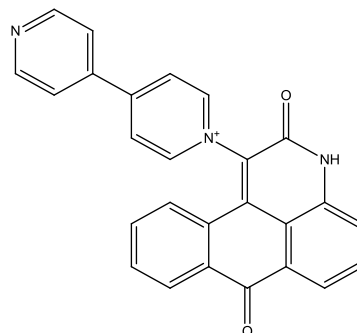


Out of these, the $V^{2+} \leftrightarrow V^{+}$ system is highly reversible (Bird et al, 1981, Qian et al, 2000). Electrochemical study of different types of molecules containing viologen has been reported for dopamine (Hsu et al, 2009), glucose (Sharrett et al, 2008) and nitrite (Silva et al, 2004) sensing. Viologens have wide applications in nanoscience and nanotechnology (Torimoto et al, 2003) because of their ability to form charge transfer complexes. These positively charged molecules have not been exploited for the electrochemical sensing of anions. On the other hand, voltammetric studies of anthrone or its viologen derivatives have not been reported so far for cation or anion detection. Anthrone derivatives have only been used as reagents for the determination of carbohydrates in the presence of serum protein, reactive diene to carry out diel alder reaction (Shen et al, 2006, Shi et al, 2007) and catalysts in reactions using oxygen as an oxidant (Shen et al, 2008). There are no reports on any kind of electrochemical study of anthrones.



1-(2,7-dioxo-3,7-dihydro-2*H*-naphtho[1,2,3-*de*]quinolin-1-yl)-1'-heptyl-4,4'-bipyridine-1,1'-dium

1 (BPODS)



1-(2,7-dioxo-3,7-dihydro-2*H*-naphtho[1,2,3-*de*]quinolin-1-yl)-[4,4'-bipyridin]-1-ium

2 (BPMS)

4.1 Results and Discussion

Cyclic voltammograms of the two new molecules **1** and **2** designed* especially to sense anionic species were recorded in acetonitrile over an applied potential range of -1.0 to 1.0V. Very interesting behavior was noticed for **1** (containing dicationic viologen motif) which showed a near ideal reversible curve with sharp peaks in anodic (-0.501V) and cathodic (-0.569V) regions (Fig. 4.1a). The value of ΔE , i.e., difference in the peak potentials of anodic and cathodic waves was 68.0 mV, which indicated a single electron exchange at the electrode. The anodic peak is due to oxidation of the -NH- group adjacent

to the carbonyl group. An electron from this nitrogen atom would be lost in preference to oxygen of either of the carbonyl groups, due to greater basic character of nitrogen.

The observed magnitude of cathodic current ($0.43\mu\text{A}$) is almost twice that of the anodic current ($0.22\mu\text{A}$) which is indicative of two reducible quaternary ammonium sites on viologen motif in the molecule, requiring exactly the same potential for the reduction and having equal opportunities to get reduced. Hence, cathodic current resulting from one e^- exchange at each N atom of dicationic viologen group is twice the magnitude to that of current resulting from $1e^-$ exchange at N atom of the anthrone derivative.

In **2**, there seems to be two independent electron exchange processes taking place in the same molecule, one in the anodic region (0.858V) and the other in the cathodic region (-0.857V). Both of these electron exchange processes are irreversible, as difference in peak potential of cathodic peak of the first redox couple and anodic peak of the second redox couple do not appear at all (Fig. 4.1b).

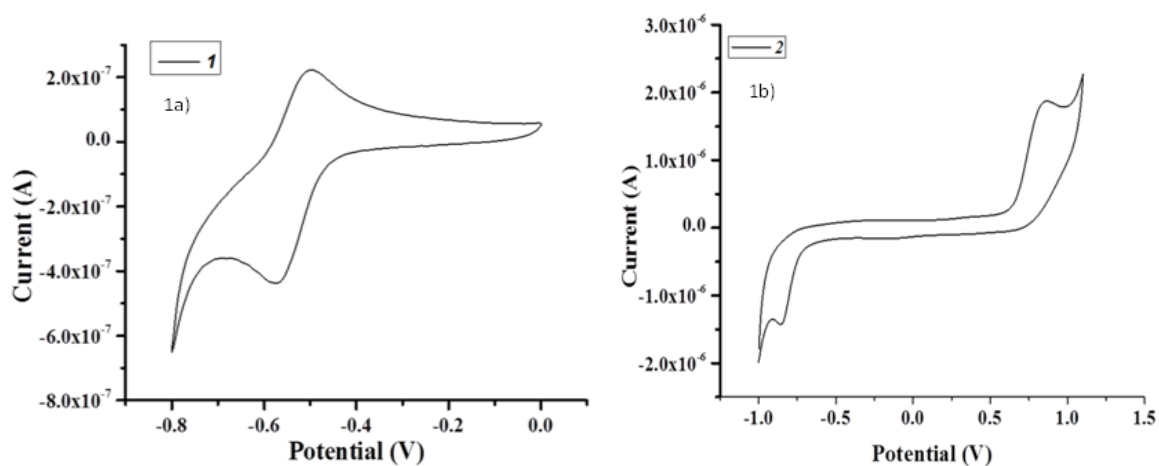
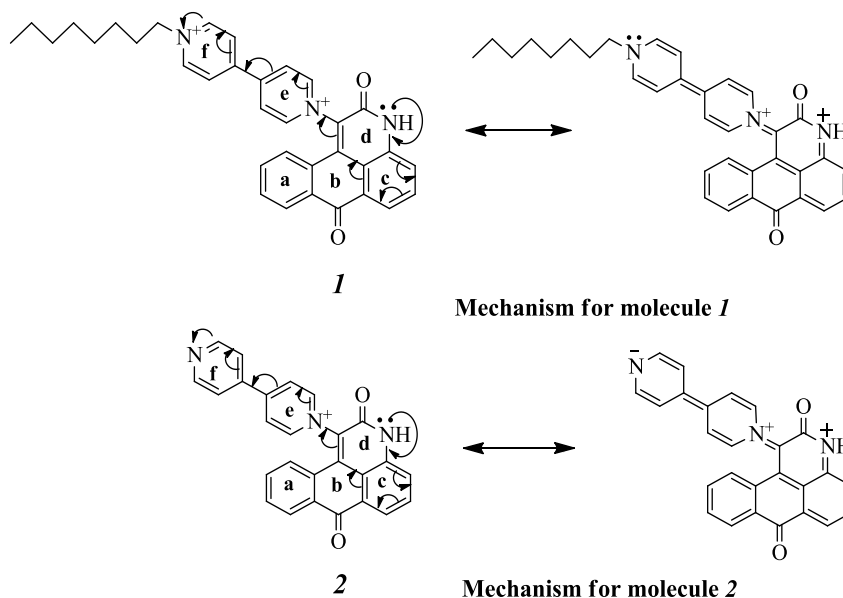


Fig. 4.1 Cyclic voltammograms of **1** and **2** in acetonitrile (ACN) medium using 0.1M TBAP supporting electrolyte (GC working electrode, scan rate 20 mVs^{-1} E vs Ag/Ag^+)

This hypothesis (the absence of peaks) can be supported with an argument that the difference in peak potentials of the two curves is about 1.0 V, which for a single electron exchange process is expected to be 59 mV. Further, the anodic peaks (-0.501 V for **1** and 0.858 V for **2**) can be assigned to the release of electrons from the lone pair on N atom of anthrone motif to quaternary nitrogen atom of the bipyridyl substituent.

4.2 Mechanism

The presence of anthrone moiety enhances stability of the viologen group by acting as a nucleophile. The lone pair on nitrogen of amine group acts as an electron rich center and through conjugation, the movement of electrons stabilizes positive charge on N of viologen (Scheme 1). Hence, anodic peaks at -0.501 V and 0.858 V are corresponding to the said electron release from the lone pairs on **1** and **2**, respectively. A lone pair on -NH- group of molecule **2** disperses charge on viologen motif through conjugation resulting in negative charge on nitrogen of the terminal pyridine ring and a positive charge on the amine nitrogen. This electronic movement results in dispersal of charge over larger part of the molecule and hence is stabilized, which is very well supported by a cathodic and an anodic peak corresponding to two separate redox processes. Separate mechanisms of e⁻ transfers in molecules **1** and **2** are shown in Scheme 1.



Scheme 4.1 Resonance stabilisation of viologen substituted anthrone molecules **1** and **2** through conjugation of lone pairs on -NH- group with bipyridyl substituent

4.3 Theoretical study

Both molecules **1** and **2** were optimized using density functional theory calculations at B3LYP/6-311++G** basis set in conjunction with conductor-like polarizable continuum model (CPCM) selecting acetonitrile as a solvent (Fig. 4.2-1 and 4.2-2). Highly occupied

molecular orbitals (HOMO) and lowest unoccupied molecular orbitals (LUMO) were located for each molecule. In both the structures, HOMO is localized over rings **c** and **d** (Fig. 4.3), i.e., containing nitrogen and carbonyl groups adjacent to each other. Domain of LUMO of structure **1** is stretching over the anthrone moiety but confined only to ring **e** of viologen motif while LUMO+1 is localized over the rings **e** and **f** (viologen motif) with no extension over the anthrone motif. All this can be probably due to +I effect of the alkyl chain attached to the ring **f** of structure **1** restricting the spread of LUMO domain until ring **e** only. This supports not only the proposed mechanism for molecule **1** (scheme 1), showing dispersal of positive charge over rings **d** and **e** but also the experimental observations where only one redox couple with double the current in cathodic region is obtained as the lobes of LUMO spread over rings **a** to **d**, as expected.

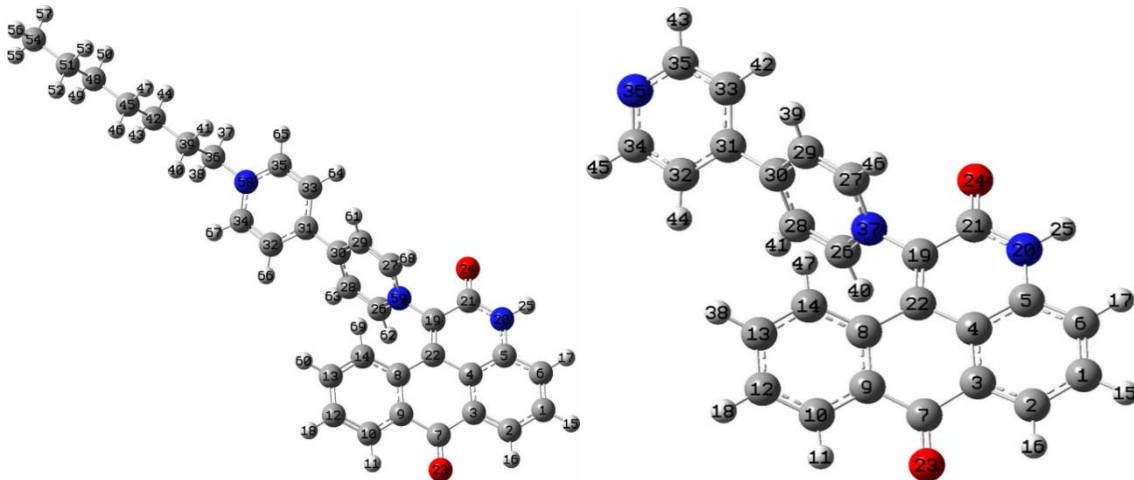


Fig. 4.2 Optimized geometries of **1** (2-1) and **2** (2-2) at B3LYP/6-311++G** level in acetonitrile with serial number of atoms using Gaussian 03W software

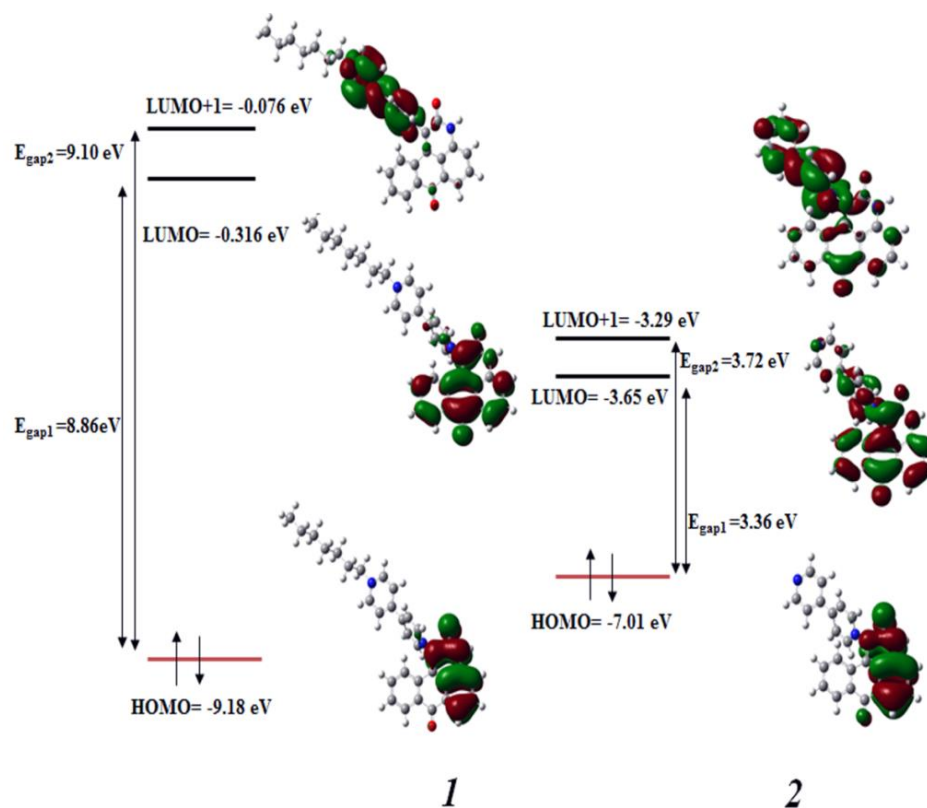


Fig. 4.3 Electronic density distribution in HOMO, LUMO and LUMO+1 states of **1** and **2** computed by the B3LYP/6-311++G** (ACN as solvent) method using Gaussian 03W software

For structure **2**, LUMO domain is dispersed over to anthrone moiety and both rings **e** and **f** (viologen motif). This supports the proposed mechanism 2 (scheme 1), that dispersal of charge extends from viologen rings **e** and **f** to anthrone ring **d** as well. There is a strong polarization of charges in structure **2**, which is also evidenced from theoretical study showing LUMO domain concentrating more towards rings **a** to **d** and weakening over rings **e** and **f** which is further supported by practical observations (Fig. 4.3) that only one anodic peak and one cathodic peak were observed as these are two clear redox processes taking place on the electrode surface. Due to their irreversible nature, either only anodic or only cathodic peak is observed. LUMO+1 structure, the domain of which is complementary to that of LUMO (oriented at right angle to each other), as anticipated theoretically. In structure **2**, a major part of LUMO+1 is localized over (viologen rings) **e** and **f** and also extended weakly extending over the anthrone moiety. The discussion above clearly

indicates that the mechanism as proposed in scheme 1 is strongly supported by DFT calculations on molecules **1** and **2**.

Calculated energies of HOMO and LUMO for molecules **1** and **2** (Table 4.1) shows an energy gap of 8.87eV and 3.36eV between the two levels and energy differences of 9.10 eV and 3.72 eV between each set of HOMO and LUMO+1 system, respectively. Although it is very difficult to explain the presence of one redox couple for molecule **1** and peaks of molecule **2** (one each in anodic and cathodic regions separately) on the basis of HOMO and LUMO+1 structures, yet the energy gap indicates more stability (Tanak *et al*, 2010) for molecule **1** and less for molecule **2**.

Table 4.1 Energies of HOMO and LUMO for molecules **1** and **2** measured using Gaussian software

Molecule	Energy in eV				
	E_{HOMO}	E_{LUMO}	$E_{\text{LUMO}+1}$	E_{gap1}	E_{gap2}
1	-9.1948	-0.3221	-0.0933	8.8727	9.1015
2	-7.0157	-3.655	-3.2947	3.3607	3.721

$E_{\text{gap1}} = E_{\text{LUMO}} - E_{\text{HOMO}}$, $E_{\text{gap2}} = E_{\text{LUMO}+1} - E_{\text{HOMO}}$

4.4 Effect of scan rate

In order to understand nature of the electrode processes taking place for **1** and **2**, peak currents of anodic waves were plotted against scan rate (Fig. 4.4a and 4.4b). A linear relation between peak current and square root of the scan rate shows that Fick's law of diffusion is obeyed and the charge transport is diffusion based process.

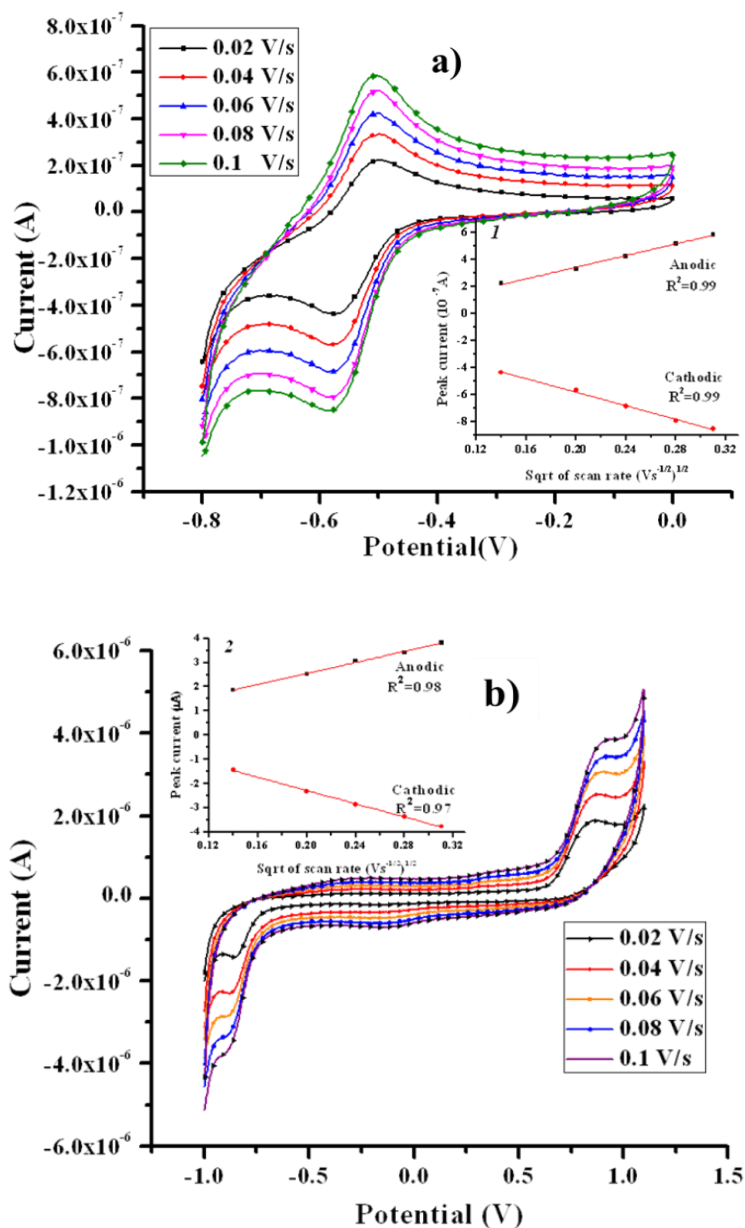


Fig. 4.4 Cyclic voltammograms of **1** and **2** in acetonitrile (ACN) at different scan rates 20, 40, 60, 80, 100 mVs^{-1} using 0.1M TBAP as supporting electrolyte and GC as Working electrode

4.5 Solvent effect

Voltammetric behavior of the anthrone derivatives was studied in different organic solvents like N, N-dimethylformamide (DMF, $\epsilon = 38.3$), acetonitrile (ACN, $\epsilon = 37.5$) and dichloromethane (DCM, $\epsilon = 9.1$). The results shown in Fig. 4.5 indicated that polarity of

the solvent had a great effect on the voltammograms. An increase in polarity of the solvent (from ACN to DMF) leads to the change in peak potentials of **1** and **2**. An interesting observation about the effect of solvent is that when a solvent with relatively more polar environment (DMF) is taken, the redox couple of **1** (-0.496 V and -0.573 V) shifts towards lesser potentials (-0.644 V and -0.726 V) indicating facilitation of oxidation for this molecule (Figure 4.5a). In case of **2** (Figure 4.5b), along with a cathodic shift in oxidation peak, quenching of the peak can also be observed on changing the solvent from ACN/DCM to DMF.

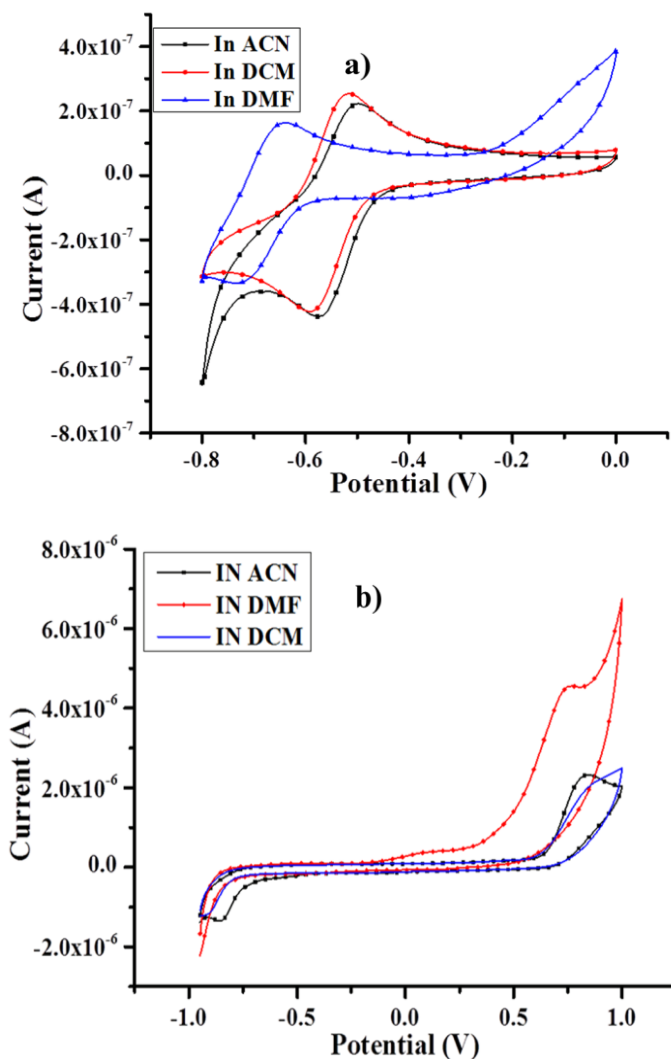


Fig. 4.5 Cyclic voltammograms of 10^{-4} M solution of a) **1** and b) **2** in different solvents using 0.1 M TBAP as supporting electrolyte (GC working electrode, scan rate 20 mVs^{-1} E vs Ag/Ag^+)

4.6 Anion selectivity

4.6.1 Colorimetric study

Anion sensing abilities of the receptors **1** and **2** have also been studied on a qualitative basis by visual examination of the anion-induced color changes in acetonitrile solution (10^{-5} M) with and without addition of the anions as their tetrabutyl ammonium salts. Fig. 4.6 shows prominent color changes of the compounds as a result of adding 2 equivalents of various anions such as CN^- , CH_3COO^- , F^- , Cl^- , Br^- , I^- and HSO_4^- . It can be seen that both the compounds are only sensitive to CN^- , CH_3COO^- and F^- . Such a distinguishable and prominent anion-specific response makes the two compounds effective colorimetric anion sensors.

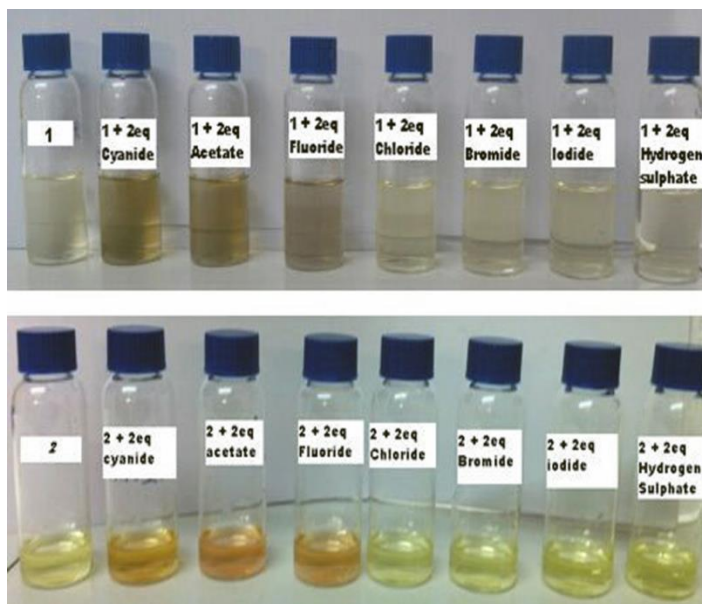
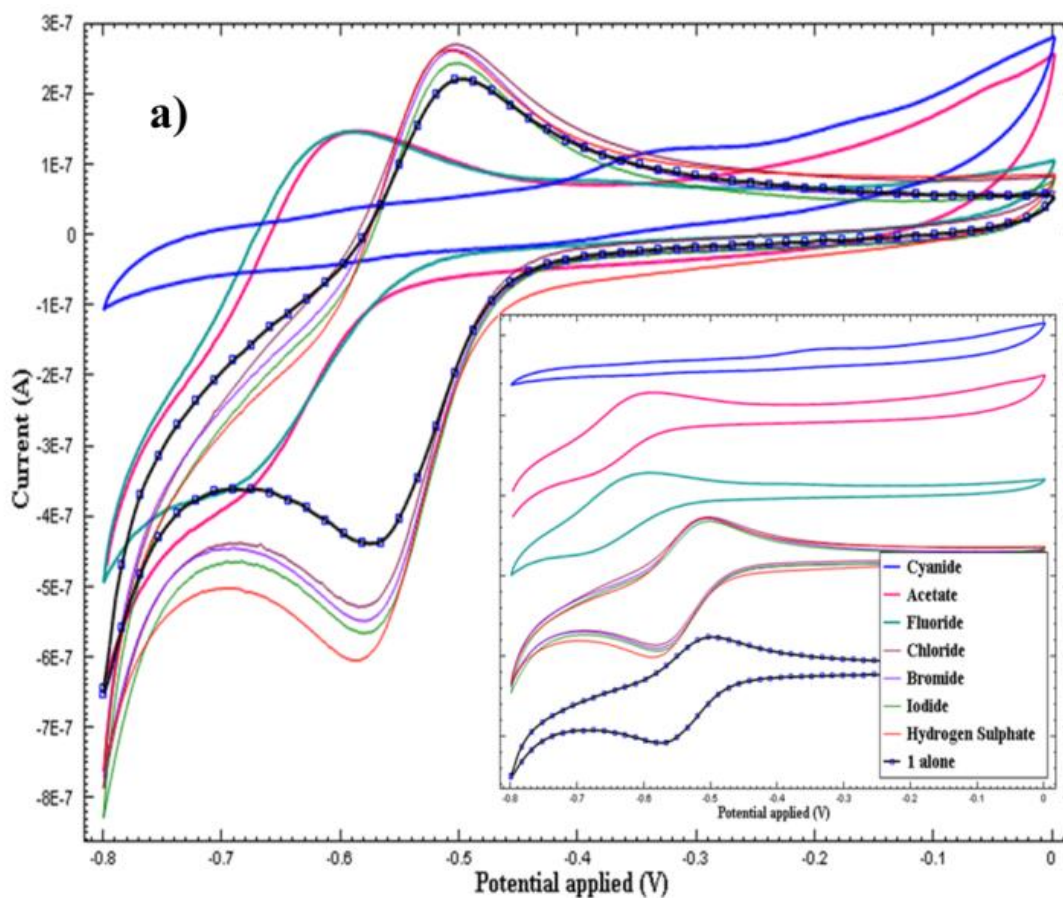


Fig. 4.6 Color changes on treatment of **1** and **2** with 2equivalents of different anions as their tetrabutyl ammonium (TBA) salts in acetonitrile

4.6.2 Analytical study

Electroanalytical study of both compounds **1** and **2** was done to check their selectivity for anions. Both **1** and **2** showed relative selectivity order as: cyanide > acetate > fluoride > chloride ~ bromide ~ iodide ~ hydrogen sulphate ions. Shift of about 100mV can be seen in the cathodic peak potential of **1** (Fig. 4.7a) on interaction with two equivalents of acetate

and fluoride ions, while with cyanide, both anodic and cathodic peaks are totally quenched because of the EC mechanism (Wang, 2000) i.e., electron transfer through a sequence of electrochemical (E) processes (e.g. redox process of **1**) followed by a chemical (C) process i.e., electrochemically inactive but chemically active complexation of **1** with the anion, as peaks in both anodic and cathodic regions are lost. This is also expected due to electrostatic interaction between positively charged quaternary N centres with anions. The same mechanism is observed in case of **2** (Fig. 4.7b), with cyanide, acetate and fluoride ions, where the cathodic peak is quenched.



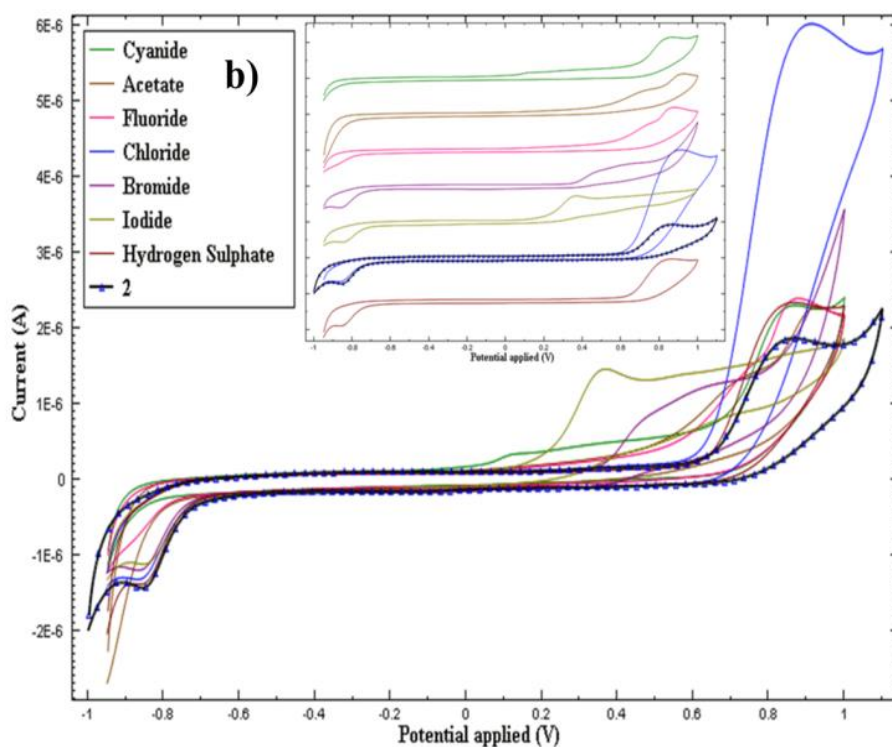


Fig 4.7 Cyclic voltammograms of **1** a) and **2** b) (10^{-4} M) with 2 equivalents of different anions using 0.1 M TBAP as supporting electrolyte (GC working electrode, scan rate 20 mVs^{-1} E vs Ag/Ag^+)

Binding constant i.e., binding affinity (Beer *et al*, 1999) of ionophore for different anions was calculated using equation 1 (Caltagirone *et al*, 2003, Schumacher *et al*, 2007). Calculated values of binding constants for various anions are given in Table 4.2.

$$E_{1/2}^{\text{complex}} - E_{1/2}^{\text{free ionophore}} = (RT/nF) \ln(K) \quad (1)$$

Binding constant values are remarkably high for cyanide (∞), acetate (74) and fluoride (53) as compared to chloride, bromide, iodide and hydrogen sulphate (less than 1.5). The observed trend for complexation is also supported with large values of ΔE_{pc} . For cyanide ions ΔE_{pc} could not be measured because the cathodic peak was quenched on complexation with the anion. Similar trends can be seen for **2**, binding constant upon interaction with anions could not be calculated because of its irreversible nature and cathodic peaks for cyanide, acetate and fluoride were fully quenched whereas for Cl^- , Br^- , I^- and HSO_4^- the ΔE_{pc} values were very less.

Table 4.2 Cathodic shift in peak potential (with binding constants) of *1* and *2* on interaction with different Anions

Anions (2 equivalents)	<i>1</i>		<i>2</i>
	$\Delta E_{pc}(mV)$	Binding constant (M^{-1})	$\Delta E_{pc}(mV)$
Cyanide	∞	∞	∞
Acetate	115	74	-
Fluoride	106	53	-
Chloride	13	1.4	9
Bromide	1	1.3	9
Iodide	1	1.3	7
Hydrogen sulphate	15	1.4	1

4.6.3 Calibration curve for cyanide ion

Experiments were conducted for the measurement of currents at the peak potential value for ionophore *1* (from CVs run separately) for different concentrations of cyanide added to the solution of *1*. Plots were drawn between different cyanide concentrations and the resulting current values recorded. The calibration was repeated five times to see reproducibility of the proposed method. The calibration curve (Figure 4.8) shows straight line with lower detection limit of 1.06×10^{-4} ($\pm 2\%$) M as indicated on the interpolation of two straight line portions of the curve. A linear decrease in cathodic current with increase in concentration of the cyanide ion results because of the progressive decrease of the compound *1* on incremental additions of the cyanide, as lesser and lesser amounts of the anthrone derivative become available for electrochemical reduction at the electrode. The residual current of the magnitude 10^{-8} A still stays even in the presence of excess of cyanide solution probably due to the presence of a very small amount of the *1* resulting from solubility product of *1*-cyanide complex in acetonitrile. Repeated measurements of the same experiment results in a calibration curve with a slope of $-0.0095 \mu A/\mu M$ with a standard deviation of 2%. This calibration curve has been used for the measurement of unknown cyanide concentrations in acetonitrile medium and has also been verified using

spectrophotometric method (Table 4.3). Comparison of the results indicates a high degree of similarity between the two sets of results.

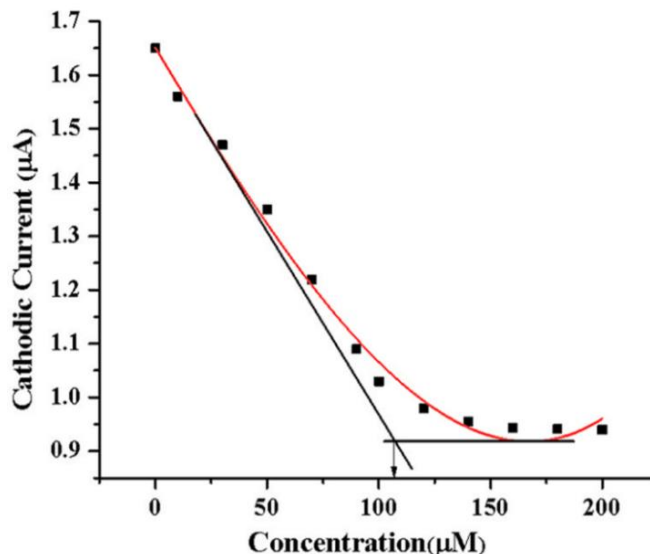


Fig. 4.8 Calibration plots between concentration of cyanide and current in acetonitrile medium using 0.1M TBAP as supporting electrolyte (GC working electrode, scan rate 20 mVs^{-1} E vs Ag/Ag^+)

Table 4.3 Concentration measurement of cyanide samples using proposed voltammetric method compared with spectrophotometric method

Unknown Samples of cyanide	Voltammetric	Spectrophotometric
	Concentration (µM)	Concentration (µM)
1	28.1	28.0
2	43.4	43.5
3	73.3	73.9
4	86.8	87.8

The proposed method of cyanide determination has also been compared with other available measurement techniques (from literature) like spectrophotometry (Isaad *et al*, 2011), spectrofluorimetry (Zang *et al*, 2012, Xiong *et al*, 2011) and potentiometry (Abbaspour *et al*, 2005, Kang *et al*, 2010) in Table 4.4. The comparison table indicates that

the proposed method is the first report of its kind in voltammetry having no interference from F^- and AcO^- unlike reported in other methods.

Table 4.4 Comparison of lower detection limits and interferences for anion detection for the reported methods with the proposed method

S.No.	Measurement techniques	Anion	Lower detection limit (μM)	Interference
1	Spectrophotometry	CN^-	10^{-5}	F^- , AcO^-
		F^-	10^{-3}	AcO^- , CN^- and $H_2PO_4^-$
2	Spectrofluorimetry	CN^-	10^{-3}	F^-
		F^-	10^{-3}	AcO^- , $H_2PO_4^-$
3	Potentiometry	CN^-	10^{-5}	Nil
		F^-	$10^{-4.5}$	Salicylate
4	Voltammetry	CN^-	10^{-4}	Nil

4.7 Interference of ions

Interference studies were carried out by adding 1 equivalent of various anions like CH_3COO^- , F^- , Cl^- , Br^- , I^- and HSO_4^- as interfering ions in 1eq concentration of CN^- ion as primary ion. Voltammograms for compound 1 in presence of cyanide did not show any change in quenching, indicating that there is no interference from these anions to the detection of cyanide with **1** (Fig. 4.9). Since no proper shaped voltammograms of the complex were obtained for **2**, the interference study from ions other than primary ion could not be completed. It can be concluded that **1** responds selectively towards cyanide ion in the presence of many other commonly available anions.

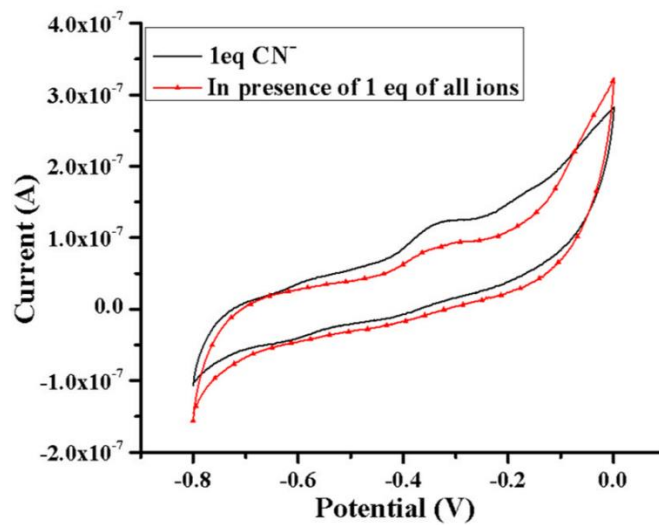


Fig. 4.9 Cyclic voltammogram of *1* showing interference of ions using TBAP as supporting electrolyte (GC working electrode, scan rate 20 mVs⁻¹ E vs Ag/Ag⁺)

4.8 Conclusions

Voltammetric study of both the molecules *1* and *2* shows the effect of substitution of viologen motif on anthrone derivative, shifting the behaviour of compounds from cation sensitive to anion sensitive species (anthrone derivatives selective for cation (Mittal *et al*, 2013)). Anthrone derivative *1* shows excellent selectivity for cyanide ions even in presence of CH₃COO⁻, F⁻, Cl⁻, Br⁻, I⁻ and HSO₄⁻ ion. A reproducible linear relationship between cathodic current and cyanide concentration establishes its application as a voltammetric chemical sensor for cyanide ion. The proposed analytical method has been compared with other prevalent measurement techniques for cyanide and is reported to perform with better selectivity and sensitivity. The cyanide ion concentration can be measured accurately (\pm 2% deviation) up to a concentration level of 10⁻⁴ M, with no interference from acetate and fluoride ions, the most common interferences in cyanide determination. Anthrone derivative *1* substituted with a dicationic viologen group (4, 4'-bipyridyl) performs as a better voltammetric sensor for cyanide ions than with a monocationic viologen i.e., *2*. Results of voltammetric sensor for cyanide ion are first of its kind using ionophore for cyanide ions is thoroughly supported by literature. The proposed mechanism for anion sensing behaviour of *1* is very well supported by theoretical calculations.

4.9 References

- Abbaspour**, A., Asadi, M., Ghaffarinejad, A., Safaei, E., 2005, A selective modified carbon paste electrode for determination of cyanide using tetra-3,4 pyridinoporphyrazinatocobalt(II), *Talanta*, 66, 931-936.
- Bianchi**, A., Bowman-James K., Garcia-Espana E. (Eds.), *Supramolecular Chemistry of Anions*, Wiley-VCH, New York (1997).
- Beer**, P.D., Gale, P.A., Chen, G.Z., 1999, Electrochemical molecular recognition: Pathways between complexation and signaling, *Journal of the Chemical Society, Dalton Transactions*, 12, 1897-1910.
- Beer**, P.D., Gale, P.A., 2001, Anion Recognition and Sensing: The State of the Art and Future Perspectives, *Angewandte Chemie International Edition* 40, 486-516.
- Bird**, C.L., Kuhn A.T., 1981, Electrochemistry of the viologens, *Chemical Society Reviews*, 10, 49-82.
- Caltagirone**, C., Gale, P.A., 2009, Anion receptor chemistry: Highlights from 2007, *Chemical Society Reviews*, 38, 520-563.
- Caltagirone**, C., Bencini, A., Demartin, F., Devillanova, F.A., Garau, A., Isaia, F., Lippolis, V., Mariani, P., Papke, U., Tei, L., Verani, G., 2003, Redox chemosensors: coordination chemistry towards Cu^{II} , Zn^{II} , Cd^{II} , Hg^{II} , and Pb^{II} of 1-aza-4,10-dithia-7-oxacyclododecane ([12]aneNS₂O) and its *N*-ferrocenylmethyl derivative, *Dalton Transactions*, 5, 901-909.
- Cametti**, M., Rissanen, K., 2009, Recognition and sensing of fluoride anion, *Chemical Communications*, 20, 2809-2829.
- Gale**, P.A., Garrido, G., Garric, S.E., 2008, Anion receptors based on organic frameworks: highlights from 2005 and 2006, *Journal of Chemical Society Review* 37, 151-190.
- Gale**, P.A., 2006, Preface to the special issue and subsequent reviews, *Coordination Chemistry Reviews*, 250, 2917.
- Hsu**, C.Y., Vasantha, V.S., Chen, P.Y., Ho, K.C., 2009, "A new stable $\text{Fe}(\text{CN})_6^{3-/4-}$ - immobilized [oly(butyl viologen)-modified electrode for dopamine determination, *Sensor and Actuators*, B 137, 313-319.
- Isaad**, J., Salaun F., 2011, Functionalized poly (vinyl alcohol) polymer as chemodosimeter material for the colorimetric sensing of cyanide in pure water, *Sensor and Actuators B*, 157, 26.
- Jia**, H., Forgie, J.C., Liu, S., Sanguinet, L., Levillain, E., Derf, F.L., Salle, M., Neels, A., Skabara, P.J., Decurtins, S., 2012, Tetrathiafulvalene-annulated dipyrrolylquinoxaline: the effect of fluoride on its optical and electrochemical behaviors, *Tetrahedron*, 68, 1590-1594.
- Kang**, Y., Lutz, C., Hong, S.A., Sung, D., Lee, J.S., Shin, J.H., Nam, H., Cha, G.S., Meyerhoff, M.E., 2010, Development of a fluoride-selective electrode based on

scandium(III) octaethylporphyrin in a plasticized polymeric membrane, *Bulletin of the Korean Chemical Society*, 31, 1601-1608.

Kim, Y.H., Rhim, S., Park, J.J., Kang J., 2012, Anion receptor interacting with anions through hydrogen bonds and charge transfer complex. *Journal of Inclusion Phenomena Macrocyclic Chemistry*, 74, 317–323.

Kirk, K.L., Biochemistry of the halogens and inorganic halides, Plenum, New York, NY, 1991, 58.

Kong, D., Weng, T., He, W., Liu, B., Jin, S., Hao, X., Liu, S., 2013, Synthesis, characterization, and electrochemical properties of ferrocenylimidazolium, *Journal of Organometallic Chemistry*, 727, 19-27.

Lindsay, A.E., O'Hare, D., 2006, The development of an electrochemical sensor for the determination of cyanide in physiological solutions, *Analytica Chimica Acta* 558, 158–163.

Lorenzo, A., Aller, E., Molina, P., 2009, Iminophosphorane-based synthesis of multinuclear ferrocenyl urea, thiourea and guanidine derivatives and exploration of their anion sensing properties, *Tetrahedron* 65, 1397–1401.

Ma, J., Dasgupta, P. K., 2010, Recent developments in cyanide detection: A review, *Analytica Chimica Acta*, 673, 117-125.

Mittal, S.K., Kaur, K., Kumar, A., Kumar, S., Kumar, A., 2013, Anthrone derivatives as voltammetric sensors for applications in metal ion detection, *Sensor letters*, 11, 223-236.

Qian, D.J., Nakamura, C., Miyake, J., 2000, Monolayers of a series of viologen derivatives and the electrochemical properties in Langmuir-Blodgett Films, *Thin Solid Films*, 374, 125-133.

Reynes, O., Bucher, C., Moutet, J., Royal, G., Saint-Aman, E., 2004, Redox sensing of anions in pure aqueous environment by ferrocene-containing 4,4'-bipyridinium-based receptors and polymer films, *Chemical Communications* 4, 428-429.

Schumacher, A.L., Hill, J.P., Ariga, K., D'souza, F., 2007, Highly effective electrochemical anion sensing based on oxoporphyrinogen, *Electrochemistry Communications*, 9, 2751-2754.

Sessler, J.L., Gale, P.A., Cho, W.S., Anion Receptor Chemistry, Royal Society of Chemistry, Cambridge, UK (2006).

Sharrett, Z., Gamsey, S., Levine, P., Cunningham-Bryant, D., Vilozny, B., Schiller, A., Wessling, R. A., Singaram B., 2008, Boronic acid-appended bis-viologens as a new family of viologen quenchers for glucose sensing, *Tetrahedron Letters*, 49, 300-304.

Shi, M., Zhi-Yu Lei, Mei-Xin Zhao, Jing-Wen Shi, 2007, A highly efficient asymmetric michael addition of anthrone to nitroalkenes with cinchona organocatalysts, *Tetrahedron Letters* 48, 5743–5746.

Shen, J., C. Hong Tan, 2008, Anthrone-Derived NHPI analogues as catalysts in reactions using oxygen as an oxidant, *Organic and Biomolecular Chemistry*, 6, 4096-4098.

Shen, J., Nguyen, T.T., Goh, Y.P., Ye, W., Fu, X., Xu, J., Tan, C.H., 2006, Chiral vicyclic guanidine-catalyzed enantioselective reactions of anthrones, *Journal of American Chemical Society*, 128, 13692-13693.

Silva, S.D., Cosnier, S., Almeida, M.G., Moura, J.J.G., 2004, An efficient poly(pyrrole-viologen)-nitrite reductase biosensor for the mediated detection of nitrite, *Electrochemistry Communications* 6, 404-408.

Tanak, H., M. Yavuz, 2010, Density functional computational studies on (E)-2-[(2-Hydroxy-5-nitrophenyl)-iminoethyl]-4-nitrophenolate, *Journal of Molecular Modeling*, 16, 235-241.

Torimoto, T., Reyes, J.P., Murakami, S., Pal, B., Ohtani, B., 2003, Layer-by-layer accumulation of cadmium sulfide core-silica shell nanoparticles and size-selective photoetching to make adjustable void space between core and shell, *Journal of Photochemistry and Photobiology A* 160, 69.

Torimoto, T., Paz Reyes, J., Iwasaki, K., Pal, B., Shibayama, T., Sugawara, K., Takahashi, H., Ohtani, B., 2003, Preparation of novel silica-cadmium sulfide composite nanoparticles having adjustable void space by size-selective photoetching, *Journal of American Chemical Society* 125, 316-317.

Wang, J., Analytical electrochemistry, A John Wiley & Sons INC., Publications 2nd edition (2004).

Xiong, J., Cui, L., Liu, W., Beves, J.E., Li, Y., Zuo, J., 2013, Large and selective electrochemical response to fluoride by a tetrathiafulvalene-based sensor, *Tetrahedron Letters*, 54, 1998-2000.

Xiong, J., Sun, L., Liao, Y., Li, G., Zuo, J., You, X., 2011, A new optical and electrochemical sensor for fluoride ion based on the functionalized boron-dipyrromethene dye with tetrathiafulvalene moiety, *Tetrahedron Letters*, 52, 6157-6161.

Zang, L., Wei, D., Wang, S., Jiang, S., 2012, A phenolic schiff base for highly selective sensing of fluoride and cyanide via different channels, *Tetrahedron*, 68, 636-641.

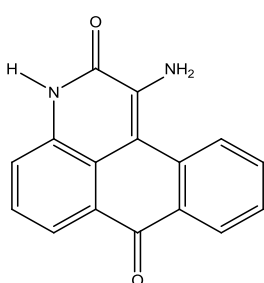
Cation sensitive anthrone derivatives

Molecules which change their easily measurable physical property on coordination with a target substrate are of special interest. Among these, new molecules are redox functionalized receptors which are able to display shift of the redox potentials upon addition of particular substrates. Molecules like cryptands, calix[4]arenes (Mahajan et al, 2008, Lyskawa et al, 2010, Chen et al, 2010), imidazole (Alfonso et al, 2011) with redox active moieties like ferrocene (Kong et al, 2013), tetrathiafulvalene (Jia et al, 2012) are commonly reported for electrochemical sensing the cations and anions. In presence of some complexing ions, the ion recognition event induces significant changes at redox active moieties like ferrocene which causes shift in its potential. Redox-active receptors for cations may be either oxidizable (and hence form less stable complexes with cations) or reducible (and hence form more stable complexes with cations), e.g., quinone, anthraquinone and nitroaromatic containing species (Beer et al, 1999). Different voltammetric methods have been used for determination of pesticides (Filho et al, 2006), drugs (He et al, 2011), cations and anions (Lloris et al, 2001). Cyclic voltammetry (CV) is widely used to monitor perturbations in electrochemical behavior of redox active receptors.

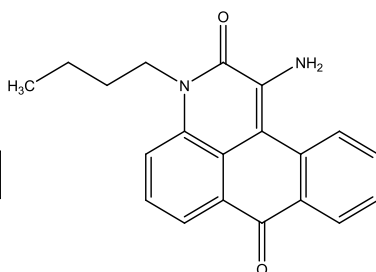
Mercury is considered as a highly toxic element and its contamination is a global problem. A major source of human exposure stems from a variety of natural and anthropogenic sources and can lead, even at low concentration, to digestive, kidney and especially neurological diseases (Firooz et al, 2013). On the other hand, copper is the third most abundant essential heavy metal ion (after Fe^{3+} and Zn^{2+}) present in the human body, playing an important role in fundamental physiological processes in organisms ranging from bacteria to mammals (Uauy et al, 1998) Nevertheless, it is also a significant metal pollutant responsible for a number of neurodegenerative diseases. The sensitive detection of mercuric ion is currently a task of prime importance for environmental or biological concerns along with other transition metal ions like Ni^{2+} , Cu^{2+} , Zn^{2+} and Cd^{2+} . To develop sensitive mercuric ion sensors, various receptors consisting of a mercuric ion recognition

unit and a probe exhibiting physical responses upon the coordination of mercuric ion have been reported. Selective electrochemical recognition of mercury in water has been reported by a redox-functionalised aza-oxa crown derivative (Costero *et al*, 2000) studied electrochemical behavior of biphenyl derivatives for different cations like Ni^{2+} , Cu^{2+} , Zn^{2+} , Cd^{2+} , Pb^{2+} and Hg^{2+} and were found to be selective for Hg^{2+} ion over other ions. Ferrocene based electrochemically active compound has also been reported for selectivity towards Hg^{2+} ion (Bui *et al*, 2008).

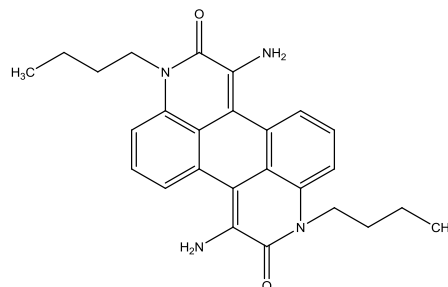
Electrochemical reduction of anthraquinone in presence of concentrated sulphuric acid gives anthrone as a product (Comninellis *et al*, 1985). Anthraquinone is a redox active moiety like ferrocene. Its derivatives have been used for various purposes: as a useful probe to measure the charge transfer (CT) through a π -stack of DNA at the metal surface (Kumamoto *et al*, 2008), as sulphonate and disulphonate salts for DNA detection via electrochemical methods (Batchelor-McAuley *et al*, 2010), as Li^+ ion selective receptor (Park *et al*, 2001), for molecular electronics (Dijk *et al*, 2006), etc. There are no reports available on the electrochemical study of any anthrone derivatives. We hereby report a study on electrochemical nature of following anthrone derivatives and their response towards different cations.



Anthrone 1



Anthrone 2



Anthrone 3

5.1 Results and Discussion

5.1.1 Electrochemical behavior of anthrone 1, 2 and 3

Cyclic voltammograms of anthrone1 and anthrone2 showed oxidation peaks at 0.640V, 0.903V, and 0.657V, 0.919V, respectively, while anthrone3 showed one redox couple

(0.189V, 0.124V) and one oxidation peak (0.984) (Table 5.1). The presence of only one weak and broad peak in the reverse cycle of anthrone1 and anthrone2 indicates a quasi-reversible redox behavior of these molecules. However, response of these compounds was quite reproducible as the intensity of the peaks in the forward as well as in the reverse reactions did not decrease on repetitive measurements. Anthrone3 shows a better reversibility, generating sharp peaks in the reverse cycle of the voltammogram (Fig. 5.1).

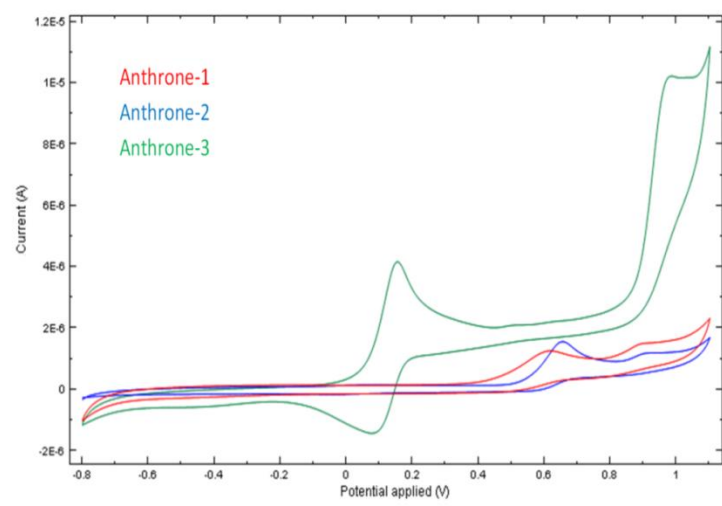


Fig. 5.1 Cyclic voltammograms of anthrone1, anthrone2 and anthrone3 (10^{-4} M) in ACN using 0.1M TBAP as supporting electrolyte, GC working electrode, scan rate 20mVs^{-1} E vs Ag/Ag^+

Table 5.1 Peak potentials (V) and peak currents (μA) values for different substrates

Compound	Peak potentials (V)			Peak current (μA)
	$E_{\text{pa}1}$	$E_{\text{pa}2}$	$E_{\text{pc}1}$	$i_{\text{pa}1}$
Anthrone1	0.640	0.904	-	1.55
Anthrone2	0.657	0.919	-	2.98
Anthrone3	0.191	0.984	0.125	4.16

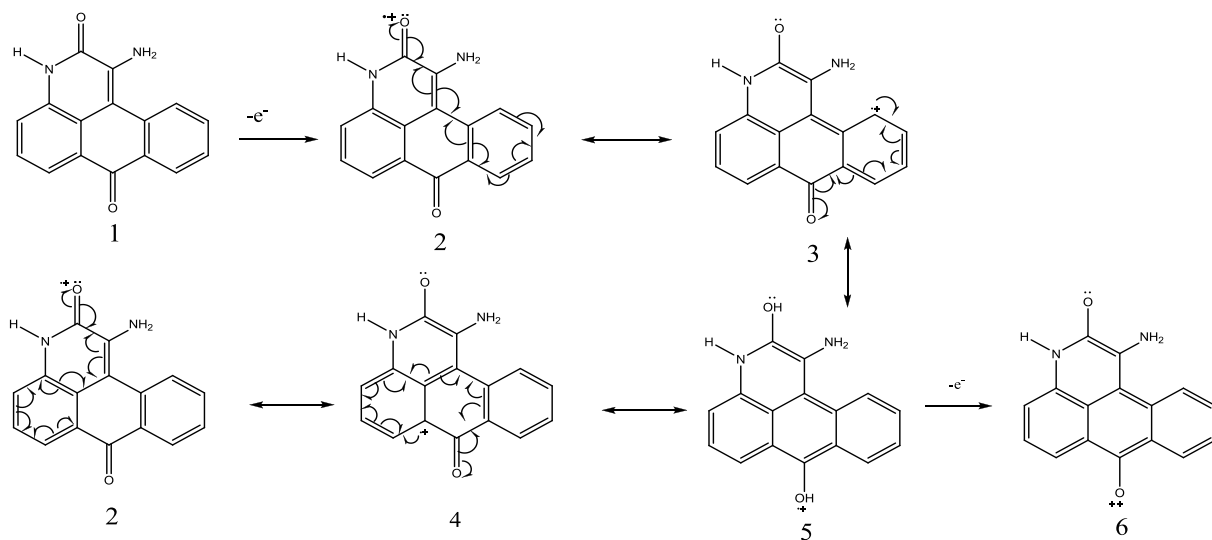
E_{pa} : anodic peak potential, E_{pc} : cathodic peak potential and i_{pa} : anodic current

Oxidative current for anthrone3 (4.16 μA) is appreciably higher than for anthrone1 (1.55 μA) and anthrone2 (2.98 μA) and appearing at much lower potential (by about 0.5V) than for the later ones. This shift of oxidative peak for anthrone3 as compared to anthrone1 and anthrone2 can be assigned to symmetry in the former and better possibility of loss of electrons from either of the two carbonyl oxygen atoms.

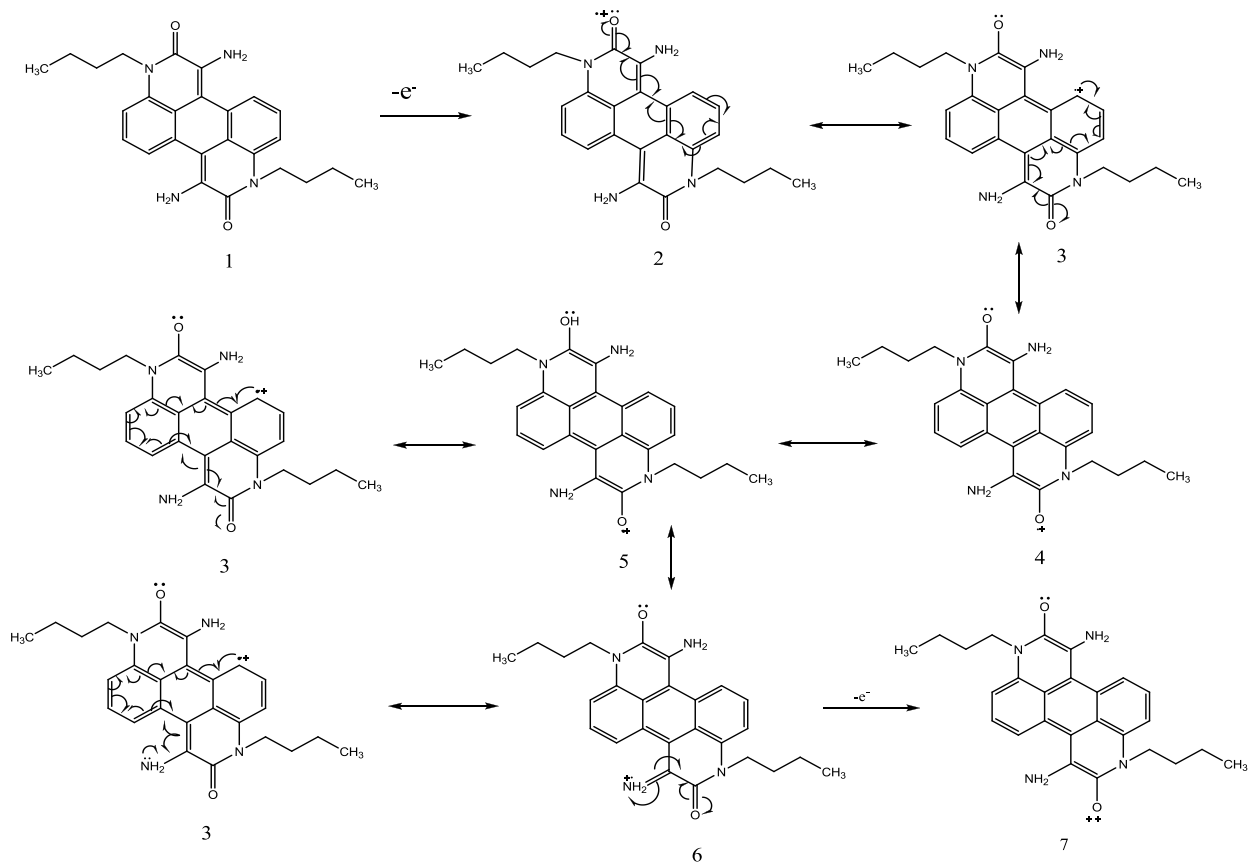
5.1.2 Mechanism of electrochemical process

Each cyclic voltammogram of anthrone1, anthrone2 and anthrone3 shows two peaks in the anodic region, and only one peak in the cathodic region, which is poorly defined for anthrone1 and anthrone2 and much improved for anthrone3. This is indicative of the fast electron exchange between anthrone3 and glassy carbon electrode.

ANTHRONE 1



ANTHRONE 3



Scheme 7.1. Mechanism scheme for the formation of radical cations for anthrone1 and anthrone3

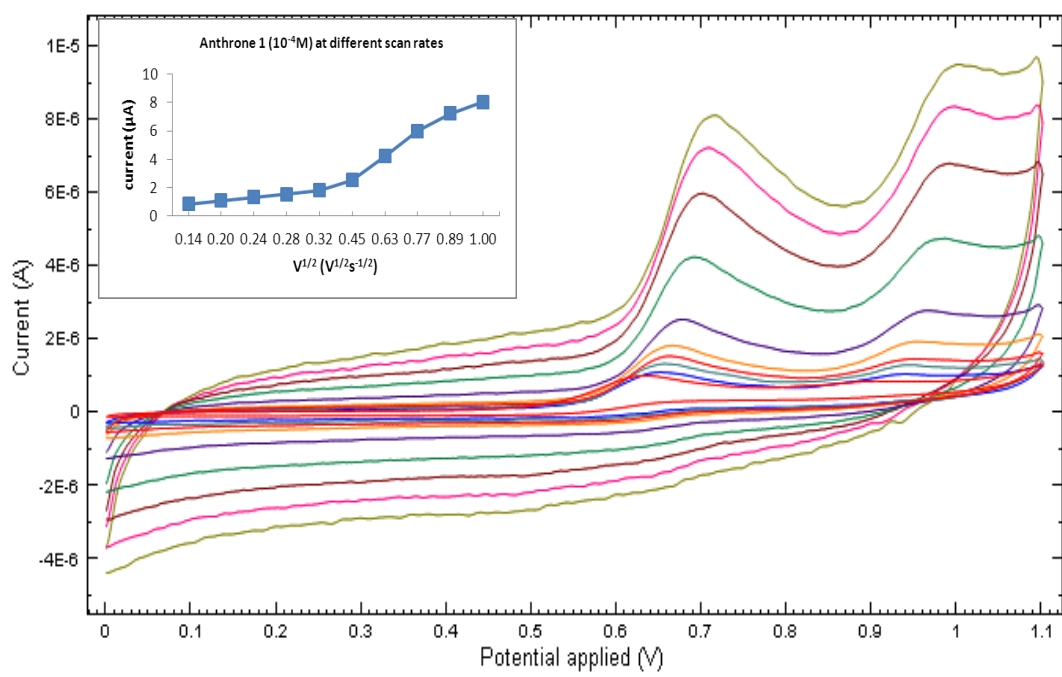
Following discussion can be made from the observations:

- 1) Shapes of all the plots are similar to each other.
- 2) The redox reaction consists of a sequence of two steps.
- 3) First step is the loss of an electron from the substrate resulting in the formation of respective radical cation.
- 4) The intermediate radical cation undergoes further loss of electron and results in the formation of the oxidized product.
- 5) The oxidized product undergoes reduction during the reverse course of cycle and two peaks, very weak in current are observed.
- 6) A sharp and intense peak for anthrone3 indicates a greater stability and better lifetime of the oxidized product which is a reactant for the second half of the reaction.
- 7) Greater intensity of the peak in cathodic region for anthrone3 is due to more number of resonating structures (Scheme 1) for the intermediate radical cation than those for anthrone1 and anthrone2, resulting in more dispersal of charge on anthrone3.
- 8) Larger number of resonating structures for anthrone3 in comparison to anthrone1 and anthrone2 strongly support the shift of anodic peak from 0.640V of anthrone1 and 0.657V of anthrone2 to 0.189V for anthrone3. Similar mechanism can be drawn for anthrone2.
- 9) Very similar shape of the plots for all the three compounds in Figure 3 show that these molecules respond in a very similar way at least in the first step of the mechanism i.e., loss of one electron to generate radical cation.
- 10) All the three compounds undergo similar steps i.e., loss of one electron and it continues till the $(\text{scan rate})^{1/2}$ is about $0.45\text{v}^{1/2}\text{s}^{-1/2}$ (Fig. 5.2).

5.1.3 Influence of scan rate

Scan rate is known to influence the magnitude of peak current (Shen *et al*, 2008). At slow scan rates, the migration of ions is supposed to be diffusion controlled and for a reversible process, the ΔE_p at 298K should be 57mV. However, peak current increases with square

root of scan rate. Voltammograms were recorded for different scan rates ranging from 20mVs^{-1} to 1000 mVs^{-1} . As expected from a reversible system, increase in scan rate resulted in increased peak current values. This was observed for all the three compounds i.e., anthrone1, anthrone2 and anthrone3 (Fig. 5.2). Further, an increase in ΔE at faster scan rate indicates a kinetic control over the electrochemical reaction than the diffusion controlled processes at the electrode. This could be observed only for anthrone3. While for anthrone1 and anthrone2, no relation could be established between ΔE and scan rate, indicating their quasi-reversible nature.



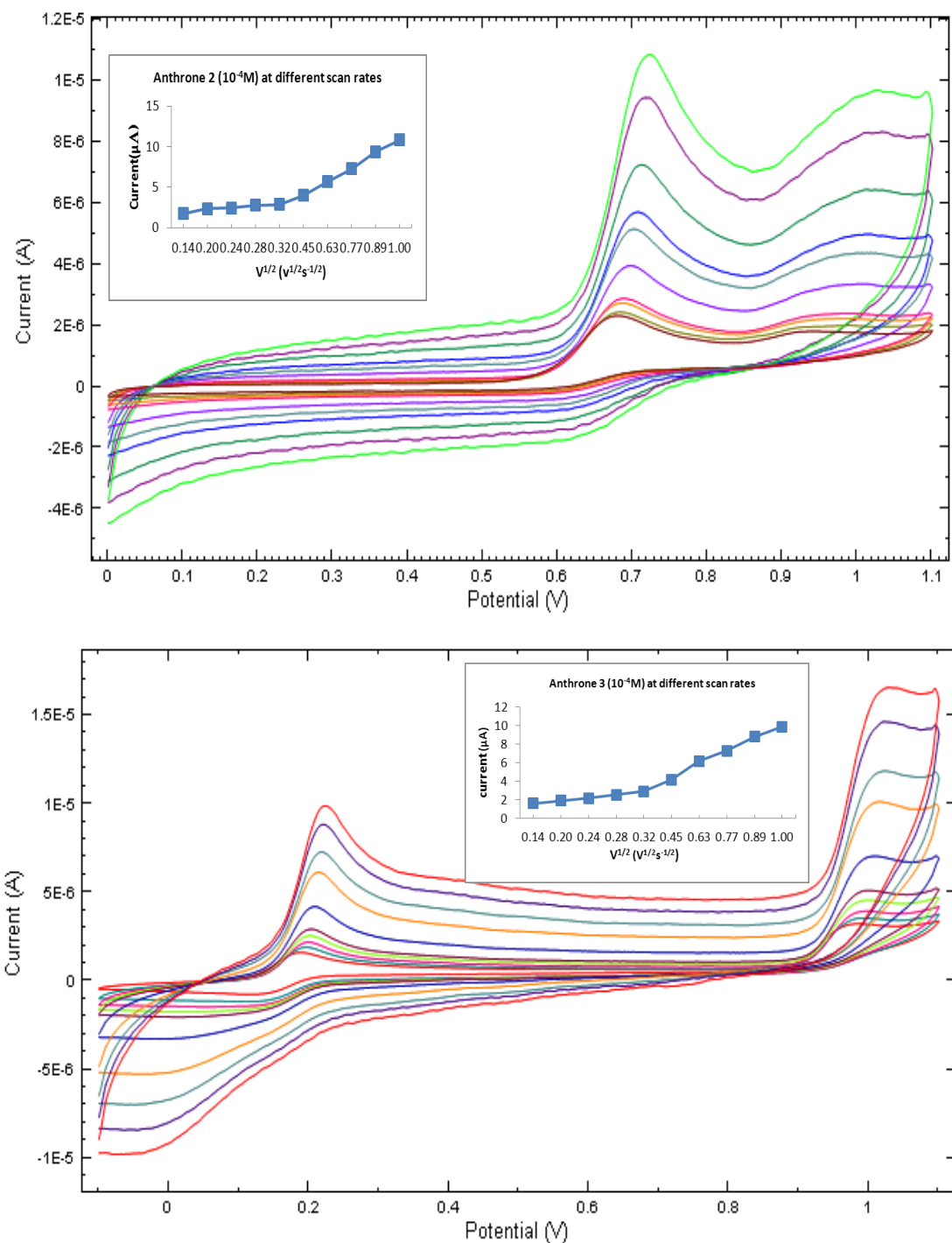


Fig. 5.2 Cyclic voltammograms showing the effect of scan rate in ACN. From inner to outer the scan rates are (20, 40, 60, 80, 100, 200, 400, 600, 800, 1000 mVs⁻¹), 0.1M TBAP, GC as working electrode. (Plots show non-linear relation between i_{pa} and $v^{1/2}$)

5.1.4 Effect of concentration of the electroactive compound

Voltammograms were drawn for different concentrations of the ligands to study the response of these compounds as shown in Fig. 5.3. With an increase in concentration of the anthrone derivatives increase in peak current was observed along with a cathodic shift in the peak potential. This is due to the reason that increase in concentration of redox substances makes the velocity of mass diffusion rapid and hence the electrode processes become more controlled by the electrode reactions.

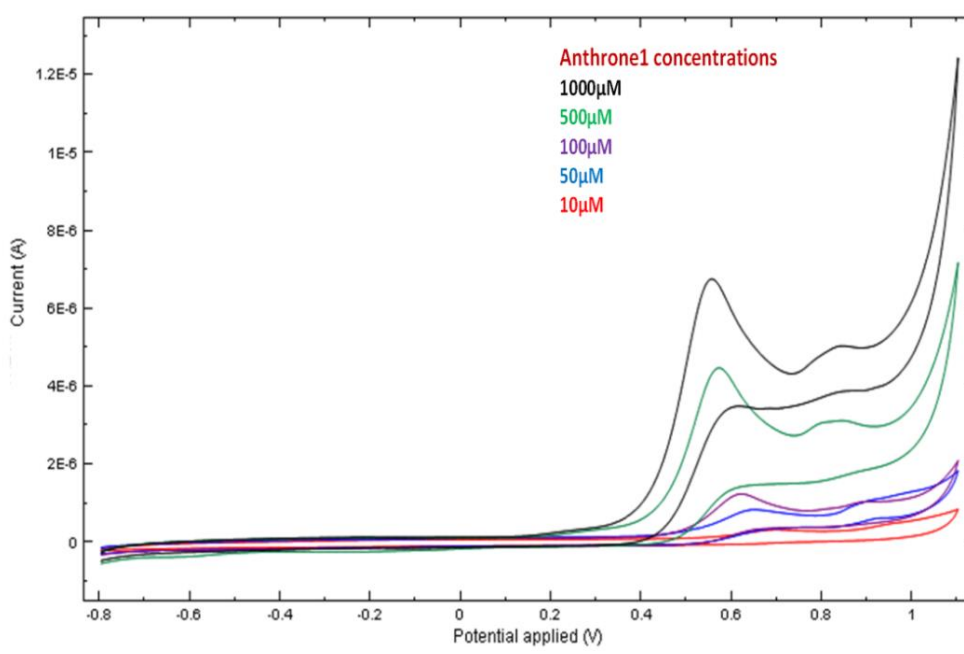


Fig. 5.3 Cyclic voltammograms of anthrone1 at GC electrode, 0.1M TBAP as supporting electrolyte and scan rate 20mVs^{-1} at different concentrations

5.1.5 Effect of change in concentration of supporting electrolyte

Fig. 5.4 shows cyclic voltammograms of anthrone1 with different electrolyte concentrations. With increase of supporting electrolyte concentration, the oxidation peaks become more distinguishable and their peak potentials are shifted cathodically, while at low concentration of the electrolyte, the second peak current becomes almost negligible. At low electrolyte concentration, the electrode process is mainly controlled by mass diffusion as the electrostatic effects are diminished, and the influence of supporting electrolyte

concentration becomes important. With an increase in the electrolyte concentration, the electrode process is mainly controlled by the diffusion process at the electrode reactions. Similar studies are conducted for anthrone2 and anthrone3. They showed the same trend.

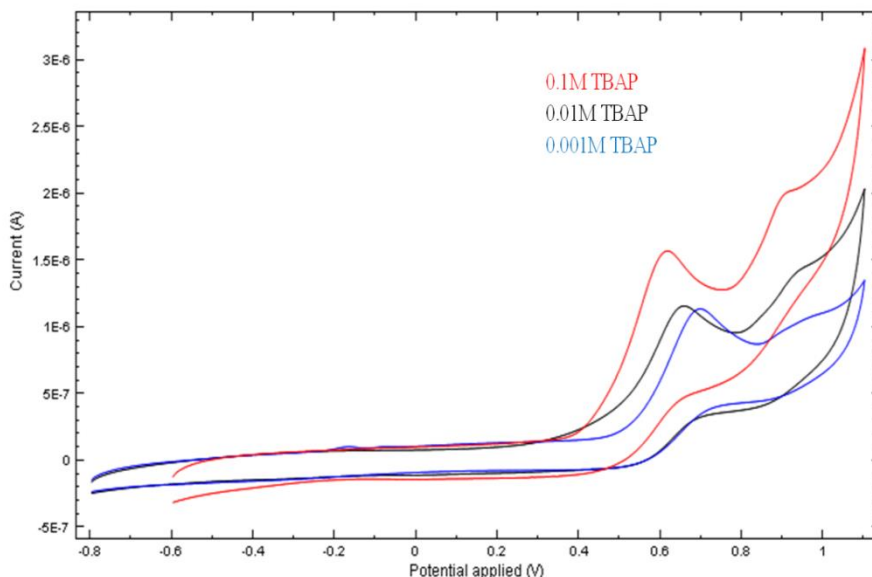


Fig. 5.4 Cyclic voltammograms curves of anthrone1 (10^{-4} M) with different electrolyte (TBAP) concentrations in ACN (GC working electrode, scan rate 20mVs^{-1} E vs Ag/Ag^+)

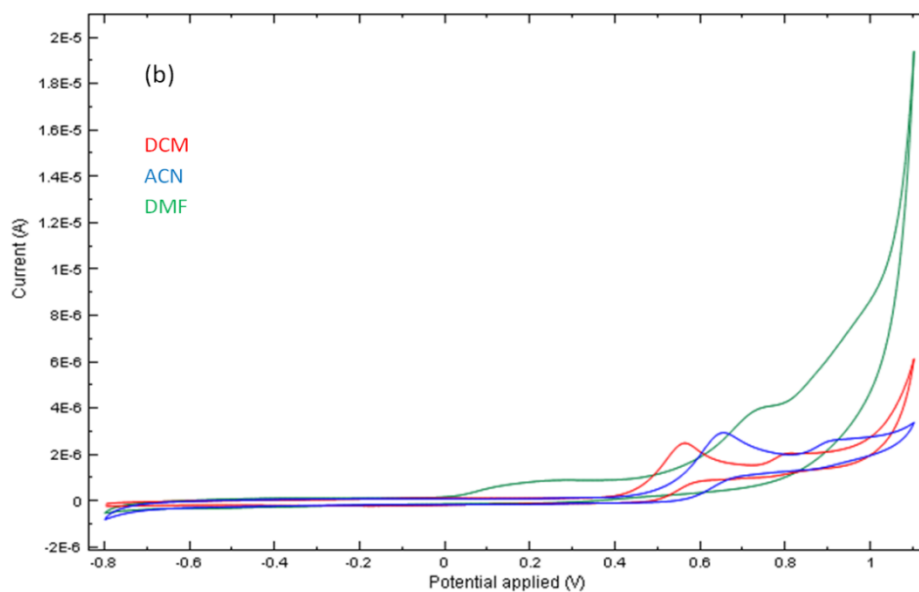
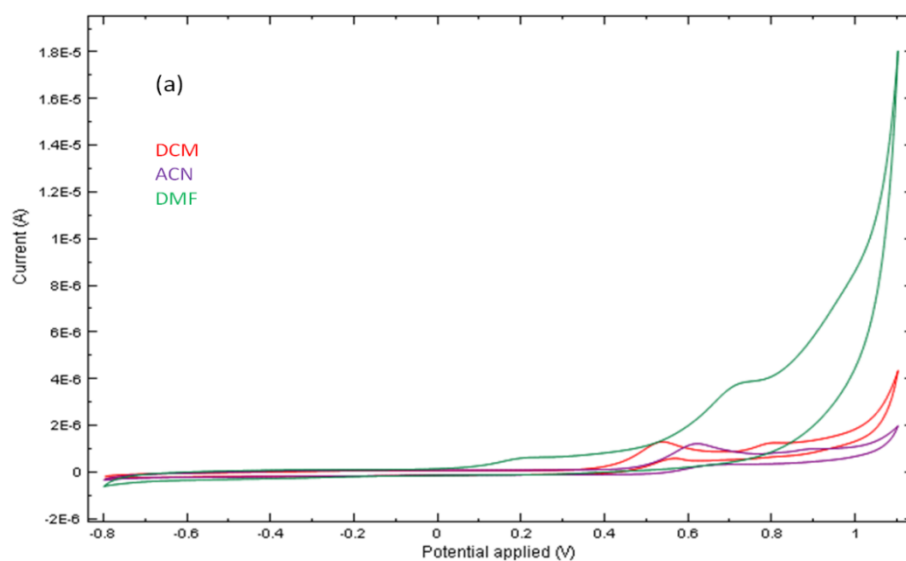
5.1.6 Effect of solvent

Voltammetric behavior of the anthrone derivatives was studied in different organic solvents like acetonitrile (ACN, $\epsilon = 37.5$), dichloromethane (DCM, $\epsilon = 9.1$) and N, N-dimethylformamide (DMF, $\epsilon = 38$). The results shown in Fig. 5.5 indicated that polarity of the solvent had a great effect on the voltammograms. An increase in polarity of the solvent (from ACN to DMF) leads to the deformation of the peak shapes. An interesting observation about the effect of solvent is that when a solvent with high dielectric constant (DMF, $\epsilon = 38$) is taken, the anodic peak shifts towards lesser potentials indicating facilitation of oxidation of these molecules in presence of the solvent (Table 5.2).

Table 5.2 Peak potentials of oxidation peaks of anthrone derivatives in different solvents

Solvent	Dielectric constant	E_a 1(V)			ΔE (mV)		
		Anthrone1	Anthrone2	Anthrone3	Anthrone1	Anthrone2	Anthrone3
DCM	9.1	0.538	0.566	0.141			
DMF	38	0.207	0.207	-	331	358	
ACN	37.5	0.641	0.657	0.191	-434	-91.2	-50

E_{pa} : anodic peak potential, ΔE : shift in peak potential



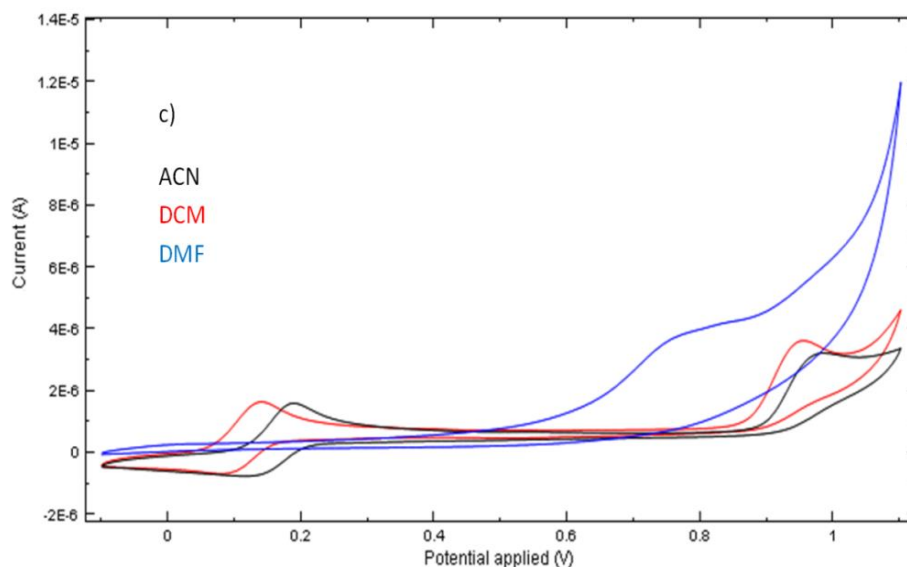


Fig. 5.5 Cyclic voltammograms of (a) anthrone1, (b) anthrone2 and c) anthrone 3 (10^{-4}M) in different solvents using 0.1M TBAP as supporting electrolyte (GC working electrode scan rate 20 mVs^{-1} E vs Ag/Ag^+)

On change of solvent from DCM to ACN, oxidation peak shifted towards higher potential values for all the three anthrones derivatives probably due to:

1. Lesser number of hetero atoms with lone pair of electrons in acetonitrile. Also, H-bonding is more probable in case of ACN which would decrease basic character of the molecules.
2. ACN has lesser basic character than DMF due to electron withdrawing nature of the Cyanide group, while in DMF the carbonyl group is attached to strongly basic dimethyl amine group.

Therefore, dimethylformamide seems to stabilise anthrone1, 2 and 3 more than that of acetonitrile, as the anodic peak is observed at lower applied potential and is totally diminished in case of anthrone3.

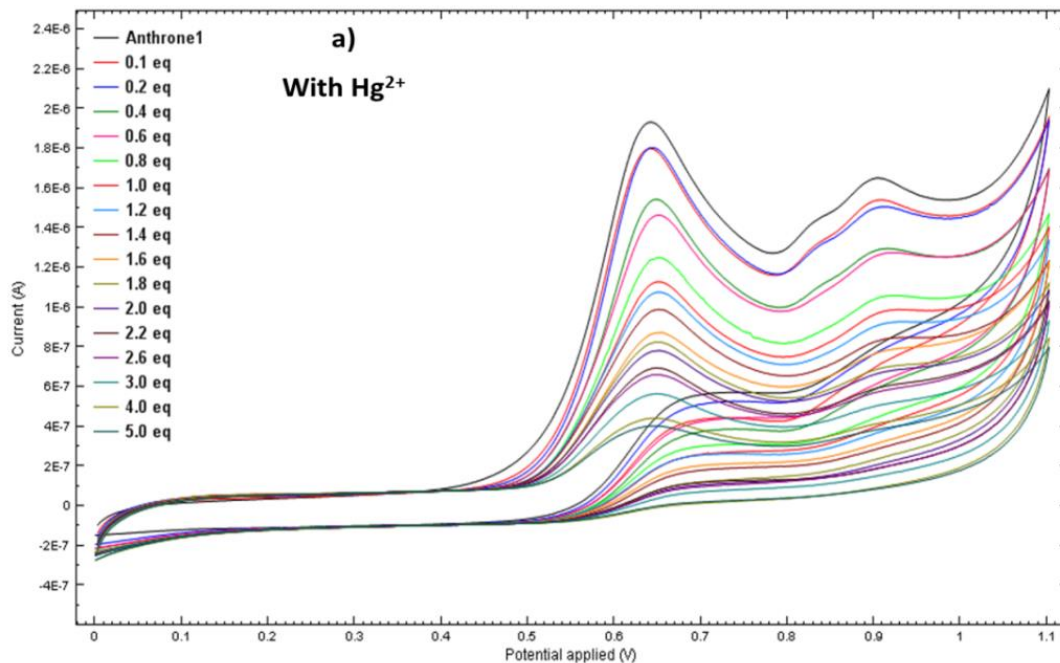
5.1.7 Electrochemical recognition of cation by anthrone 1, 2 and 3

Experiments were conducted with different transition metal ions like Co^{2+} , Ni^{2+} , Cu^{2+} , Zn^{2+} , Pb^{2+} and Hg^{2+} in acetonitrile at a scan rate of 20 mVs^{-1} to understand complexation behaviour of anthrone derivatives with the metal ions. In presence of Hg^{2+} ions, the

voltammograms of anthrone1 and anthrone3 are different from that in presence of anthrone2 (Figures 5.6-5.13). However, cyclic voltammogram for Cu^{2+} -anthrone complex showed an additional peak, as shown in Fig. 5.6b. A detailed study was done with different concentrations of ions ranging from 0.1equivalents to 20 equivalents of the anthrone derivatives.

Anthrone1

In voltammogram of anthrone1, intensity of the anodic peaks decrease with increase in concentration of Hg^{2+} ions. At 2 equivalents of the metal ion concentration, the second oxidation peak becomes almost negligible while the first oxidation peak current falls with broadening of the peak suggesting complexation between anthrone1 and Hg^{2+} ions. An almost linear change in anodic peak current was observed (for peak at 0.640 V) for different concentrations indicating a quantitative response of anthrone1 for Hg^{2+} ions (Fig. 5.6a).



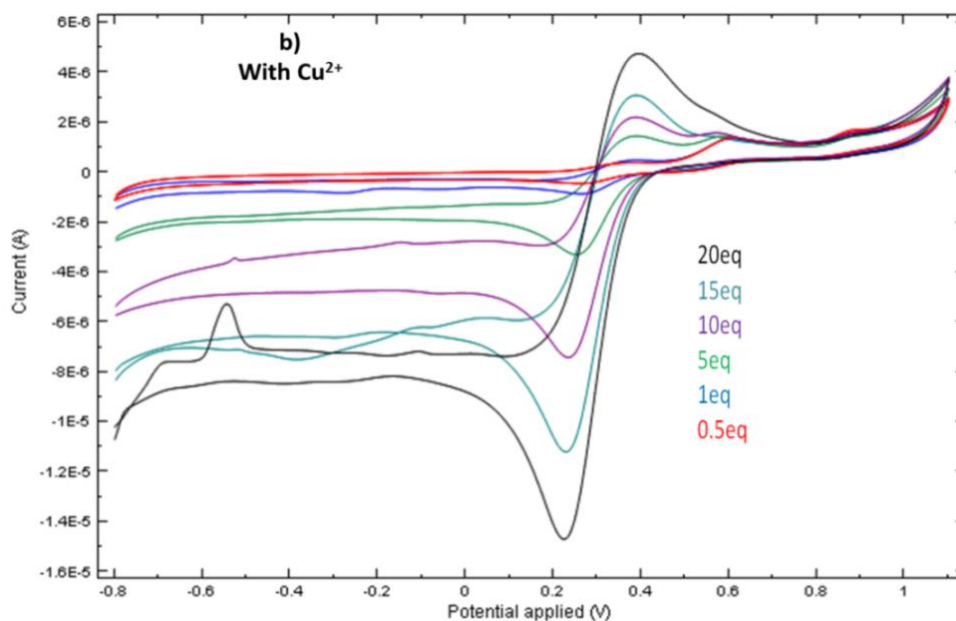


Fig. 5.6 Cyclic voltammograms of anthrone1 with different equivalents of a) Hg^{2+} and b) Cu^{2+} ion in ACN with 0.1M TBAP supporting electrolyte (GC working electrode, scan rate 20 mVs^{-1} E vs Ag/Ag^+)

Table 5.3 Peak potential (V) values for of anthrone1 alone and with different metal ions

Metal ions (1eq)	Peak potentials (V)			
	E_{pa1}	E_{pa2}	E_{pa3}	E_{pc}
Anthrone1 alone	0.640	0.903	-	-
With Cu^{2+}	0.609	0.885	0.375	0.264
With Ni^{2+}	0.629	0.907	-	-
With Pb^{2+}	0.630	0.907	-	-
With Zn^{2+}	0.630	0.905	-	-
With Co^{2+}	0.618	0.889	-	-
With Hg^{2+}	0.651	0.916	-	-

E_{pa} : anodic peak potential and E_{pc} : cathodic peak potential

In presence of Cu^{2+} ions, anthrone1, shows a new redox couple (oxidation peak at 0.375 V and reduction peak at 0.264 V) (Table 5.3), in addition to oxidation peaks at 0.657 V and 0.919 V. The increase in cathodic peak current is comparatively more than the anodic peak

current, on gradual addition of Cu^{2+} ions (Fig. 5.6b), which is probably because of the electroactive nature of the product formed upon complexation. At higher concentration of Cu^{2+} ions, the oxidation peaks of anthrone1 diminish and only the peaks of new redox couple remain. On complexation with Cu^{2+} ions, a cathodic shift of about 30 mV in the oxidation peak potential is observed while in presence of other metal ions (listed above) a shift of 10-20 mV is recorded and their peak currents remain almost same even at high concentration. This indifference of peak current in the presence of metal ions other than Cu^{2+} indicates that anthrone1 is more selective toward Cu^{2+} ions.

Anthrone2

Anthrone 2 on the other hand does not show any kind of response towards Hg^{2+} ion in terms of peak potential shift or magnitude of peak current (Figure 5.7a). Voltammogram of anthrone2 in the presence of different concentrations of Cu^{2+} ion show different peak heights (Figure 5.7b). For anthrone2- Cu^{2+} complex, a trend similar to that of anthrone1- Cu^{2+} was observed i.e., formation of new redox couple with oxidation peak at 0.374V and reduction peak at 0.264V (Table 5.4). This generation of new redox couple instead of shift in peak potentials of anthrone2 (and anthrone1 also) shows that ECE mechanism (Wang, 2000) is taking place. Hence, anthrone derivatives can also be used for copper ion determination in a large range of 0.5 to 20 equivalents of the metal ion with respect to anthrone2.

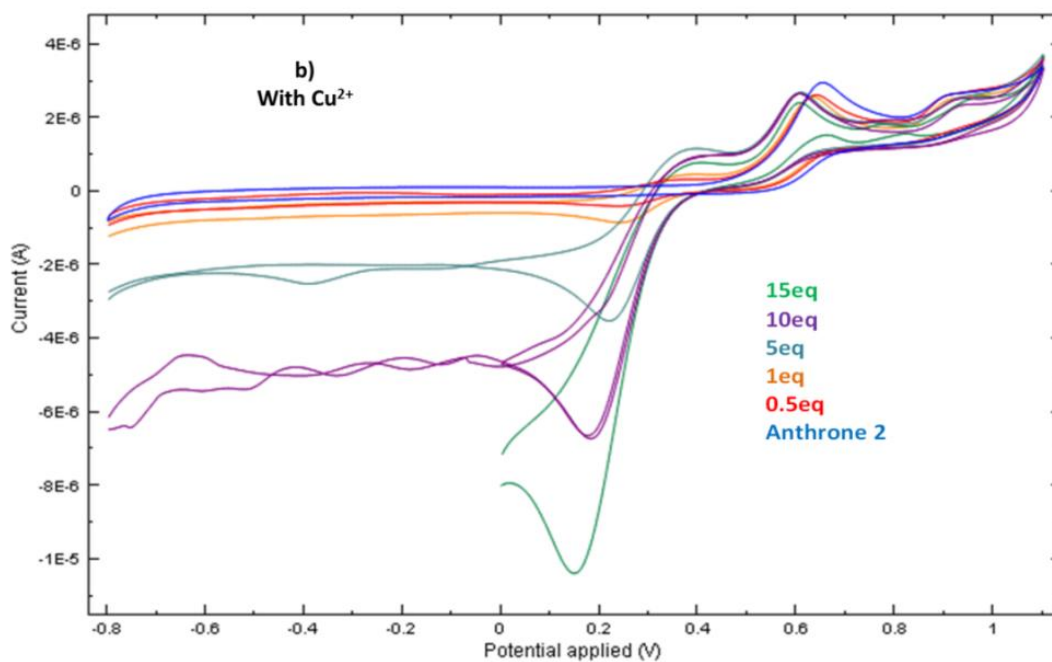
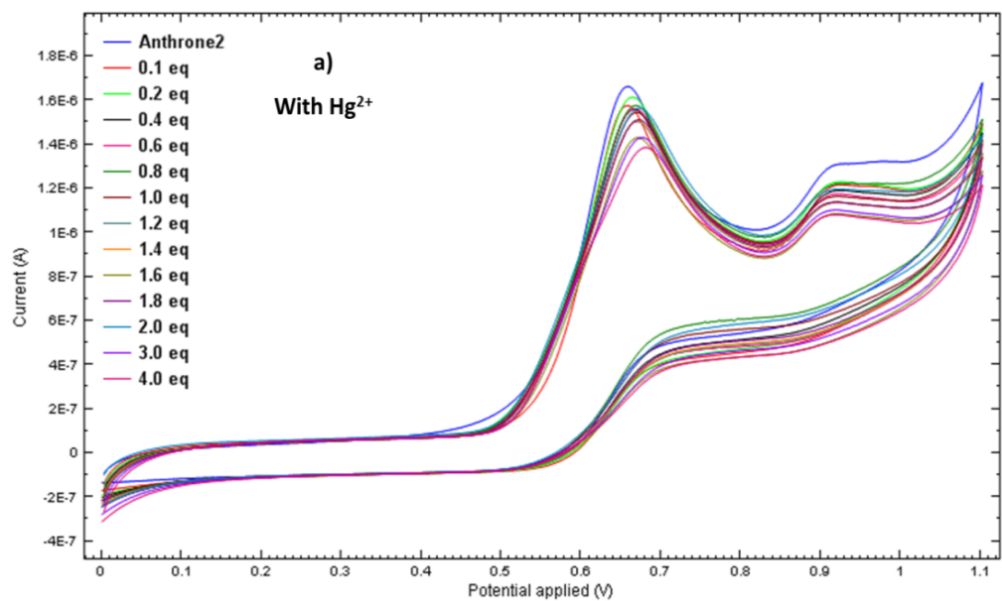


Fig. 5.7 Cyclic voltammograms of anthrone2 with different equivalents of a) Hg^{2+} ion and b) Cu^{2+} in ACN with 0.1M TBAP supporting electrolyte (GC working electrode, scan rate 20 mVs^{-1} and E vs Ag/Ag^+)

Table 5.4 Peak potential (V) values for anthrone2 alone and with different metal ions

Metal ions (1eq)	Peak potentials (V)			
	E _{pa1}	E _{pa2}	E _{pa3}	E _{pc}
Anthrone2 alone	0.657	0.919	-	-
With Cu ²⁺	0.634	0.928	0.376	0.248
With Ni ²⁺	0.659	0.905	-	-
With Pb ²⁺	0.645	0.904	-	-
With Zn ²⁺	0.621	0.892	-	-
With Co ²⁺	0.635	0.895	-	-
With Hg ²⁺	0.665	0.919	-	-

E_{pa}: anodic peak potential and E_{pc} : cathodic peak potential

Anthrone3

For anthrone3, its electrochemical data with respect to Hg²⁺ and Cu²⁺ ions can be seen in Table 5.5. On addition of 0.5 equivalents of Cu²⁺, the cathodic peak almost diminishes accompanied by decrease in anodic peak currents. On further addition of Cu²⁺ concentration, the anodic peak current decreases and is ultimately lost. This is due to the possibility of formation of the product which is electrochemically inert at that potential. On addition of 2 equivalents of the metal ion, a new cathodic peak (0.153V) was observed while the anodic peak (0.168V) diminishes with the addition of 3 equivalents addition (Fig. 5.8a) of the metal ion.

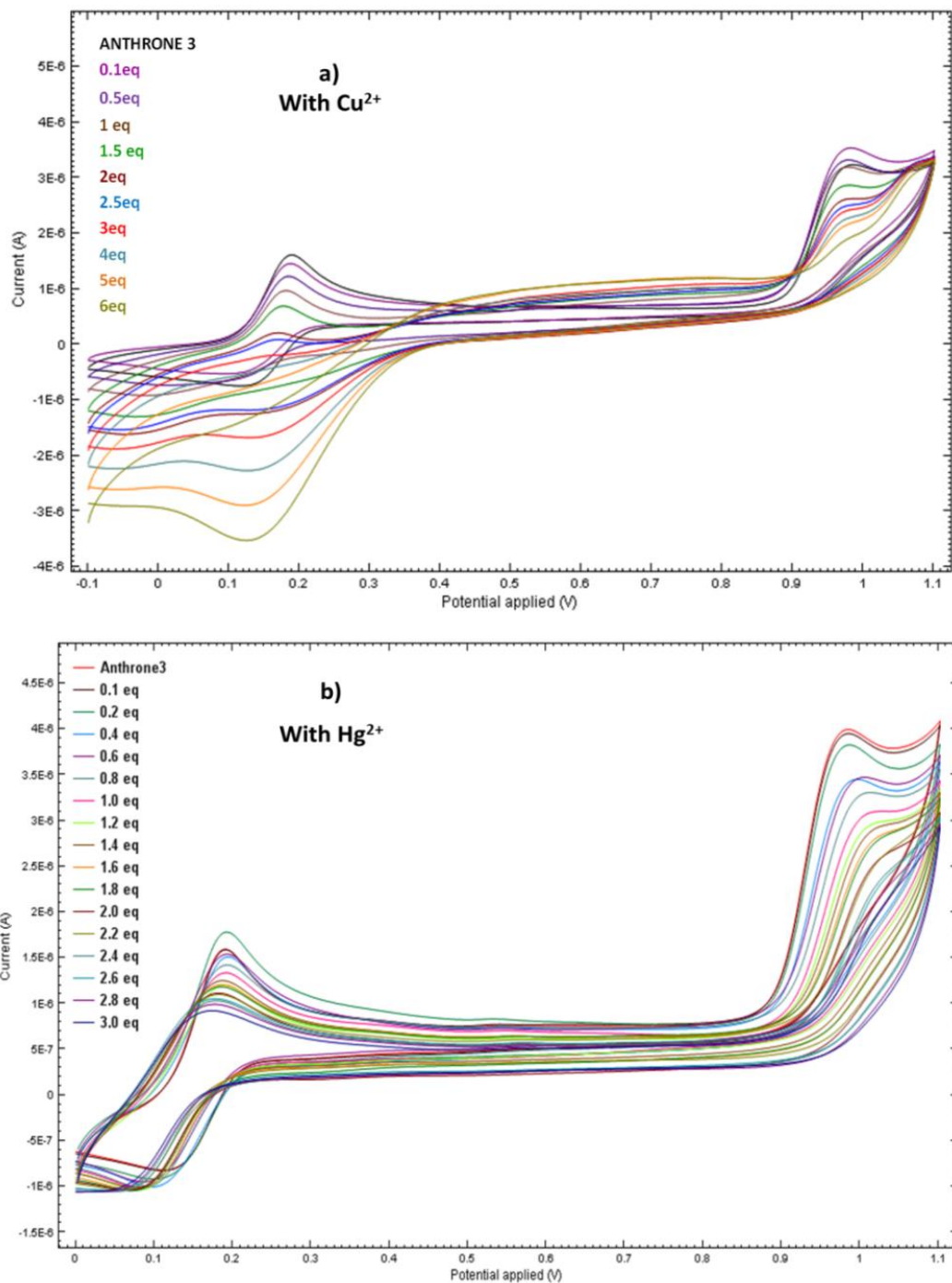


Fig. 5.8 Cyclic voltammograms of anthrone3 with different concentrations of Cu²⁺ a) and b) Hg²⁺ ion, in ACN with 0.1M TBAP supporting electrolyte (GC working electrode, scan rate 20mVs⁻¹ and E vs Ag/Ag⁺)

Table 5.5 Peak potential (V) values of anthrone3 alone and with different equivalents of Cu^{2+} ion

Concentration of Cu^{2+} (Equivalents)	Peak Potentials, V		
	E_{pa1}	E_{pc1}	E_{pa2}
0.0	0.191	0.125	0.984
0.1	0.186	0.112	0.982
0.5	0.184	-	0.98
1.0	0.18	-	0.976
1.5	0.176	-	0.976
2.0	0.168	0.153	0.976
2.5	0.168	0.151	0.976
3.0	-	0.143	0.976
4.0	-	0.138	0.974
5.0	-	0.126	0.974
6.0	-	0.126	-

E_{pa} : anodic peak potential and E_{pc} : cathodic peak potential

Anthrone3 shows a quantitative response towards Hg^{2+} metal ion (at 3 equivalent onwards) as a cathodic shift of about 26 mV can be observed in the oxidation peak (Fig. 5.8b), while the second oxidation peak of anthrone3 at 0.984 decreases with each addition of the metal ion and is finally lost. Cyclic voltammograms of anthrone derivatives with other metal ions shows that these derivatives are responsive to Cu^{2+} and Hg^{2+} metal ions only (Fig. 5.9, 5.10, 5.11).

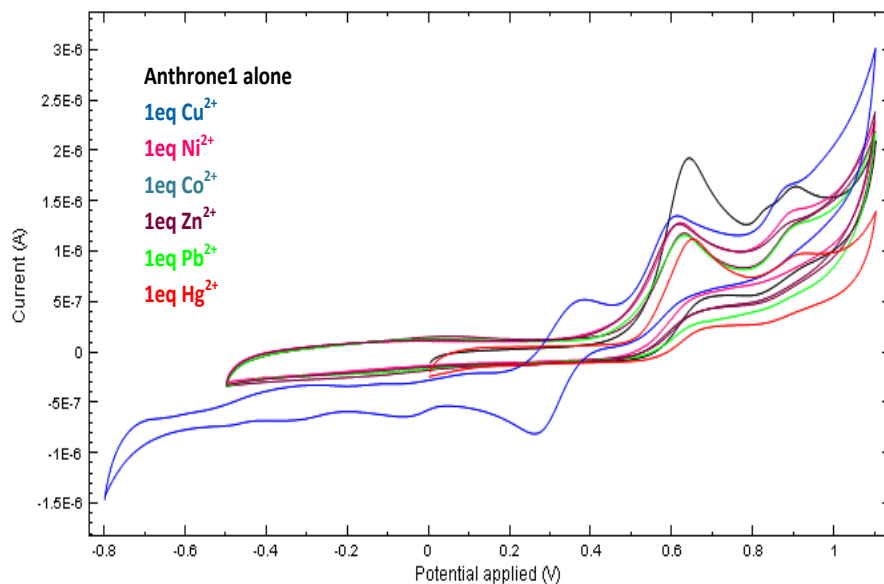


Fig. 5.9 Cyclic voltammograms of anthrone1 with 1 equivalent of different metal ions in ACN with 0.1M TBAP supporting electrolyte, GC working electrode (scan rate 20 mVs^{-1} and E vs Ag/Ag^+)

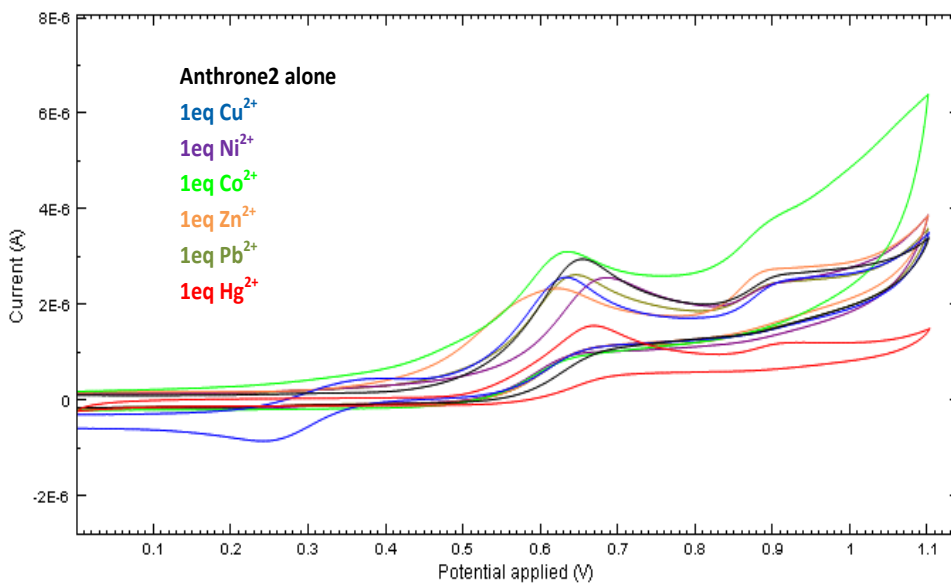


Fig. 5.10 Cyclic voltammograms of anthrone2 with 1 equivalent of different metal ions in ACN with 0.1M TBAP supporting electrolyte (GC working electrode, scan rate 20 mVs^{-1} and E vs Ag/Ag^+)

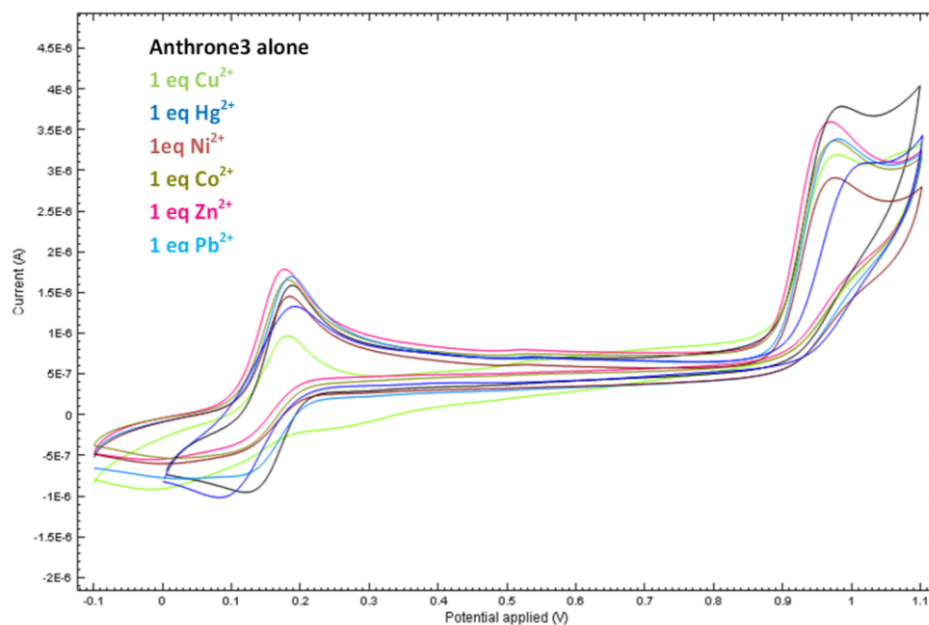


Fig. 5.11 Cyclic voltammograms of anthrone3 with 1 equivalent of different metal ions in ACN with 0.1M TBAP supporting electrolyte, (GC working electrode, scan rate 20 mVs^{-1} and E vs Ag/Ag^+)

5.1.8 Anthrone3 in ACN: Water system

Effect of solvent was observed on CV curves of anthrone3 (Fig.5.12). Anthrone3 voltammogram in 1:1 water: ACN solvent system shows only one redox couple with almost same magnitude of current as observed in pure acetonitrile but with a cathodic shift of about 100mV in peak potentials of redox couple. Also the second oxidation peak as observed in pure acetonitrile is absent in this solvent system. This observation indicates that presence of solvent with high dielectric constant like water results in hydrogen bonding and hence stabilizing anthrone3 to the extent that the second anodic peak does not appear at all. At the same time the redox couple shifts to lower potential. But even on changing the solvent system from pure acetonitrile to 1:1 water: ACN anthrone3 shows more selectivity toward Hg^{2+} and Cu^{2+} ions (Fig. 5.13).

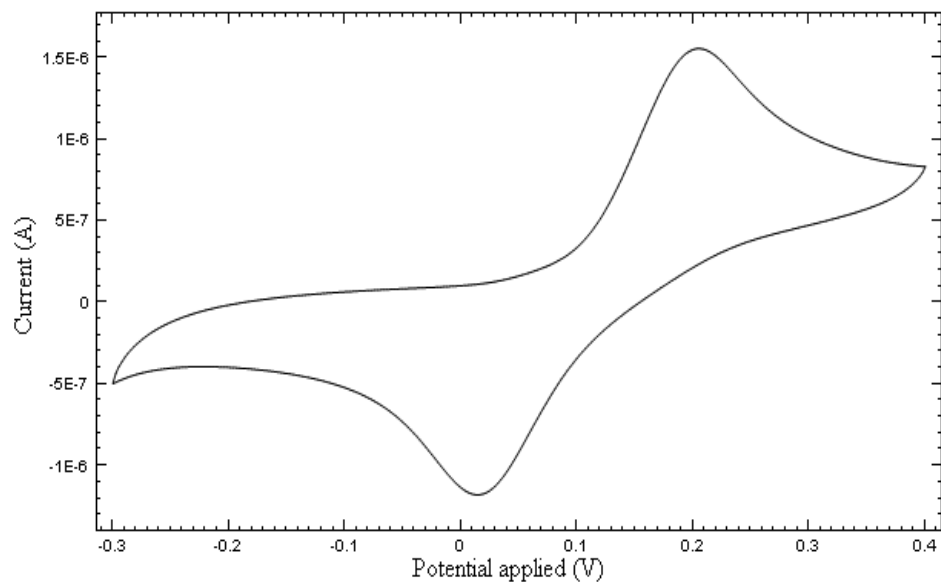


Fig. 5.12 Cyclic voltammograms of anthrone3 10^{-4} M in 1:1 water : ACN with 0.1M HEPES buffer/KCl (pH-7) supporting electrolyte (GC working electrode, scan rate 20 mVs^{-1} and E vs Ag/AgCl)

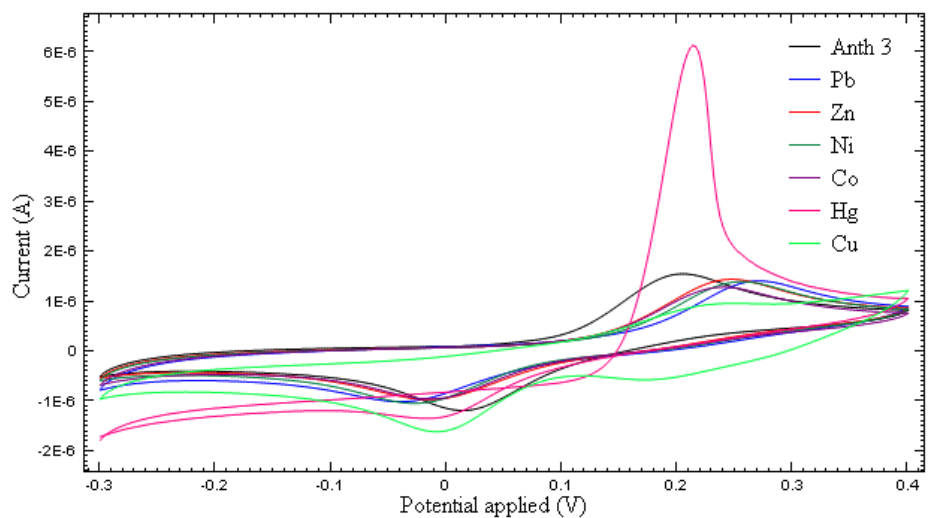


Fig. 5.13 Cyclic voltammograms of anthrone3 with 2 equivalents of different metal ions in 1:1 water : ACN with 0.1M HEPES buffer/KCl (pH-7) supporting electrolyte (GC working electrode, scan rate 20 mVs^{-1} and E vs Ag/AgCl)

5.1.9 Interference study

Voltammetric study was done to know the effect of the presence of other ions on the response of anthrone derivatives for Cu^{2+} and Hg^{2+} ions. All the three derivatives responded selectively to copper ions even in presence of other metal ions (Table 5.6) but for Hg^{2+} ions a very small amount of interference was noticed from Cu^{2+} indicated from the decrease in peak current.

Table 5.6 Peak potential (V) values for anthrone3 alone and with different metal ions

Metal ions (1eq)	Peak potentials (V)		
	E_{pa1}	E_{pa2}	E_{pc}
Anthrone3 alone	0.191	0.984	0.125
With Cu^{2+}	0.180	0.976	-
With Ni^{2+}	0.183	0.975	-
With Pb^{2+}	0.186	0.978	-
With Zn^{2+}	0.177	0.969	-
With Co^{2+}	0.181	0.975	-
With Hg^{2+}	0.190	1.012	0.083

E_{pa} : anodic peak potential and E_{pc} : cathodic peak potential

5.2 Conclusions

1. Anthrone derivatives are electroactive at glassy carbon electrode for cyclic voltammetric studies.
2. Anthrone3, a derivative of anthrone with a center of symmetry is oxidized at a much lower potential than those derivatives with no centre of symmetry (anthrone1 and anthrone2). Better stability of the species is also supported by the electronic resonance structures of the possible intermediate species.
3. Scan rate study indicates the electrochemical reaction for high concentration of the electrolyte, a kinetically controlled process than a diffusion-controlled process.
4. Anodic peak current for ligands increases linearly with increase in their concentration.
5. Increase in polarity of the solvent leads to deformation of the peak shapes and a shift in peak potential also.
6. Anthrone derivatives respond quantitatively with no interference for copper ions in presence of Co^{2+} , Ni^{2+} , Zn^{2+} , Pb^{2+} and Hg^{2+} ions. Hg^{2+} however interferes.

5.3 References

Alfonso, M., Tarraga, A., Molina, P., 2011, A bisferrocene-benzobisimidazole triad as a multichannel ditopic receptor for selective sensing of hydrogen sulfate and mercury ions, *Organic Letters*, 13, 24, 6432-6435.

Batchelor-McAuley, C., Li, Q., Dapin, S.M., Compton, R.G., 2010, Voltammetric characterization of DNA intercalators across the Full pH Range: Anthraquinone-2,6-disulfonate and Anthraquinone-2-sulfonate, *Journal of Physical Chemistry B*, 114, 4094–4100.

Beer, P.D., Gale, P. A., Chen, G. Z., 1999, Mechanisms of electrochemical recognition of cations, anions and neutral guest species by redox-active receptor molecules, *Coordination Chemistry Reviews*, 185–186, 3–36.

Bui, N., Hong, J., Sun-il Mho, Jang, H., 2008, A ferrocene derivative redox sensor for mercuric Ion: synthesis and electrochemical study, *Bulletin of Korean Chemical Society*, 29, 7 1395,

Comminellis, Ch., Plattner, E., 1985, The electrochemical reduction Of anthraquinone to anthrone in concentrated H₂SO₄. *Journal of Applied Electrochemistry*, Short Communications 15.

Chen, S., Webster, R.D., Talotta, C., Troisi, F., Gaeta, C., Neri, P., 2010, Electrochemistry and ion-sensing properties of calix[4]arene derivatives, *Electrochimica Acta*, 55, 7036-7043.

Costero, A.M., Monrabal, E., Andreu, C., Martínez-Máñez, R., Soto, J., Padilla-Tosta, M., Pardo, T., Ochando, L. E., M.Amigó, J., 2000, Synthesis, solution and electrochemical behaviour

of new aza-crown ethers derived from biphenyl, *Journal of Chemical Society, Dalton Transaction*, 361-367.

Dijk V.E.H., Myles, D.J.T., Veen, V., M.H., Hummelen, J.C., 2006, Synthesis and properties of an anthraquinone-based redox switch for molecular electronics, *Organic Letters*, 8, 2333-2336.

Firooz, A.R., Ensafi, A.A., Hajyani, Z., 2013, A highly sensitive and selective bulk optode based on dithiacyclooctadecane derivative incorporating chromoionophore V for determination of ultra trace amount of Hg(II), *Sensors and Actuators B*, 177, 710- 716.

Filho, N.C., E.C. Venancio, E.S. de Medeiros, S.T. Tanimoto, S.A.S. Machado, L.H.C. Mattoso, 2006, *Sensor Letters*, 4, 1, ,6, 11-16.

He, N., Xu, L., Du, J., Li, Z., Deng, Y., Li, S., Ge, S., 2011, Preparation and characterization of porous electrochemical sensor and its application in voltammetric determination of paracetamol, *Sensor Letters*, 9, 1, 199-205.

Jia, H.P., Forgie, J. C., Liu, S.X., Sanguinet , L., Levillain, E., Derf, F. L., Salle, M., Neels, A., Skabara, P. J., Decurtins, S., 2012, Tetrathiafulvalene-annulated dipyrrolylquinoxaline:

the effect of fluoride on its optical and electrochemical behaviors, *Tetrahedron* 68, 1590-1594.

Kong, D., Weng, T., He, W., Liu, B., Jin, S., Hao, X., Liu, S., 2013, Synthesis, characterization, and electrochemical properties of ferrocenylimidazolium, *Journal of Organometallic Chemistry*, 727, 19-27.

Kumamoto, S., Watanabe, M., Kawakami, N., Nakamura, M., Yamana, K., 2008, 2'-anthraquinone- conjugated oligonucleotide as an electrochemical probe for DNA mismatch, *Bioconjugate Chemistry*, 19, 65-69.

Lloris, J.M., Manez, R. M., Soto J., Pardo, T., 2001, An electrochemical study in acetonitrile of macrocyclic or open-chain ferrocene-containing oxa-aza or polyaza receptors in the presence of protons, metal cations and anions, *Journal of Organometallic Chemistry*, 637-639, 151 - 158.

727, 19-27.

Lyskawa, J., Canevet, D., Allain, M., Sallé, M., 2010, An electron-rich three dimensional receptor based on a calixarene-tetrathiafulvalene assembly, *Tetrahedron Letters*, 51, 5868-5872.

Mahajan, R. K., Kaur, R., Bhalla, V., Kumar, M., Hattori, T., Miyano S., 2008, Mercury(II) sensors based on calix[4]arene derivatives as receptor molecules, *Sensors and Actuators B*, 130, 290-294.

Park, D. H., Kang, S. O., Lee, H., Nam, K. C., Jeon, S., 2001, Synthesis and electrochemistry of

diester-anthraquinone as lithium-ion selective receptor, *Bulletin of Korean Chemical Society*, 22, 6.

Shen, J., Hong Tan, C.: 2008, Anthrone-derived NHPI analogues as catalysts in reactions using oxygen as an oxidant, *Organic and Biomolecular Chemistry*, 6, 4096-4098.

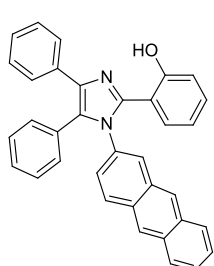
Uauy, R., Olivares, M., Gonzalez, M., 1998, Essentiality of copper in humans, *American Journal of Clinical Nutrition*, 67, 952 S-959S.

Yildiz, E., Keles, T.A., 2009, Synthesis and Characterization of New Cobalt (II), Iron (III) Complexes with Anthraquinone and s-Triazine Moieties, *Synthesis and Reactivity in Inorganic, Metal-Organic, and Nano-Metal Chemistry*, 39, 455-461.

Chemical Sensors Based on Imidazole Derivatives

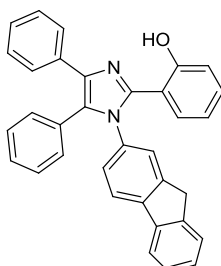
Excessive levels or even small doses of very toxic metals like lead, cadmium, mercury, etc. can cause serious problems on the environment and human health (Scoullou et al, 2001). Accumulation of such metals on the human body can cause diseases in the central nervous system, liver and kidneys, or skin, bones, and teeth (Buica et al, 2009). Sensing and recognition of heavy and transition metal ions by artificial receptors have been receiving considerable attention (Amendola et al, 2006, Wannalarse et al, 2008).

Imidazole is one of the frequently used molecular scaffolds to make supramolecular systems for highly sensitive and selective ion sensing. These molecules are commonly used for anion sensing, because of the presence of -NH- group which acts as the binding site for anions (Gale, 2006). But there have also been reports of imidazole based derivatives capable of exhibiting sensitivity and selectivity towards the metal ions like Fe^{2+} (Chaoliang et al, 2010, Bhaumik et al, 2011), Pb^{2+} (Zapata et al, 2008, Alfonso et al, 2011), Hg^{2+} (Alfonso et al, 2011), Cu^{2+} (Wysiecka et al, 2007, Li et al, 2008), Ni^{2+} and Cu^{2+} (Pyrkosz et al, 2012), Zn^{2+} (Kim et al, 2012) etc. Almost all the reported imidazole based receptors have imidazole substituted at the C-2 position. Molecules studied here along with substitution at C-2 position had amine hydrogen of imidazole ring substituted with anthracene and fluorene groups, making these molecules capable receptors for cation sensing.



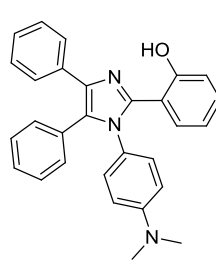
2-(1-(anthracen-2-yl)-4,5-diphenyl-1H-imidazol-2-yl)phenol

TPAN



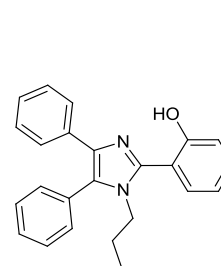
2-(1-(9H-fluoren-2-yl)-4,5-diphenyl-1H-imidazol-2-yl)phenol

TPF



2-(1-(4-(dimethylamino)phenyl)-4,5-diphenyl-1H-imidazol-2-yl)phenol

TPIAM



2-(1-butyl-4,5-diphenyl-1H-imidazol-2-yl)phenol

TPIM

6.1 Results and discussion

6.1.1 Electrochemical behavior of the molecules

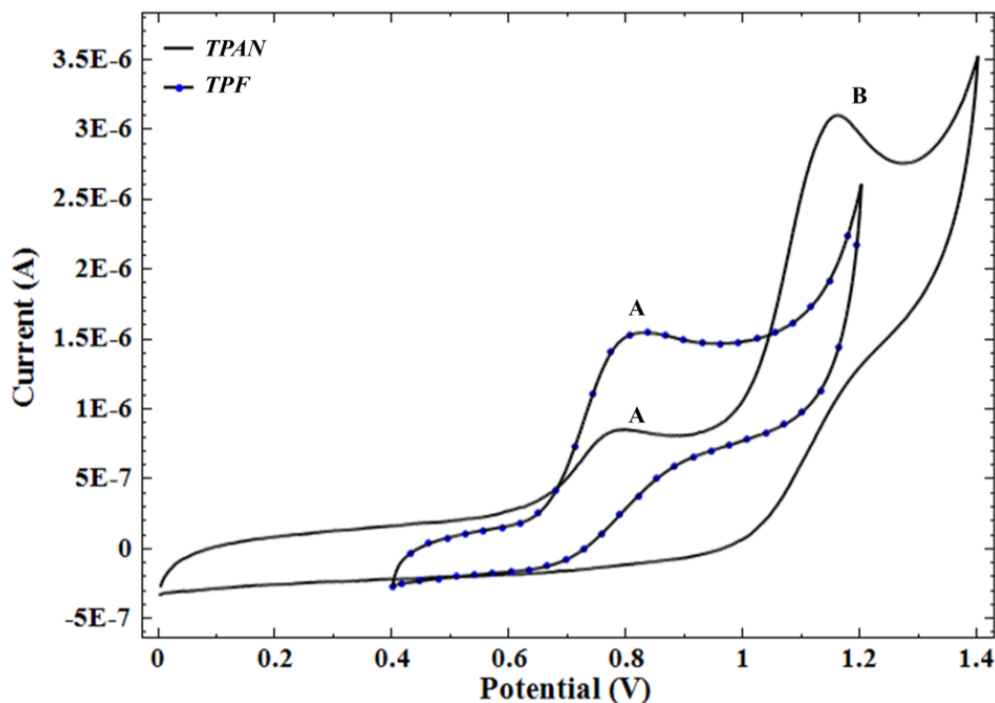


Fig. 6.1 Cyclic voltammograms of TPAN and TPF (10^{-4} M) in acetonitrile (ACN) medium using 0.1M TBAP supporting electrolyte (GC working electrode, scan rate 20 mVs^{-1} E vs Ag/Ag^+)

Voltammetric study of the new molecules 2-(1-(anthracen-2-yl)-4, 5-diphenyl-1H-imidazol-2-yl) phenol (TPAN), 2-(1-(9H-fluoren-2-yl)-4,5-diphenyl-1H-imidazol-2-yl)phenol (TPF), 2-(1-(4-(dimethylamino)phenyl)-4,5-diphenyl-1H-imidazol-2-yl)phenol (TPIAM) and 2-(1-butyl-4,5-diphenyl-1H-imidazol-2-yl)phenol (TPIM) was done in acetonitrile medium under nitrogen environment and at a scan rate of 0.02V/s (Fig. 6.1 and Fig. 6.2). The voltammograms showed two oxidation peaks at 0.75V and 1.15V for TPAN while for TPF showed only one oxidation peak at 0.78V was observed (Fig. 6.1). The voltammograms in Fig. 6.2 showed three oxidation peaks at 0.632V, 0.757V, 0.918V for TPIAM while for TPIM two oxidation peaks were observed at 0.714V, 1.31V. Both TPAN and TPIM showed peaks at almost same potential.

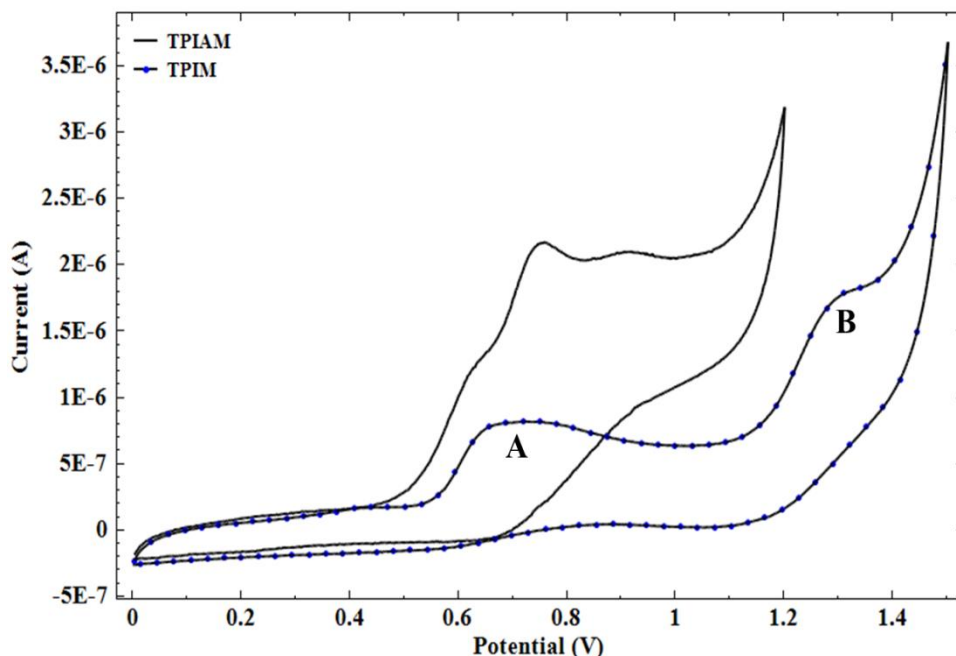


Fig. 6.2 Cyclic voltammograms of TPIAM and TPIM (10^{-4} M) in acetonitrile (ACN) medium using 0.1M TBAP supporting electrolyte (GC working electrode, scan rate 20 mVs^{-1} E vs Ag/Ag^+)

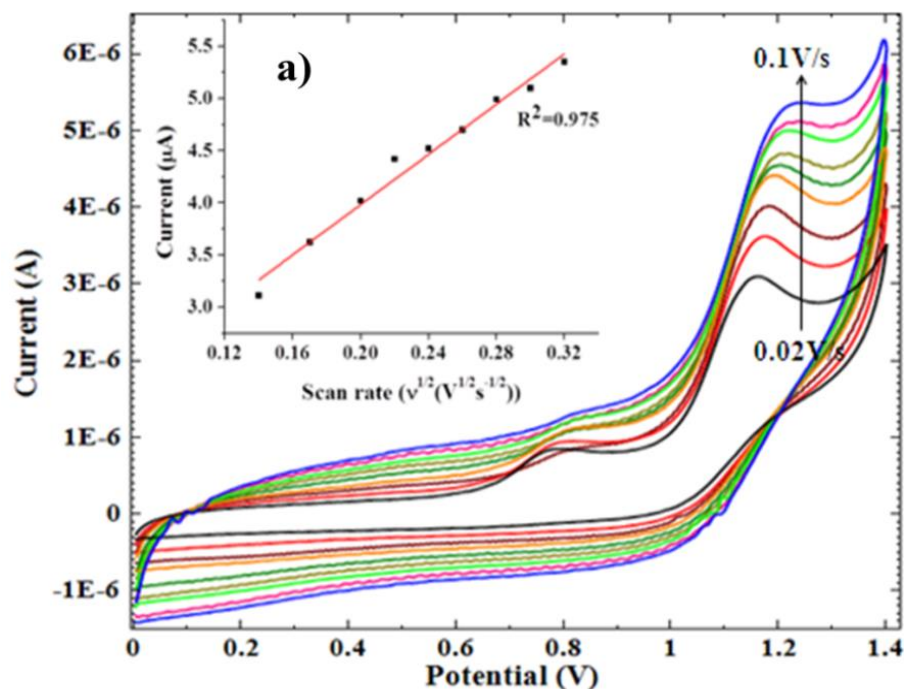
The peak at 0.75V is probably due to electron pair available on hydroxyl group of the substituent of the imidazole base while the stronger oxidation peak at 1.16V is due to the lone pair on N_1 of the imidazole ring. The peak at A is much weaker than the peak B because of the relatively different degrees of respective basicity of the two lone pairs. It needs to be understood here that the lone pair on hetero atom which is conjugated over less no of carbon atoms should behave more basic and would need less energy to be oxidized in comparison to the pair of electrons which is extensively conjugated and should show less basicity hence appear at higher oxidation potential.

This hypothesis is very clearly observed in terms of the appearance of peak A at relatively lower potential (0.75V) than the peak at (1.16V). The shape (broad) and position (0.78V) of the only peak of TPF can be explained on the basis of electronic environment around the lone pairs on oxygen of $-\text{OH}$ group and lone pair on N_1 atom of imidazole group because of the similar electronic environment around these lone pairs. Individual oxidation peaks are merged to appear as a single intense and broad oxidation peak at 0.78V. The appearance of weak peaks in the reverse cycle of the voltammograms indicate a quasi

reversible to irreversible nature of the redox couples of TPAN and TPF ionophore in ACN medium which is further verified with the scan rate study. While for TPIAM the three oxidation peaks observed in close proximity of each other can be because of the presence of three oxidisable sites present in the molecule i.e., -OH group, lone pair on N₁ atom of imidazole ring and lone pair on N₃ atom of the dimethylaminophenyl group.

6.1.2 Effect of scan rate

Scan rate effect was studied to know the behavior of molecules at different scan rates from 20mVs⁻¹ to 100mVs⁻¹. Peak currents of anodic waves were plotted against square root of scan rates separately. A linear relation between peak current and the square root of scan rate indicated a diffusion based process. In Fig 6.3a and 6.3b it can be seen that at scan rates higher than 40mVs⁻¹, the peak potential is shifting linearly with scan rate. While for TPIAM and TPIM scans taken at above scan rate of 40mVs⁻¹, showed huge disturbance and totally irreversible nature. So rest of the study was conducted at lower scan rate (20mVs⁻¹) only.



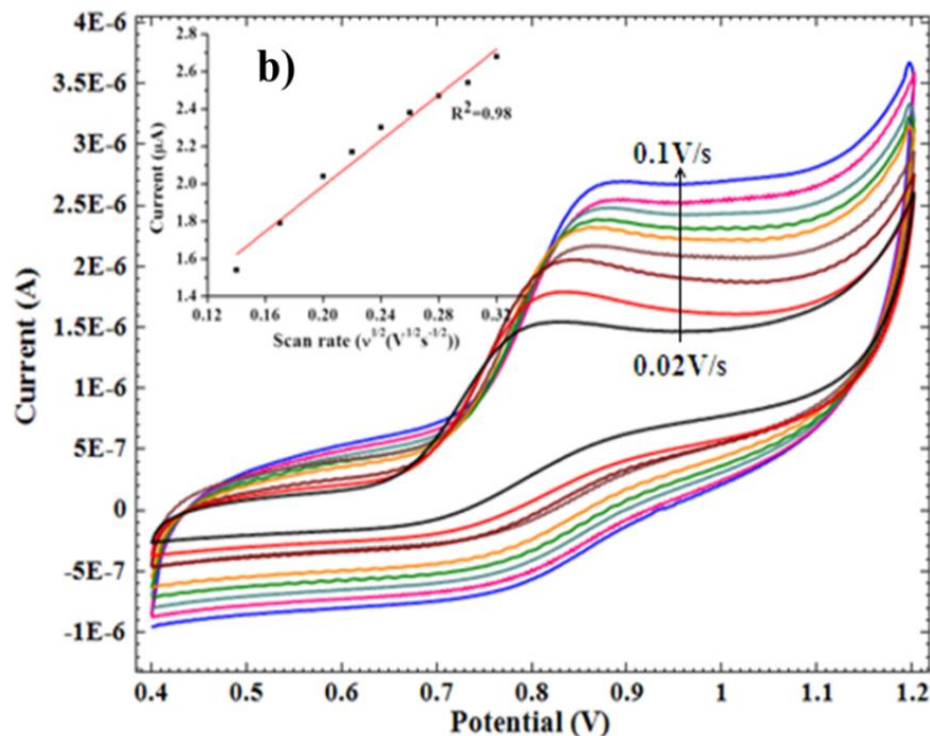
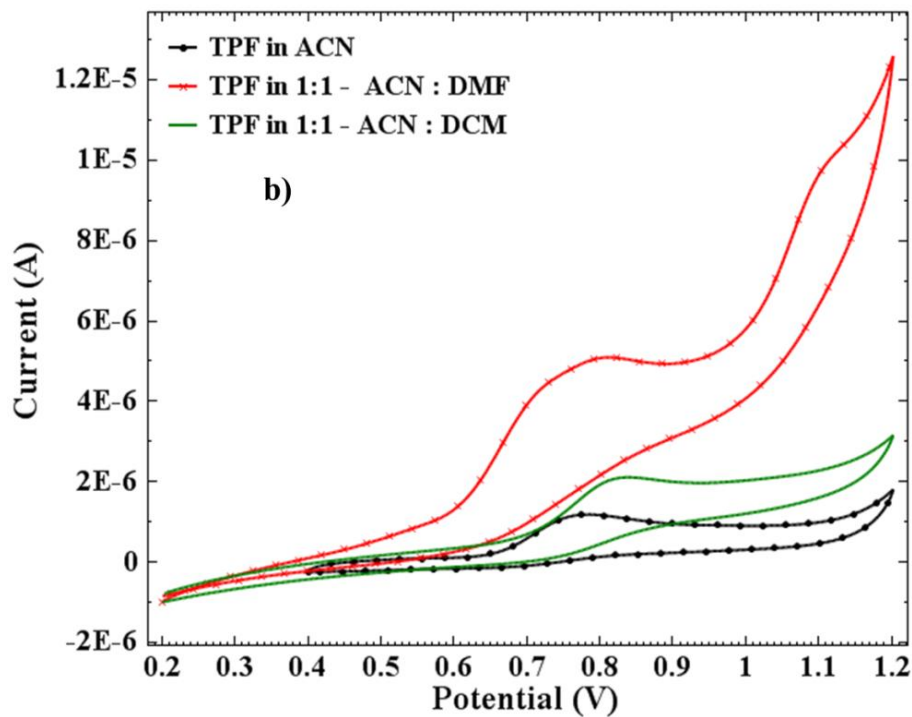
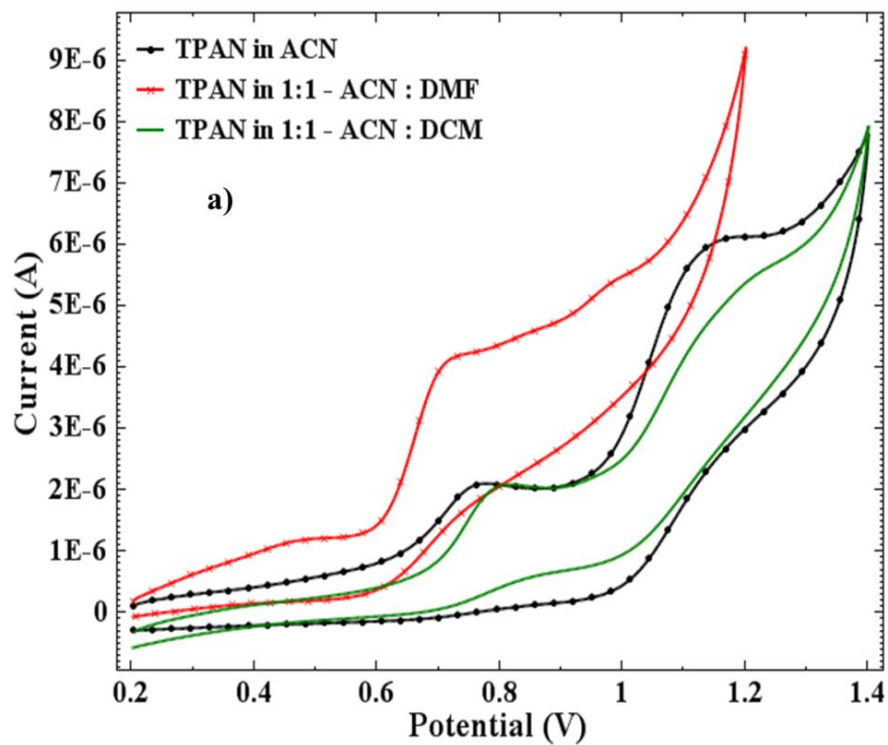


Fig. 6.3 Cyclic voltammograms of TPAN and TPF in acetonitrile (ACN) at different scan rates (10 to 100 mVs⁻¹) using 0.1M TBAP as supporting electrolyte and GC as working electrode

6.1.3 Solvent effect

Voltammetric behavior of the imidazole derivatives was studied in different organic solvents like acetonitrile (ACN, $\epsilon = 37.5$, DN=14.1 kcalmol⁻¹), N,N-dimethylformamide (DMF, $\epsilon = 38.3$, DN=26.6 kcalmol⁻¹) and dichloromethane (DCM, $\epsilon = 9.1$, DN=1 kcalmol⁻¹). Voltammograms show deformation and shift in peaks of both the molecules in DMF. The higher the donor number (DN), the stronger the interaction between solvent and acceptor (Reichardt *et al.*, 2010). Here, donor number of DMF is more than other two solvents, which shows higher ability of solvent to stabilise the molecules leading to deformed peaks with a cathodic shift though dielectric constant of ACN and DMF are almost same. Results shown in Fig 6.4 indicated the great effect of polarity of solvent on the molecules.



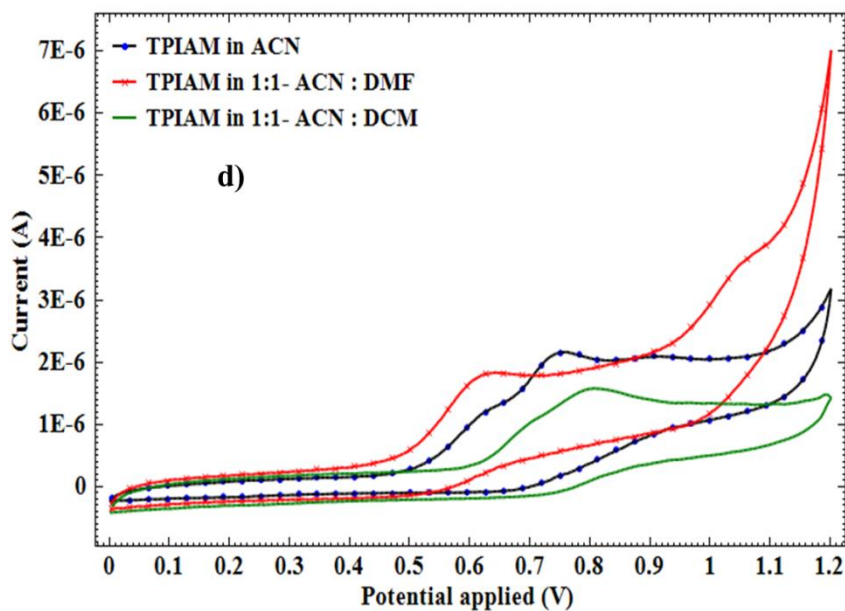
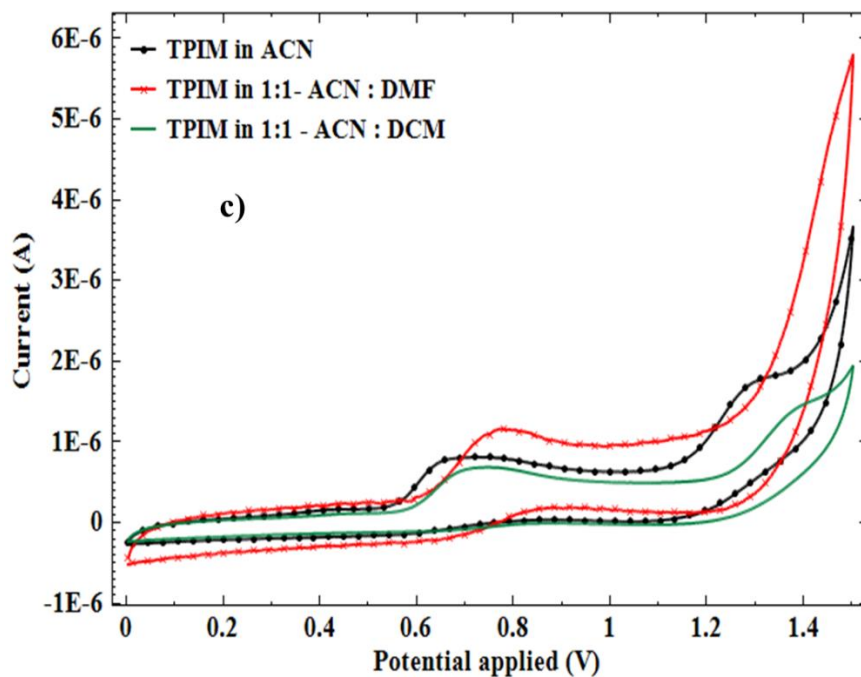


Fig. 6.4 Cyclic voltammograms of 10^{-4} M solution of a) TPAN, b) TPF, c) TPIM and d) TPIAM in different solvents using 0.1M TBAP as supporting electrolyte (GC working electrode, scan rate 20 mVs^{-1} E vs Ag/Ag^+)

6.1.4 Cation interaction

One of the main applications of voltammetric studies of the imidazole derivatives is the quantitative detection of species which can form sufficiently strong complex with the molecules so that a visible change in current magnitude can be correlated to concentration of the target species. To learn more about the properties of TPAN, TPF, TPIM and TPIAM as a cation receptor voltammetric titrations were done with cations like Cu^{2+} , Hg^{2+} , Zn^{2+} , Pb^{2+} , Co^{2+} and Ni^{2+} . TPIM and TPIAM - metal ion interactions were studied on the basis of results obtained from cyclic voltammetry while for TPAN and TPF-ion interaction, cyclic voltammetric studies were accompanied with differential pulse voltammetry.

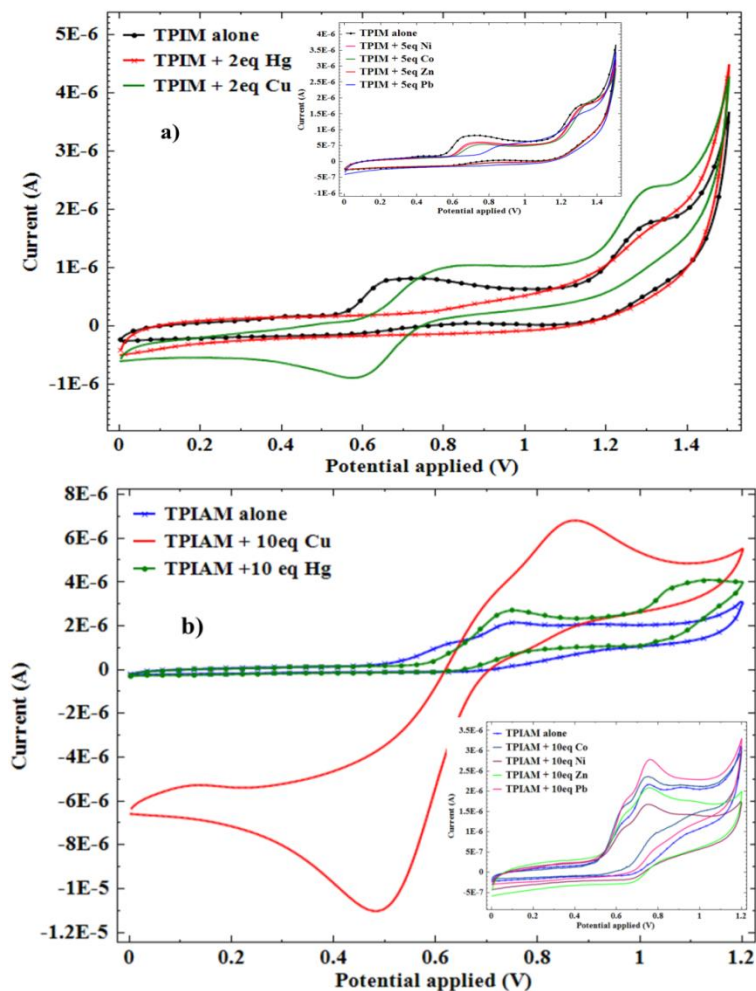


Fig. 6.5 Cyclic voltammograms of a) TPIM and b) TPIAM (10^{-4}M) with different concentrations of Hg^{2+} and Cu^{2+} ions in acetonitrile and in inset- CVs with other metal ions at scan rate 0.02Vs^{-1} , 0.1M TBAP, GC as working electrode.

Cyclic voltammograms of TPIM and TPIAM (Fig 6.5a and 6.5b) after interaction with metal ions show that both the molecules showed substantial change in peak potentials and current for Hg^{2+} and Cu^{2+} ions. While with other metal ion like Ni^{2+} , Co^{2+} , Zn^{2+} and Pb^{2+} negligible changes in peak potential and currents were observed even at 10 equivalents of these metal ions. In case of TPIM on interaction with Hg^{2+} ion both the peaks got diminished showing that EC mechanism has been followed i.e., electrochemical process followed by a chemical reaction giving electrochemically inactive product. On the other hand interaction with Cu^{2+} ion gave a 140mV of anodic shift in peak potential of peak at 0.71V along with a generation of new reduction peak at 0.58V. TPIAM showed similar trend on interaction with Cu^{2+} ion with a reduction peak emerging at 0.486V accompanied by an anodic shift of 100 mV in the oxidation peak at 0.75V. For Hg^{2+} ions, TPIAM showed a new oxidation peak at around 1.1V, alongwith the shift in potential of its other oxidation peaks. Out of these two molecules, TPIM showed better sensing toward

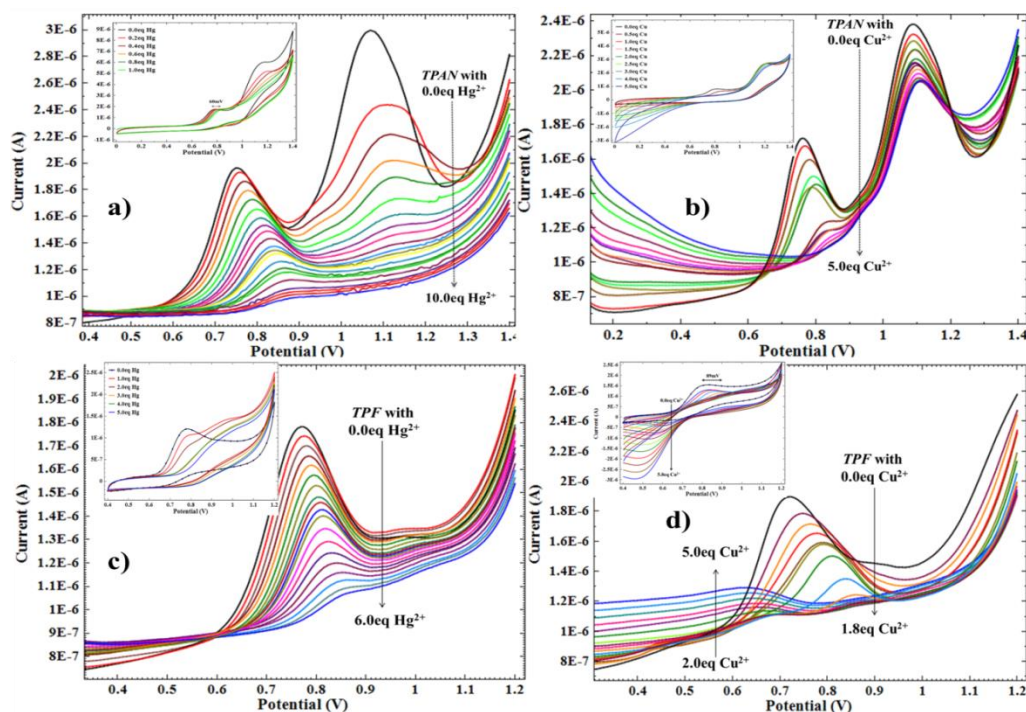


Fig. 6.6 Differential pulse voltammograms of TPAN and TPF (10^{-4}M) with different concentrations of Hg^{2+} and Cu^{2+} ions in acetonitrile and corresponding CV studies (in inset)

The changes in the peak current and peak potential of TPAN and TPF on addition of these metal ions were used to monitor their binding behavior with differential pulse voltammetry. All the voltammetric titrations were carried out by taking standard solution of molecules (10^{-4} M) in pure acetonitrile medium by adding aliquots of metal ions ($0-10^{-3}$ M). The changes were observable only upon addition of Hg^{2+} and Cu^{2+} ions. While for other metal ions, no significant changes were observed under the same conditions from which it was concluded that both TPAN and TPF show selectivity towards Cu^{2+} and Hg^{2+} ions.

6.1.5 Differential pulse voltammetry- a quantitative study

TPAN

Voltammogram of TPAN were recorded in acetonitrile medium at 20 mVs^{-1} scan rate for successive additions of Hg^{2+} ion solution over a concentration range of 0.0eq to 10.0eq of Hg^{2+} . The plots are shown in Fig. 6.6a. As per our previous observation, current intensity of peak B decreased successively from $3 \times 10^{-6} \text{ A}$ to $1 \times 10^{-6} \text{ A}$ on increasing the addition of Hg^{2+} ions from 0 to 10eq. Although decrease in current intensity of peak B was accompanied by relatively much less decrease in current intensity for the peak A, it is important to notice here that the peak A does not get quenched even at 10-fold increase in concentration of Hg^{2+} ions to that of TPAN. This behavior of the molecule can be used for selective quantification of the Hg^{2+} ions. From DPV response curves in presence of different concentration of copper ions (Fig. 6.6b), it is observed that with each successive addition of copper ions there is a fall in the current magnitude of peak A accompanied with relatively small changes in current of Peak B.

TPF

The TPF molecule also behaves the same way the TPAN did, as with successive additions of Hg^{2+} ions from 0.0eq to 6.0eq peak current intensity of the only peak in the anodic region decreases successively and linearly with corresponding increased presence of Hg^{2+} ions. This trend in current magnitude is shown in Fig. 6.6c. In the presence of copper ions the TPF responds in an interesting way. Here, with each successive addition of Cu^{2+} ions

from 0.0eq to 1.8eq of Cu^{2+} ions the peak current intensity decreases linearly with simultaneous appearance of a new peak at 0.65 V (Fig. 6.6d). It is still difficult to explain appearance of the new peak. Probably, the TPF copper complex is behaving as a lewis base. This observation was, however, not seen in case of TPAN.

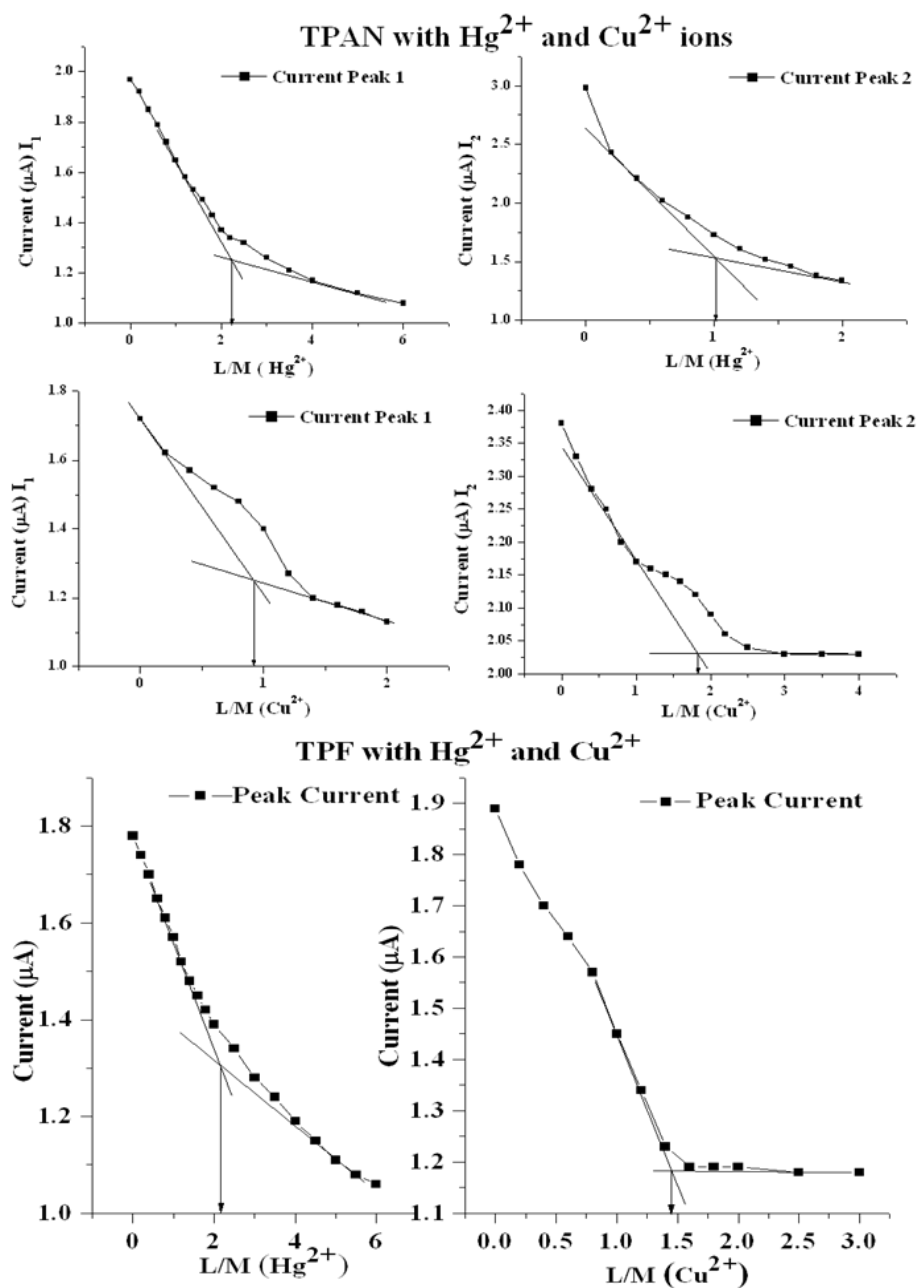


Fig 6.7 Plots of current vs L/M ratio for TPAN and TPF with Hg^{2+} and Cu^{2+} ions

Most possible sites for interaction in both the molecules are the two nitrogen atoms present in imidazole ring which can interact with cations because of the availability of lone pair of electrons on them. From the voltammograms of TPAN in presence of Hg^{2+} and Cu^{2+} , it can be concluded that mercury and copper ions interact with the molecules from different binding sites. Quantitatively, TPAN binds Hg^{2+} in 1:2 ratio at site 1 and 1:1 ratio at site 2 as per ratiometric method (Fig. 6.7). While DPV for TPF with Hg^{2+} and Cu^{2+} ions show that both ions interact differently with it. TPF forms 1:2 complex with Hg and 1:1 complex with copper. Other metal ions show very weak interaction with both the molecules.

It can be very clearly concluded that the change in current of peak A can be associated with the presence of copper ions and that of peak B with mercury ions. The hypothesis presented above is confirmed from the following observation: DPV for TPAN are recorded in presence of both mercury and copper ions taken in equal concentrations; both the peaks A and B are seen as quenched, confirming that the two peaks are responding independently to the concentration of Cu^{2+} and Hg^{2+} ions.

6.1.6 Interference study

Interference studies were done to know the selectivity of both the molecules (Fig 6.8). Differential pulse voltammograms were taken for TPAN(10^{-4} M) and TPF (10^{-4} M) in presence of Hg^{2+} (2eq), Cu^{2+} (2eq) individually and then in presence of other metal ions like Co^{2+} , Ni^{2+} , Zn^{2+} and Pb^{2+} . Even the presence of 10-fold concentration of these ions (Co^{2+} , Ni^{2+} , Zn^{2+} and Pb^{2+}), did not show any change in voltammetric response TPAN and TPF towards Hg^{2+} and Cu^{2+} ions, indicating that there is no interference from these cations.

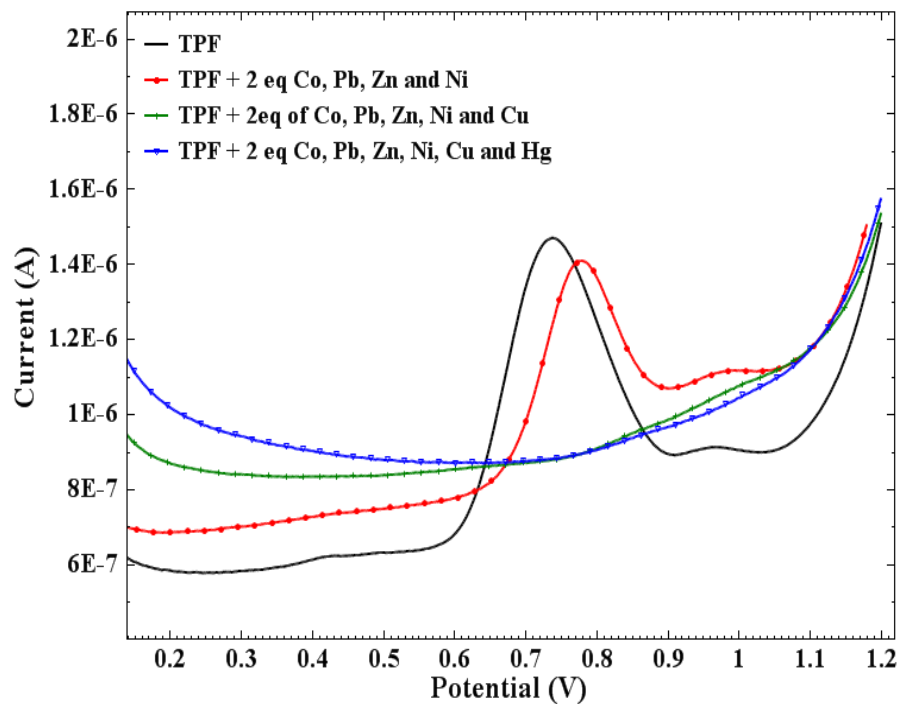
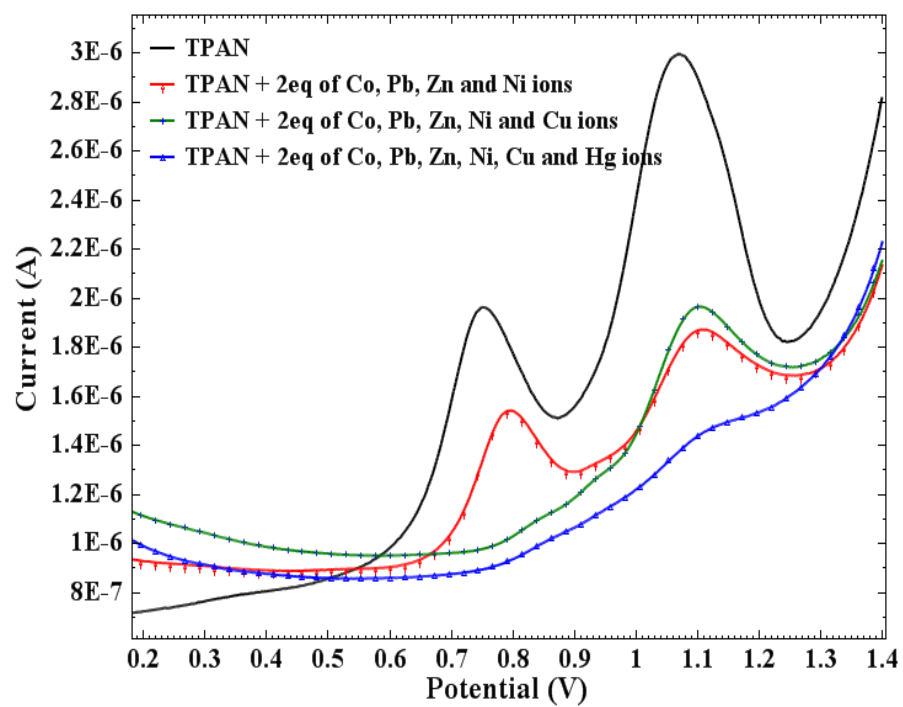


Fig. 6.8 Differential pulse voltammograms of TPAN and TPF (10⁻⁴M) in presence of different metal ions, at amplitude 25mV, scan rate 0.02Vs⁻¹

6.1.7 Sensitivity (LOD and LOQ)

Sensitivity of molecules was determined from the limit of detection (LOD) and limit of quantification (LOQ) values based on 3-sigma method. A plot of current (μA) versus concentration (μM) resulted in a straight line. The experiment was repeated 3 times and the representative curve from the 3 sets of data was used for further calculations of LOD and LOQ. By using 3-sigma method the limit of detection was found to be $1.1 \mu\text{M}$ and limit of quantification value comes out to be $3.3 \mu\text{M}$ by both the molecules for Hg^{2+} and Cu^{2+} ions.

6.2 Conclusions

Cyclic voltammetric study of imidazole based molecules TPAN, TPF, TPIM and TPIAM showed irreversible electrochemical nature. Further on interaction with Hg^{2+} , Cu^{2+} , Co^{2+} , Ni^{2+} , Zn^{2+} and Pb^{2+} metal ions, all the molecules showed qualitative and quantitative selectivity toward Hg^{2+} and Cu^{2+} ions only, even in presence of other interfering ions. From DPV studies it was also concluded that Hg^{2+} and Cu^{2+} interact differently with TPAN and probably at its different sites.

6.3 References

- Alfonso, M., A.,** Tarraga, P., Molina, 2011, A bisferrocene-benzobisimidazole triad as a multichannel ditopic receptor for selective sensing of hydrogen sulfate and mercury ions, *Organic Letters*, 13, 24, 6432-6435.
- Alfonso, M.,** Espinosa, A., Tarraga, A., Molina, P., 2011, A simple but effective dual redox and fluorescent ion pair receptor based on a ferrocene-imidazopyrene dyad, *Organic Letters*, 13, 8, 2078-2081.
- Amendola, V.,** Fabbrizzi, L., Forti, F., Licchelli, M., Mangano, C., Pallavicini, P., Poggi, A., Sacchi, D., Taglieti, A., 2006, Light-emitting molecular devices based on transition metals, *Coordination Chemistry Review*, 250, 273–299.
- Bhaumik, C.,** Das, S., Maity D., Baitalik, S., 2011, A terpyridyl-imidazole (tpy-HImzPh₃) based bifunctional receptor for multichannel detection of Fe²⁺ and F⁻ ions, *Dalton Trans.*, 40, 11795–11808.
- Buica, G.O.,** Bucher, C., Moutet, J.C., Royal, G., Saint-Aman, E., Ungureanu, E.M., 2009, Voltammetric sensing of mercury and copper cations at Poly(EDTA-like) film modified electrode, *Electroanalysis*, 21, 77.
- Chaoliang, T.,** Qianming, W., 2010, Anion/Cation (H₂PO₄⁻ and Fe³⁺) induced dual luminescence quenching effect based on terbium solid sensor, *Journal of Rare Earths*, 28, 6, 888-892.
- Gale, P.A.,** 2006, Special issue for anion complexation, *Coordination Chemistry Reviews*, 250.
- Kim, M.J.,** Kaur, K., Singh, N., Jang, D.O., 2012, Benzimidazole-based receptor for Zn²⁺ recognition in a biological system: A chemosensor operated by Retarding the excited state proton transfer, *Tetrahedron*, 68, 27–28, 5429-5433.
- Li, Z.,** Lou, X., Yu, H., Li, Z., J., Qin, 2008, An imidazole-functionalized polyfluorene derivative as sensitive fluorescent probe for metal ions and cyanide, *Macromolecules*, 41, 7433-7439.
- Reichardt, C.,** Welton, T., 2011, Solvents and Solvent Effects in Organic Chemistry, Edn. 4, WILEY-VCH, ch-2, pp. 26.
- Scoullos, G.H.,** Vonkeman, M.J., Thorton, L., Makuch, Z., 2001, In Mercury, Cadmium, and Lead: Handbook for Sustainable Heavy Metals Policy and Regulation (Environment & Policy); Kluwer Academic: Norwell, MA,; Vol. 31.
- Wannalarse, B,** Tuntulani, T., Tomapatanaget, B., 2008, Synthesis, optical and electrochemical properties of new receptors and sensors containing anthraquinone and benzimidazole units, *Tetrahedron*, 64, 10619-10624.
- Wysiecka, E.W.,** Jamrogiewicz, M., Fonarib, M.S., J.F., Biernat, 2007, Azomacrocyclic derivatives of imidazole: synthesis, structure, and metal ion complexation properties, *Tetrahedron* 63, 4414–4421.

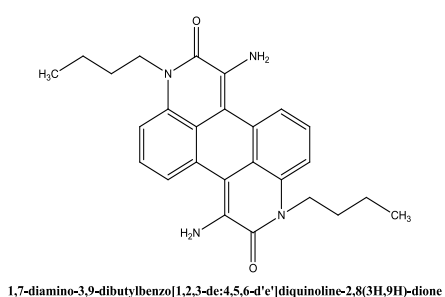
Chemical Sensing with Electrode Modification

Electrochemical analysis based on electrode modification is an interesting field used for heavy metal ion sensing (Heitzmann et al, 2005). Electrode modification with screen printing technology is now a well-established technique for both chemical and biosensors (Kampouris et al, 2009, Somerset et al, 2010, Emanuel et al, 2010 Sljukic et al, 2011). Screen printing has been developed over many years and one of its best known applications is the production of low cost disposable glucose sensors for diabetics to monitor blood glucose levels (Montessino et al, 2001, Grennan et al 2001). There are lots of reports on modified SPEs for detection of heavy metal ions using stripping voltammetry. Bernalte et al, 2011 used screen printed gold electrodes for the determination of mercury by square wave anodic stripping voltammetry while Hallam et al, 2010 reported electrochemical sensing of Cr (VI) with graphite screen printed electrodes. There are no reports on anthrone derivatives being studied as modified voltammetric sensors for cations.

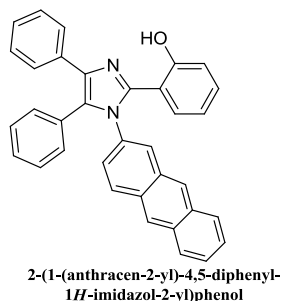
Another improved and miniature alternative to the conventional GC electrodes are chemically modified electrodes. Conducting polymers are widely used to make sensors by modification of electrodes. The use of an electrode modified with a ligand having a high affinity for a given metal cation will ensure highly sensitive and selective measurements, and can reduce interferences compared to conventional voltammetric techniques. From application point of view, polyaniline in the semioxidized, i.e. polyemeraldine form (PANI), seems to be the most promising conducting polymer as it is easy to prepare, low cost, environmentally as well as thermally stable. Polyaniline modified electrodes have been widely used for biosensing (Tahir et al, 2005, Dhand et al, 2011), as potentiometric sensor for Ag^+ ions using thiacalix[4]arene as neutral carrier (Evtugyn et al, 2007) as conductometric Hg^{2+} sensor (Muthukumar et al, 2007) and as a gas sensor for ammonia (Xu et al, 2007, Manigandan et al, 2008). Reports of polyaniline modified with organic molecules/receptors for voltammetric ion sensing are almost negligible.

This chapter is comprised of two parts based on studies of screen printed electrode and polyaniline modified electrode. Voltammetric behaviour of screen printed electrodes of anthrone derivatives (SPE-A) was studied and their response towards different cations is reported here. Reports of SPE modified with synthesized organic molecule used for ion sensing purpose are rare (Hallam et al, 2010). The results were compared with those on bare glassy carbon electrode using anthrone³ in solution phase. Surface morphology of screen printed electrodes is also reported.

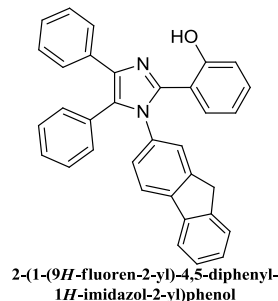
An attempt was made to project imidazole based molecules (TPAN and TPF) as voltammetric cation sensors. Concept of this sensor is based on the imidazole derivatives (as receptors) immobilized onto polyaniline modified glassy carbon electrode (as transducer), interacting with cations through hydrogen bonding. Modification of electrode with polyaniline enhanced the response and sensitivity toward Hg²⁺ ions.



Anthrone 3



TPAN



TPF

7.1 Anthrone modified screen printed electrode (SPE-A)

7.1.1 Voltammetric study of anthrone³ using glassy carbon electrode and screen printed electrode modified with anthrone³

Cyclic voltammetric studies were carried out using screen printed electrode modified with anthrone³ (SPE-A) as well as with bare GC electrode in 1:1 water-acetonitrile solution mixture of anthrone³. Voltammograms with both electrodes displayed sharp and distinct peaks of reversible nature for anthrone³. A redox couple was obtained at 0.076 V, 0.019 V

and 0.03 V, 0.21 V for SPE-A and anthrone3, respectively, which can be explained on the basis of mechanism shown in Scheme 1.

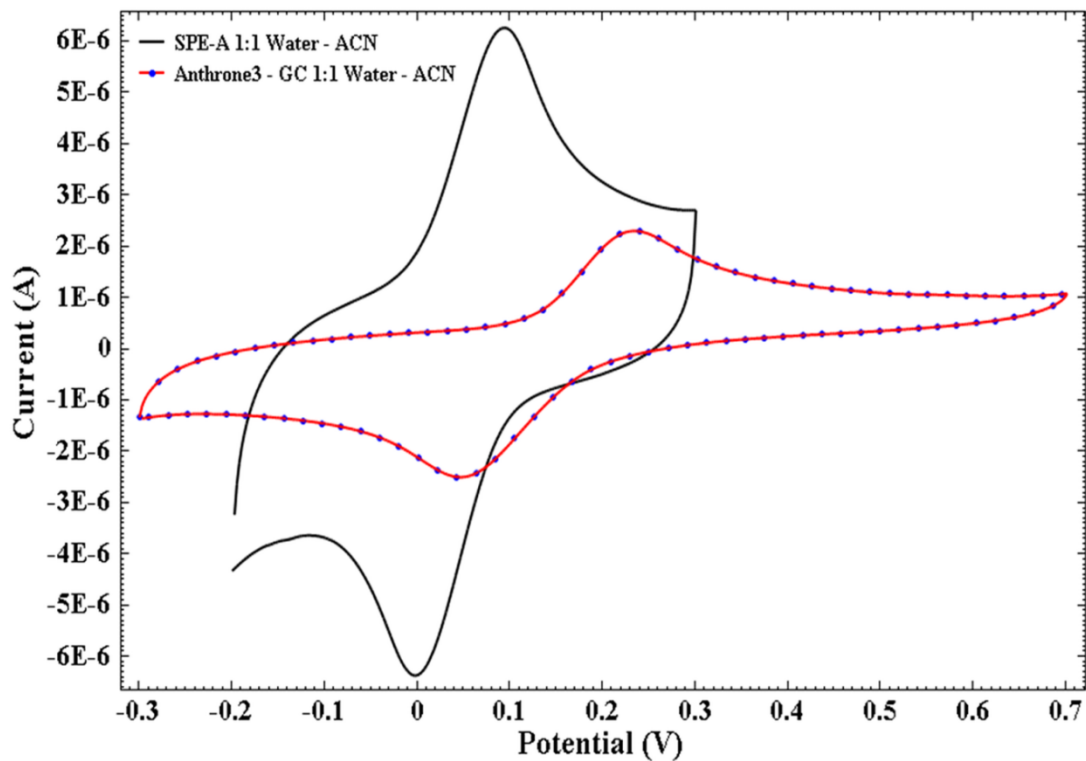
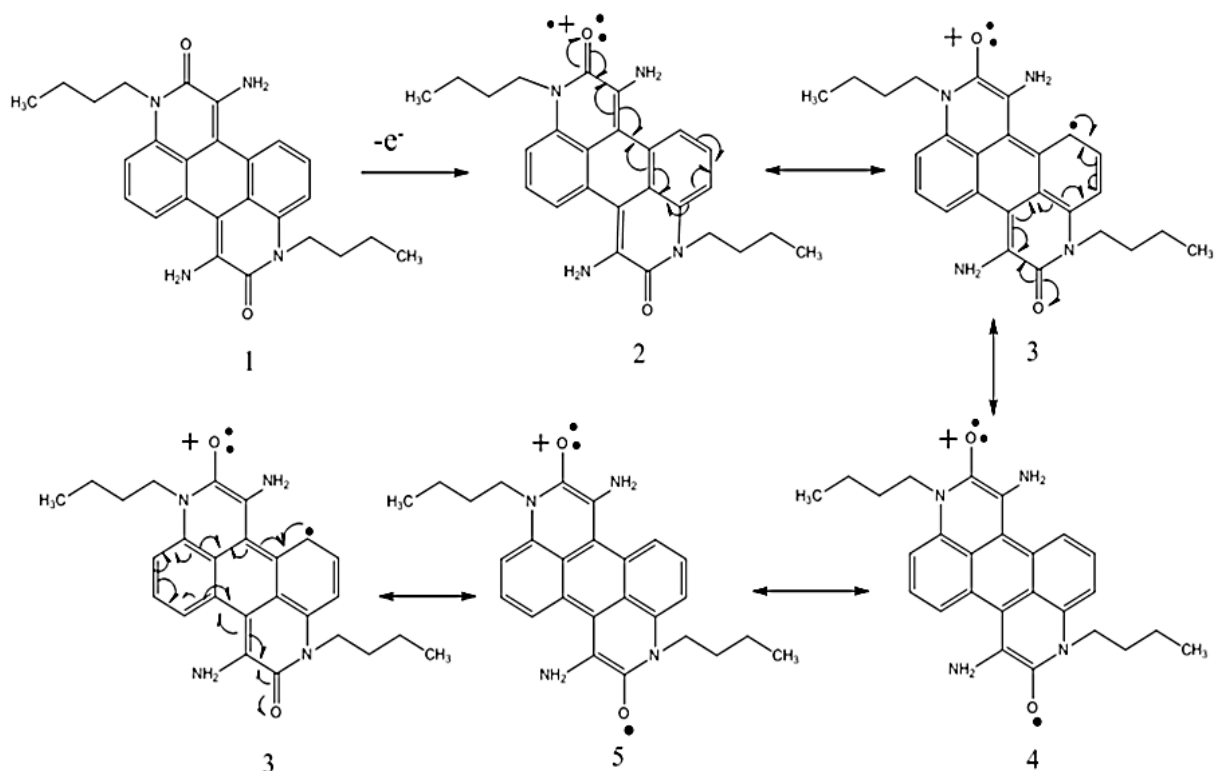


Fig. 7.1 Cyclic voltammogram of anthrone3 (solution phase) with GC as working electrode and SPE-A, in 1:1 Water - ACN solvent system. Scan rate: 0.02Vs^{-1} ; Supporting electrolyte: 0.1M KCl, pH 7, E vs Ag/AgCl)



Scheme 1 Resonance stabilisation of substituted anthrone3 through conjugation of lone pairs on oxygen of -CO group

Current magnitude (6.4 mA) of anodic peak of anthrone3 impregnated in SPE was about three times the current obtained with GC electrode for the same substrate and the solvent media (Fig. 7.1). Voltammograms with SPE showed a cathodic shift of about 100 mV in anodic region and about 50 mV in cathodic region. Both the curves were reproducible and were recorded several times. The differences in shifts in peak potentials (100 mV and 50 mV, respectively in anodic and cathodic regions) can be explained in terms of the $\Delta E_{\text{SPE-A}}$ (57 mV) and ΔE_{GC} (180 mV). The lesser value of $\Delta E_{\text{SPE-A}}$ is due to faster electron transfer in SPE than in GC because of the fast charge transfer between the ionophore and the ink of the SPE matrix working as the carbon electrode as compared to the GC electrode.

7.1.2 Solvent effect

To understand the effect of different solvent mixtures, experiments were conducted to record voltammograms for both SPE-A and anthrone3 in solution phase. The water-

acetonitrile solvent mixtures were taken in different volume ratios of 10:0, 7:3 and 1:1 (Fig. 7.2 and Fig. 7.3). The results with 1:1 water: acetonitrile were the most reproducible and stable. The voltammograms in this selected solvent mixture using GC electrode showed only one redox couple and a cathodic shift of about 100 mV from that of peak potential in pure acetonitrile medium (Fig. 7.4).

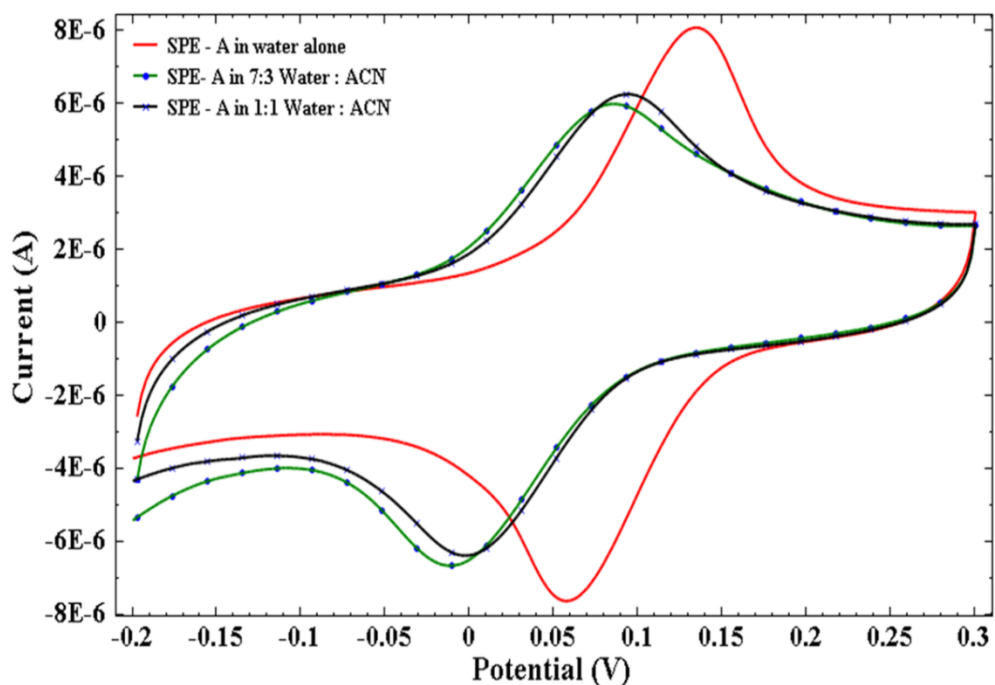


Fig. 7.2 Effect of solvent system on anthrone3 modified screen printed electrode (scan rate 0.02Vs^{-1} , supporting electrolyte 0.1M KCl, pH 7, E vs Ag/AgCl)

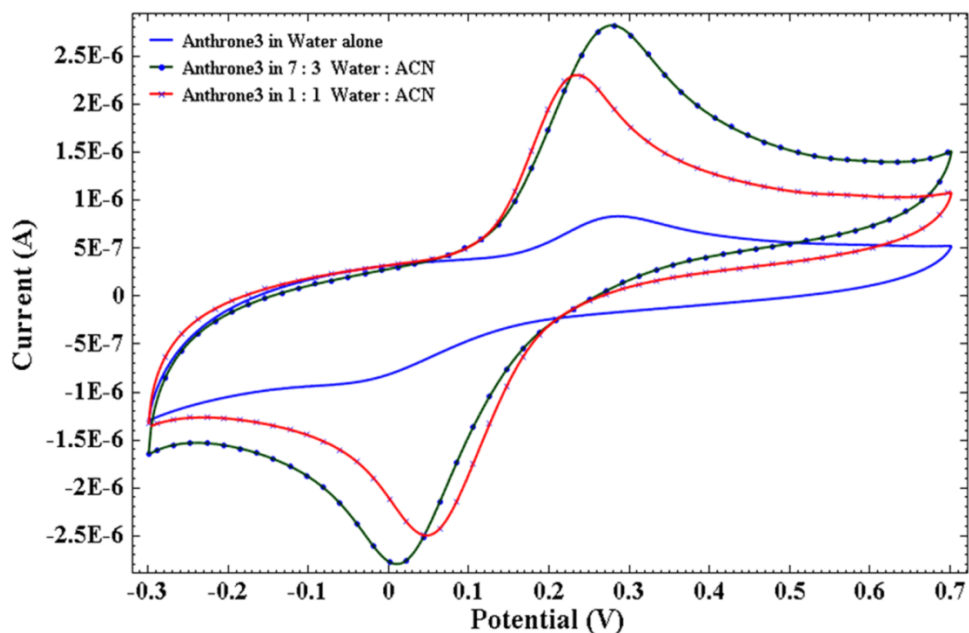


Fig. 7.3 Effect of solvent system on anthrone3 (solution phase) with GC as working electrode (scan rate 0.02V s^{-1} , supporting electrolyte 0.1M KCl , pH 7, E vs Ag/AgCl)

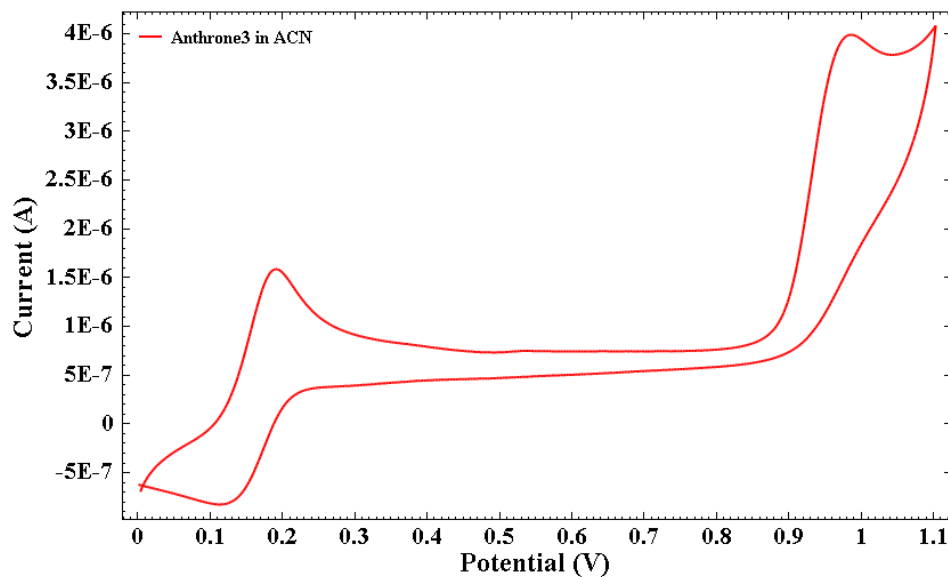


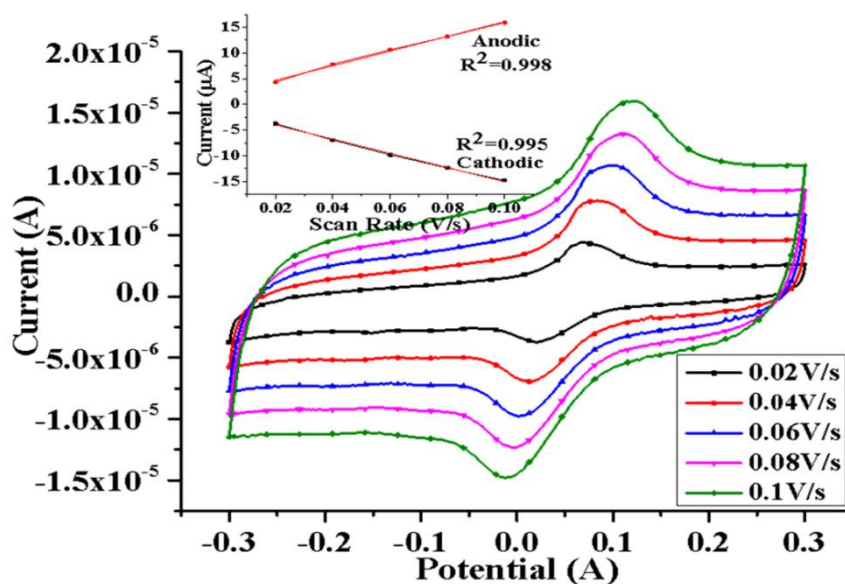
Fig. 7.4 Cyclic voltammogram of anthrone3 in acetonitrile solvent, with 0.1M TBAP as supporting electrolyte (GC working electrode, scan rate 20 mVs^{-1} E vs Ag/Ag⁺)

The oxidation peak at 0.98 V was found quenched in the solvent mixture medium. Similar behaviour was observed with SPE-A but with increased current magnitude. This

voltammetric behaviour in the solvent mixture may be due to high dielectric constant of water which was involved in hydrogen bonding with anthrone³ resulting in its stabilization to the extent that the second peak is not observed at all, accompanied with shifting of the redox couple to the lower potential. On the basis of better stability and reproducibility of voltammograms in water-acetonitrile solvent mixture (1:1) all subsequent studies were carried out in this solvent mixture composition.

7.1.3 Effect of scan rate

Peak currents of anodic waves were plotted against square root of scan rates separately for modified screen printed electrode (Fig. 7.5a) and anthrone³ in solution phase using GC electrode (Fig. 7.5b). A linear plot between peak current and the square root of scan rate indicated a diffusion based process. As per the Randles-Sevcik equation (1), for a reversible system peak potential is independent of scan rate and $\Delta E = 59 \text{ mV/n}$ (Wang, 2000).



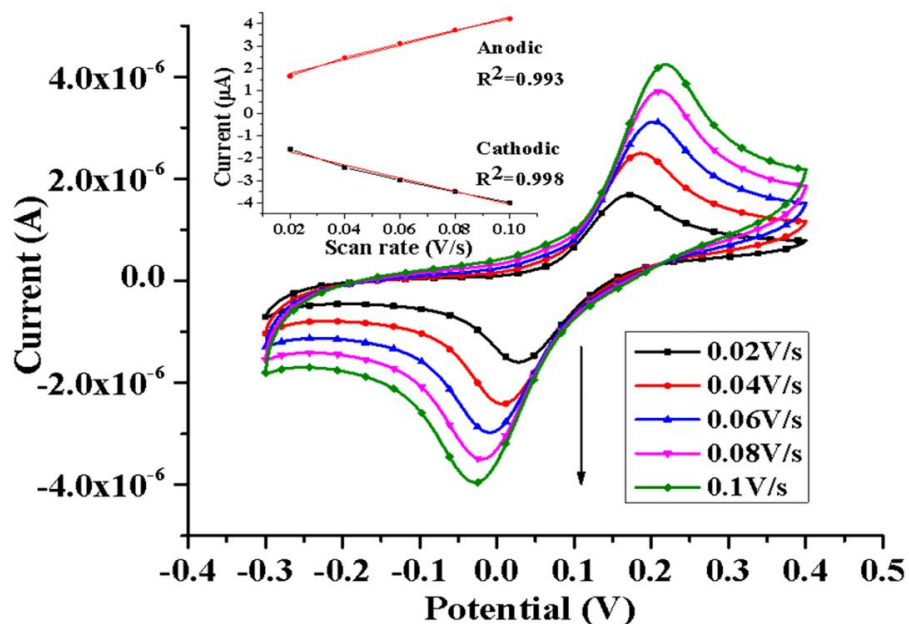


Fig. 7.5 Cyclic voltammograms of SPE-A (4a) and anthrone3 (4b) in 1:1 water-ACN at different scan rates (supporting electrolyte 0.1M KCl, pH 7, E vs Ag/AgCl)

It can be seen from Fig 7.5a and 7.5b that at lower scan rate i.e., $20 \text{ mVs}^{-1/2}$ reversibility conditions are followed (in Table1 the ΔE value for SPE-A is 57 mV) while at scan rate $40 \text{ mVs}^{-1/2}$ and above, response of the electrode tends to be quasi-reversible (ΔE value between 60-200 mV).

$$I_p = (2.69 \times 10^5) n^{3/2} ACD\nu^{1/2} \quad (1)$$

I_p is the peak current (A), n is the number of electrons, A is the area of electrode (cm^2), C is the concentration (mol cm^{-3}) D is diffusion coefficient (cm^2s^{-1}) and ν is the scan rate (Vs^{-1}).

7.1.4 Cation selectivity behavior

Experiments were conducted with SPE-A electrode in presence of different metal ions in 1:1 water-acetonitrile medium. The presence of different metal ions like Co^{2+} , Ni^{2+} , Cu^{2+} , Zn^{2+} , Hg^{2+} and Pb^{2+} resulted in the shift of peak potentials to different extents (see Table 7.1). Taking the magnitude of shift in peak potential as criteria of selectivity, the metal ions can be put in the following decreasing order of selectivity:

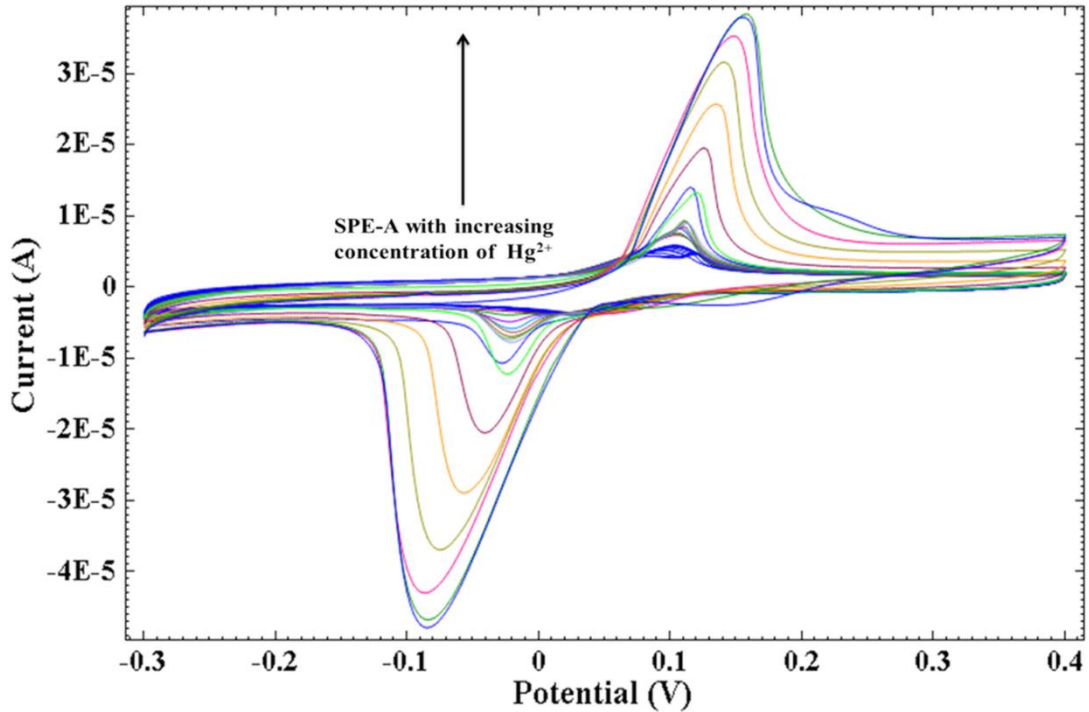
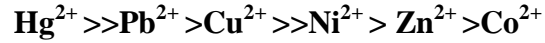


Fig. 7.6 Cyclic voltammograms of SPE-A with different equivalents of Hg^{2+} ions in 1:1 water- ACN (scan rate 0.02V s^{-1} , supporting electrolyte 0.1M KCl , pH 7, E vs Ag/AgCl)

Studies were further extended taking different concentrations of Hg^{2+} ions. It can be observed that the current magnitude of anodic peak at 0.083 V increases continuously with increasing concentration of Hg^{2+} ions (Fig. 7.6). The concentration range selected for the study was $5 \times 10^{-6}\text{ M}$ to $3.5 \times 10^{-3}\text{ M}$. A similar behavior was also noticed in the cathodic peak current as well. There was very small shift in peak potential, probably due to quasi-reversible nature of the electrochemical reaction at the cathode. With screen printed electrode, a selective behavior for copper ions was also established (Fig. 7.7). A better selectivity for mercury ions over copper ions was noticed with SPE-A.

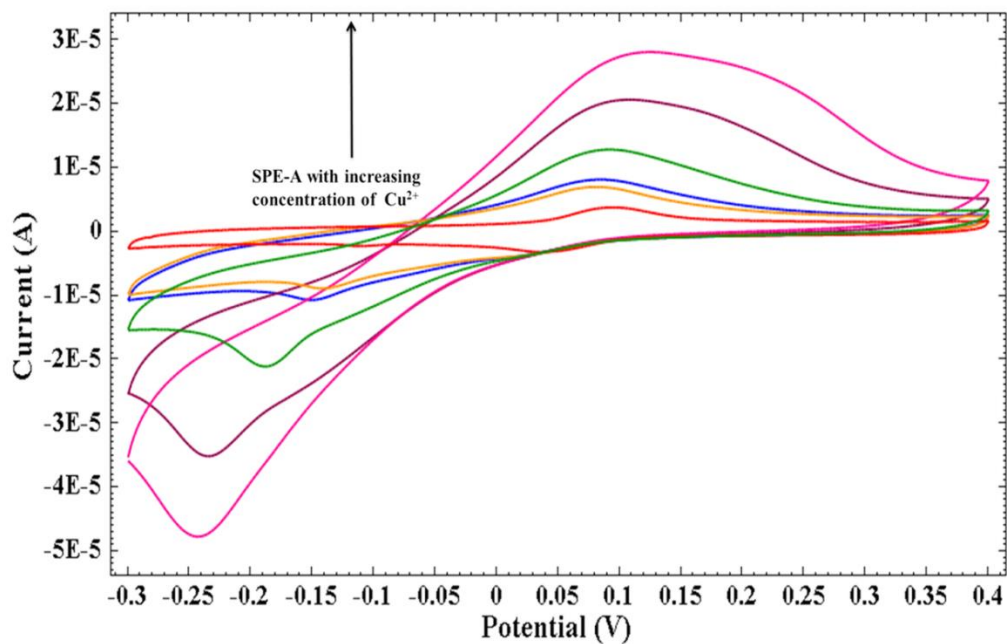


Fig. 7.7 Cyclic voltammograms of anthrone3 (solution phase) with different equivalents of Cu^{2+} ions in 1:1 water-ACN (scan rate 0.02V s^{-1} , supporting electrolyte 0.1M KCl, pH 7, E vs Ag/AgCl)

Table 7.1 Voltammetric data of SPE-A (SPE-Anthrone3) with different metal ions

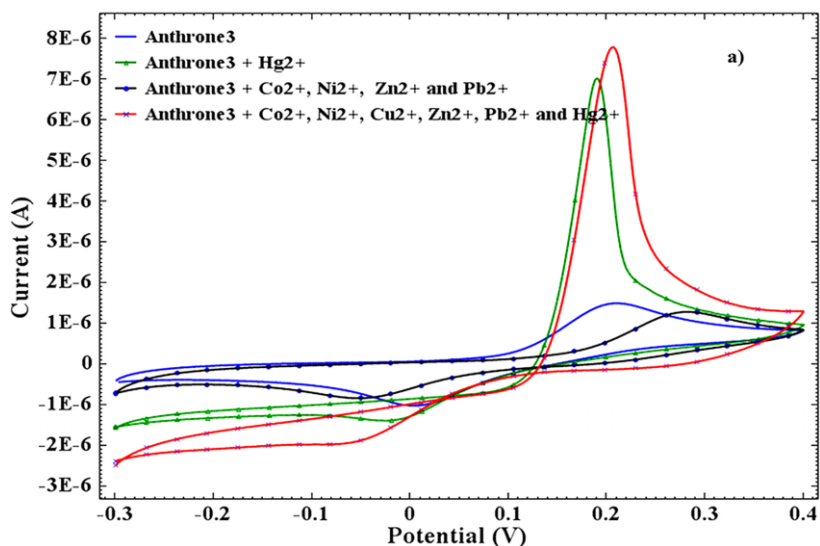
Working Electrode	$E_a(\text{V})$	$E_c(\text{V})$	$\Delta E_p = E_a - E_c(\text{V})$	$\Delta E_a(\text{V})$
SPE-A alone	0.076	0.019	0.057	--
SPE-A with Co^{2+}	0.071	0.011	0.060	0.005
SPE-A with Ni^{2+}	0.081	0.021	0.060	-0.005
SPE-A with Cu^{2+}	0.104	-0.232	0.336	-0.028
SPE-A with Zn^{2+}	0.073	0.011	0.062	0.003
SPE-A with Hg^{2+}	0.122	-0.071	0.193	-0.046
SPE-A with Pb^{2+}	0.112	0.047	0.065	-0.036

E_a = Anodic peak potential, E_c = Cathodic peak potential, ΔE_p = Difference of peak potentials, ΔE_a = Difference of anodic peak potential

Voltammetric study of Anthrone3 was also conducted in solution phase (1:1 water-acetonitrile) which shows sensitivity towards Hg^{2+} and Cu^{2+} ions. Even in presence of other heavy metal ions Pb^{2+} , Ni^{2+} , Zn^{2+} and Co^{2+} , anthrone3 shows high sensitivity toward Hg^{2+} ions. As the concentration of Hg^{2+} ions increased from $5 \times 10^{-6} \text{M}$, curve crossing in the voltammograms was observed, which shows that ECE mechanism is taking place as curve crossing has been quoted as diagnostic of a series of chemical reactions (presumably electrochemical processes run through a chemical process) occurring within the electrochemical time scale of a cyclic voltammetric scan (Fox and Akaba, 1983).

7.1.5 Interference of ions

Interference study was done to know selectivity of both anthrone3 in solution phase and SPE-A. Cyclic voltammograms were run for both these systems in the presence of Hg^{2+} ions and the resulting curves shown in Fig. 7.8a and 7.8b.



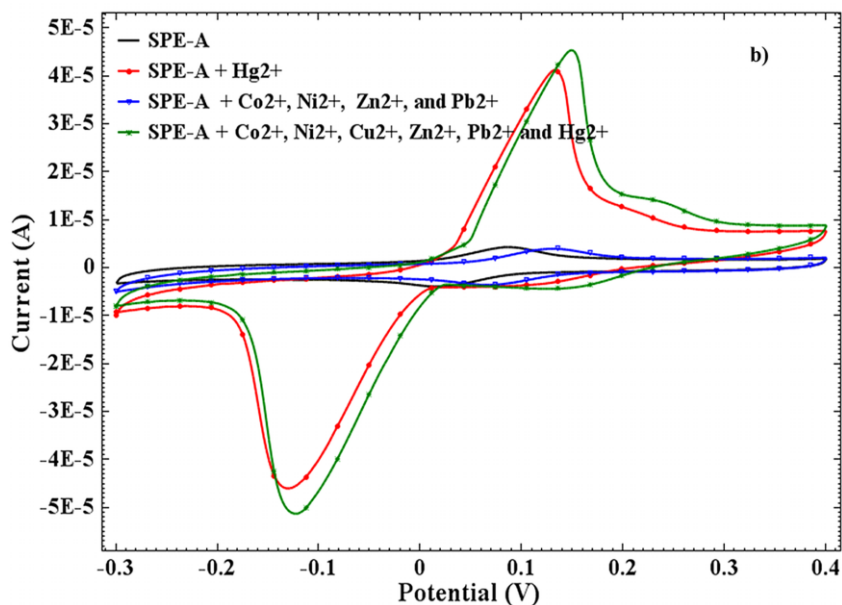


Fig. 7.8 Interference study of a) Anthrone3 in solution phase and b) SPE-A with different metal ions in 1:1 water-ACN (scan rate 0.02Vs^{-1} , supporting electrolyte 0.1M KCl, pH 7, E vs Ag/AgCl)

Even the presence of 10-fold concentration of ions like Co^{2+} , Ni^{2+} , Zn^{2+} and Pb^{2+} , did not show any change in voltammetric response of anthrone3 (in solution phase) and SPE-A towards Hg^{2+} ions, indicating that there is no interference from these cations. It can be concluded that both the systems respond selectively towards mercury ions in the presence of many other commonly available cations.

7.1.6 Sensitivity (LOD and LOQ)

Sensitivity of the method based on SPE was determined from the limit of detection (LOD) and limit of quantification (LOQ) values based on 3-sigma method. A plot of current (μA) versus concentration (μM) resulted in a straight line. The experiment was repeated 3 times and the representative curve from the 3 sets of data was used for further calculations of LOD and LOQ. By using 3-sigma method the limit of detection was found to be $0.61\ \mu\text{M}$ and limit of quantification value comes out to be $1.86\ \mu\text{M}$. However, methods like fluorescence are reported to sense mercury up to $1.0\ \mu\text{M}$ level (Kima et al, 2012), tripodal rhodamine based chemosensor for Cu^{2+} and Hg^{2+} with detection limit of $0.30\ \mu\text{M}$ (Zeng et

al, 2009], mercury/copper- plated screen printed electrodes for lead with a detection limit of 0.81 μM (Zen, 2000)

7.1.7 Regeneration of Screen printed electrodes

Anthrone³ modified screen printed electrodes showed highly reversible nature after its exposure to EDTA solution for 5-10 minutes, after it is used to sense Cu^{2+} ions in water - acetonitrile medium (Fig. 7.9). The disposable electrode was found to respond again as a fresh SPE-A, after its regeneration with EDTA. The electrode was regenerated at least for 3-4 times, after which the response becomes irregular. This observation could not be repeated with Hg^{2+} ions probably because of greater stability of anthrone³- Hg^{2+} complex than EDTA- Hg^{2+} complex (Fig. 7.10). Similar results were obtained with anthrone³ in solution medium (1: 1 water-acetonitrile) (Fig. 7.11 and Fig. 7.12).

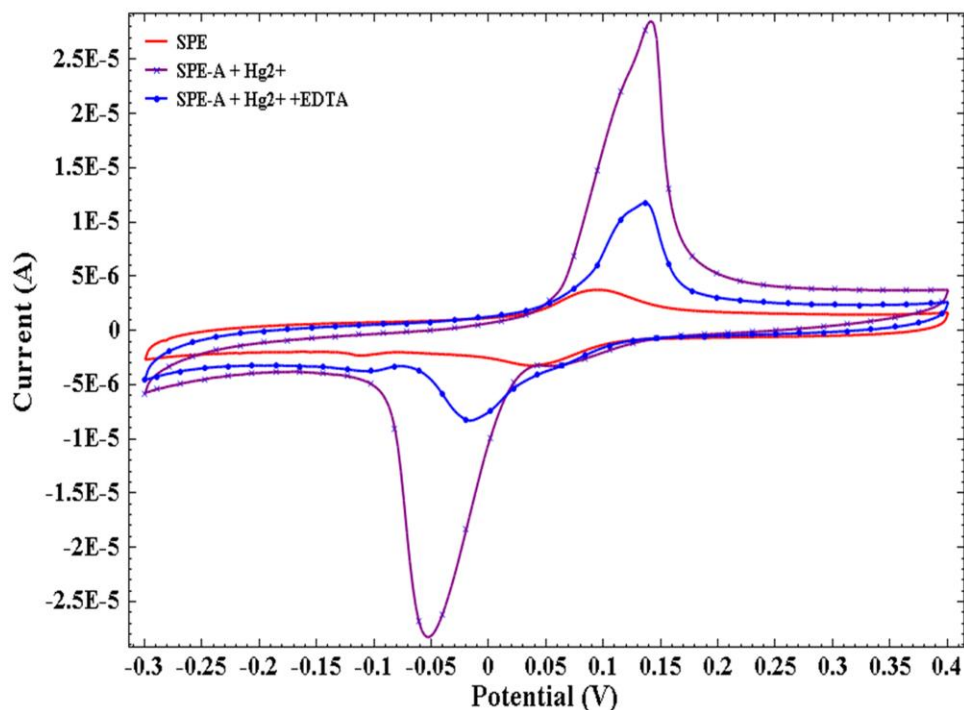


Fig. 7.9 Cyclic voltammograms of SPE-A after treating it with Cu^{2+} ions and EDTA in 1:1 water- ACN (scan rate 0.02V s^{-1} , supporting electrolyte 0.1M KCl, pH 7, E vs Ag/AgCl)

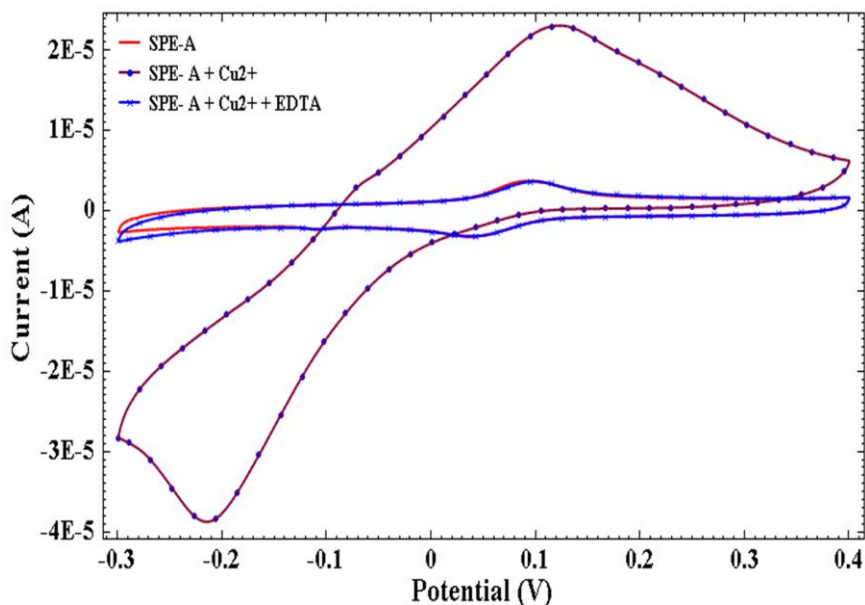


Fig. 7.10 Cyclic voltammograms of SPE-A after treating it with Hg^{2+} ions and EDTA in 1:1 water-ACN (scan rate 0.02V s^{-1} , supporting electrolyte 0.1M KCl, pH 7, E vs Ag/AgCl)

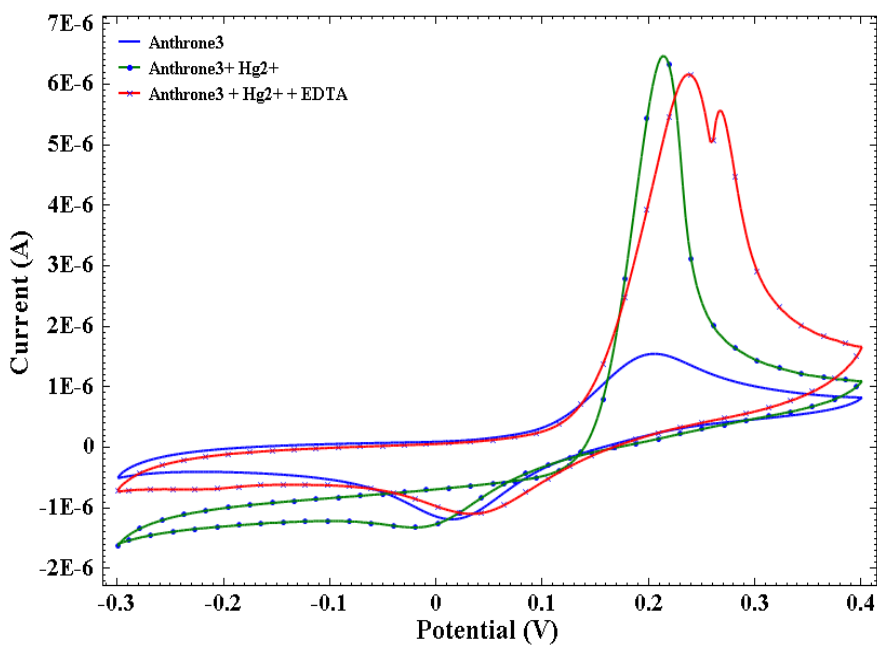


Fig. 7.11 Cyclic voltammograms of anthrone3 after addition of Hg^{2+} ions and EDTA in 1:1 water-ACN (scan rate 0.02V s^{-1} , supporting electrolyte 0.1M KCl, pH 7, E vs Ag/AgCl)

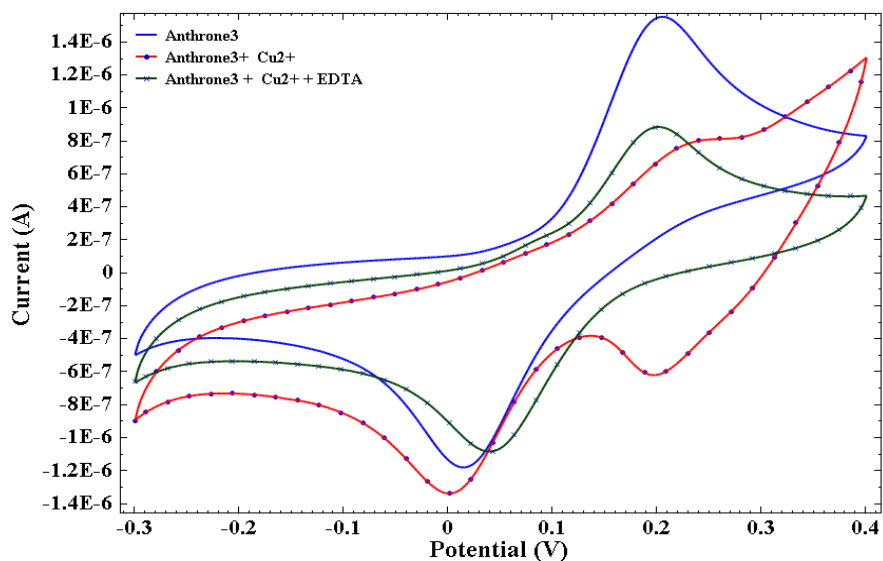


Fig. 7.12 Cyclic voltammograms of anthrone3 after addition of Cu^{2+} ions and EDTA in 1:1 water-ACN (scan rate 0.02V s^{-1} , supporting electrolyte 0.1M KCl, pH 7, E vsAg/AgCl)

7.1.8 SEM images of EDTA-treated and non-treated SPE-A electrodes

SEM images were recorded for SPE electrodes modified with anthrone3 (Fig. 7.13). Images of SPE-A were also recorded after sensing mercury and copper ions and their subsequent treatment with EDTA. It can be seen from Fig.7.14a that white spots encircled in the image are due to the presence of mercury ions which stay even after treatment with EDTA (Fig. 7.14b) for reasons discussed above. SEM images of SPE with copper ions present as white spots (encircled) (Fig. 7.14c) are found missing in the image (Fig. 7.14d) after treatment with EDTA. This hypothesis supports experimental observation that using EDTA treated SPE after Cu^{2+} detection could reproducibly give same curve as before.

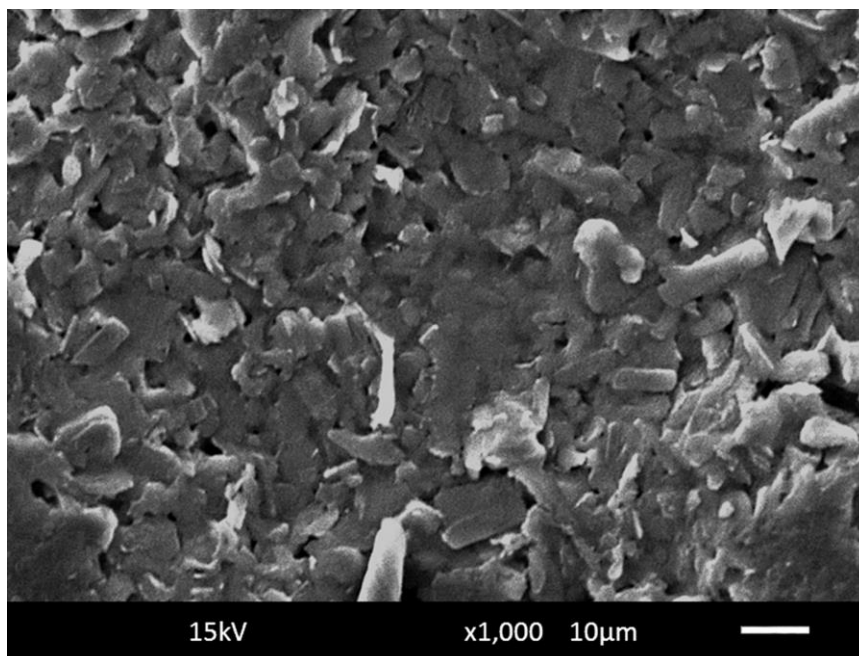


Fig. 7.13 SEM image of anthrone3 modified screen printed electrode

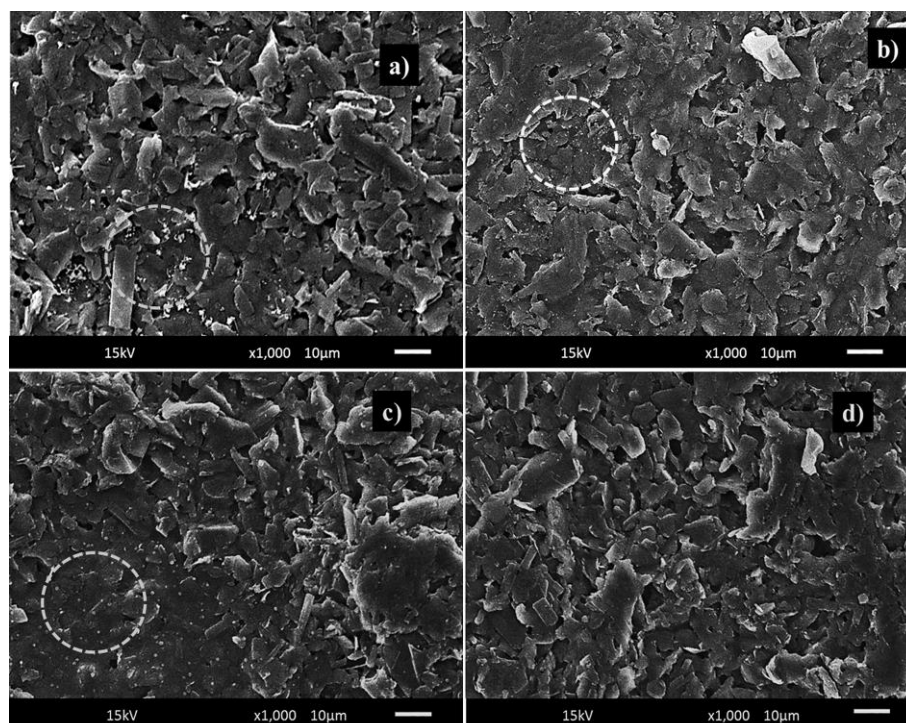


Fig. 7.14 SEM images of anthrone3 modified screen printed electrode a) after treatment with Hg^{2+} b) Hg^{2+} treated electrode after treatment with EDTA solution, c) after treatment with Cu^{2+} , d) Cu^{2+} treated electrode after treatment with EDTA solution

7.1.9 Validation of mercury determination using SPE-A with AAS

SPE-A was tested for the analysis of artificial samples of Hg^{2+} ions. Atomic absorption spectroscopy was used to verify the results obtained with voltammetric method. Table 7.2 shows that the results obtained with SPE-A voltammetrically are in complete agreement with the results obtained with AAS for Hg^{2+} ion.

Table 2. Real time sample analysis of laboratory tap water and its verification with atomic absorption spectroscopy for Hg^{2+} ions

Samples	AAS (μM)	Voltammetry (with SPE-A) (μM)
Lab tap water	--	--
ARS1	10.0	10.5
ARS2	24.9	25.4
ARS3	35.9	36.4
ARS4	44.9	45.4

ARS = Artificial real sample

7.2 Polyaniline modified electrode

7.2.1 Electrode modification

Polyaniline coating was done chrono-amperometrically at a constant current of 1mAcm^{-2} by varying the time of deposition (Fig. 7.2.1) from 100s to 300s. Cyclic voltammograms corresponding to PANI deposited for particular duration of time (inset Fig. 7.2.1) were taken to optimize the deposition time duration in acetonitrile containing 0.1 M TBAP as supporting electrolyte. Overlay of the chronoamperometric and voltammetric scans showed that most stable PANI deposition was obtained at 300s. Increasing the deposition duration increases the thickness of the polymer layer but too much thick layer can cause ineffective interaction between the solution and surface of electrode leading to decrease in

conductivity. So optimizing the deposition time becomes an important part of modification of electrode with conducting polymers.

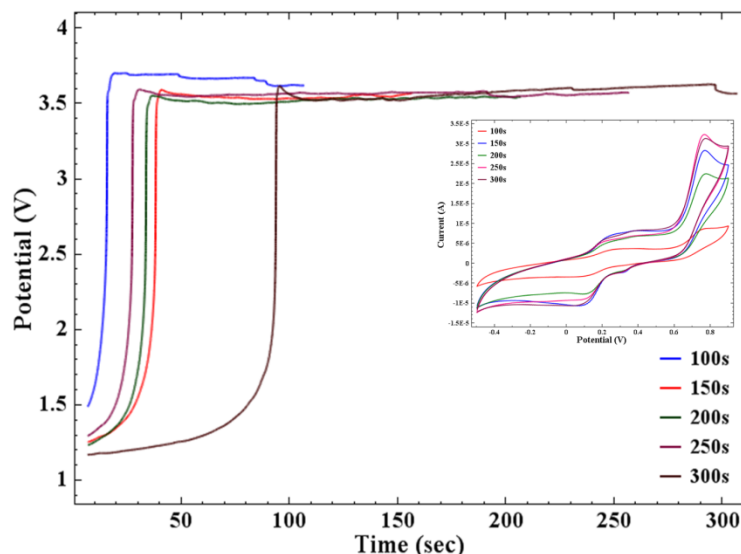


Fig.7.2.1 Chronoamperometric deposition of PANI on glassy carbon electrode in acetonitrile containing 0.1M CF_3COOH , 0.1M TBAP, as supporting electrolyte, time varying from 100 to 300 s, Inset contains CVs corresponding to PANI formed, E vs Ag/Ag^+)

7.2.2 Electrochemistry of PANI in acetonitrile

Cyclic voltammogram of PANI (Zhang et al, 2009) coated on GC electrode (chronoamperometrically), was drawn in acetonitrile containing 0.1M TBAP at a scan rate of 20mVs^{-1} , shows three reversible redox couples, aa', bb' and cc' Fig. 7.2.2. The first oxidation peak **a** (0.23V) belongs to the formation of a leucoemeraldine cation radical from leucoemeraldine. The reverse reduction process corresponds to peak **a'** at 0.1V. The leucoemeraldine cation radical further oxidized to emeraldine at the peak **c** with a potential of 0.729 V, with a corresponding cathodic peak (**c'**) at 0.64 V belonging to the reduction process. The third pair of peaks **bb'** (0.36/0.32V) corresponds to defects in linear structure of polyaniline polymer. Galvanostatic polymerization leads to formation of polyaniline in its conductive form in acetonitrile medium.

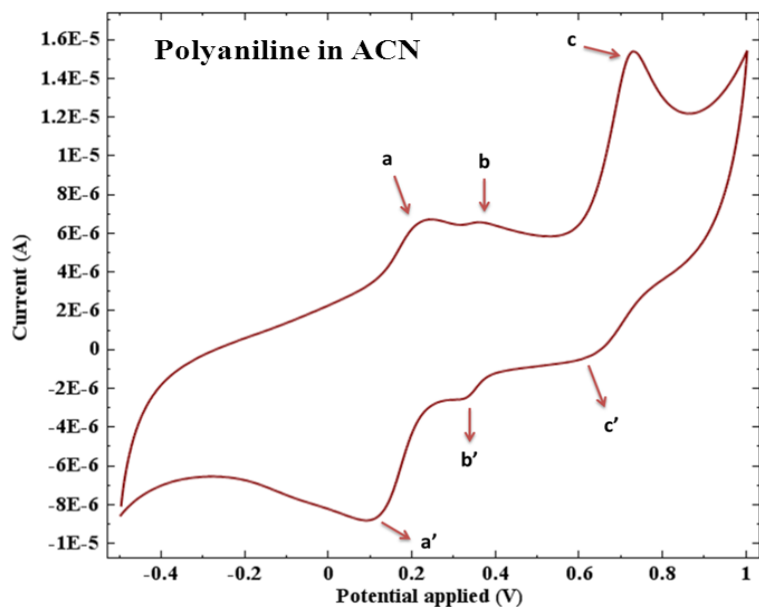


Fig. 7.2.2 Cyclic voltammogram of PANI coated on glassy carbon electrode in acetonitrile containing 0.1M TBAP as supporting electrolyte, scan rate 0.02Vs^{-1} , E vs Ag/Ag^+)

7.2.3 Permeability of PANI coating on working electrode

Cyclic voltammetric studies of PANI modified GC electrode were done with ferrocene to confirm its permeability. Fig 7.2.3 shows PANI modified GC gave much better results with ferrocene than the bare glassy carbon electrode in terms of current magnitude in acetonitrile medium at 20mVs^{-1} scan rate. This showed that PANI coating done from acetonitrile is highly conductive and doesn't cause any hindrance to the mobility of ions and can be used for further application.

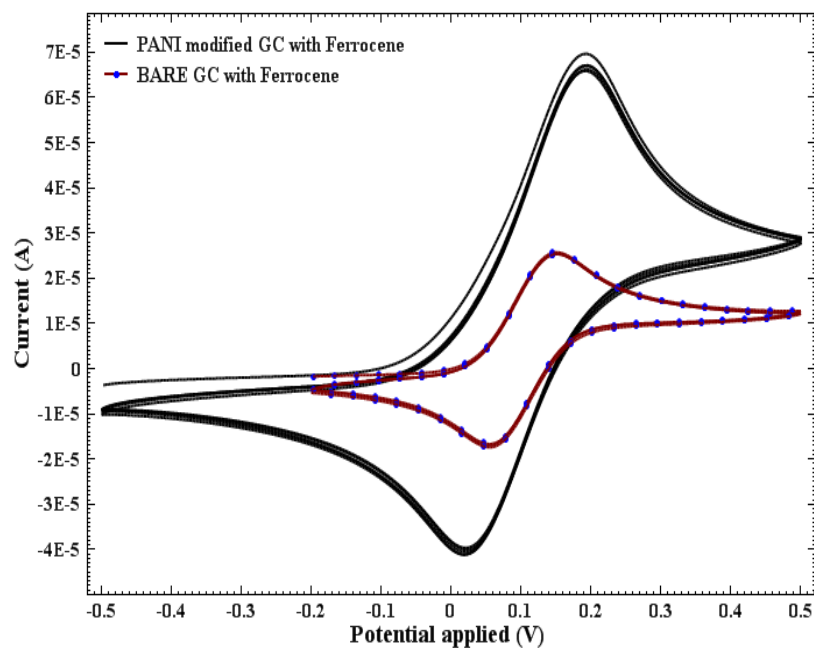


Fig. 7.2.3 Cyclic voltammogram of PANI coated and Bare glassy carbon electrode with 0.01M ferrocene in acetonitrile containing 0.1M TBAP as supporting electrolyte, scan rate 0.02Vs^{-1} , E vs Ag/Ag^+)

7.2.4 Application of PANI modified electrode

PANI modified electrode was treated at 0.3V for 300 secs chrono-potentiometrically, before coating the ionophores, to get an extended or open morphology of polymer giving more porous nature (Muthukumar et al, 2007) as can be seen in Fig. 7.2.4a. Ionophores TPAN and TPF, dissolved in THF were then drop coated ($40\mu\text{l}$) onto PANI modified glassy carbon electrode. Fig. 7.2.4b shows porous polyaniline coated with ionophore (encircled area). After drying the modified electrode voltammetric study was done in acetonitrile medium containing tetrabutylammonium perchlorate as the supporting electrolyte. Result obtained with ionophore coated electrode were compared with the results of bare GC electrode. It was observed that the CV study of molecules with modified electrode gave better results with higher magnitude of current of the oxidation peaks (Fig 7.2.5a and 7.2.5b).

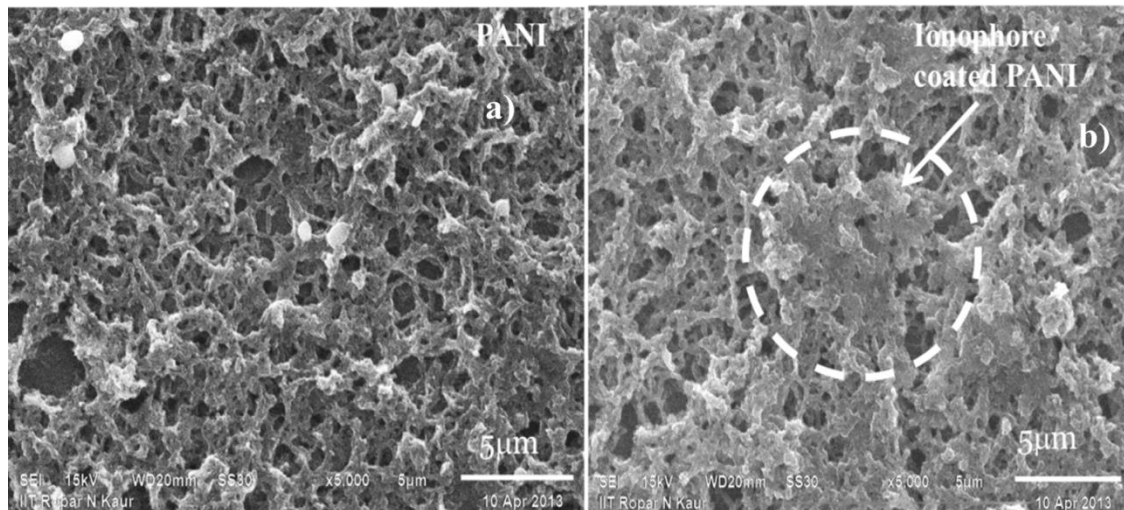
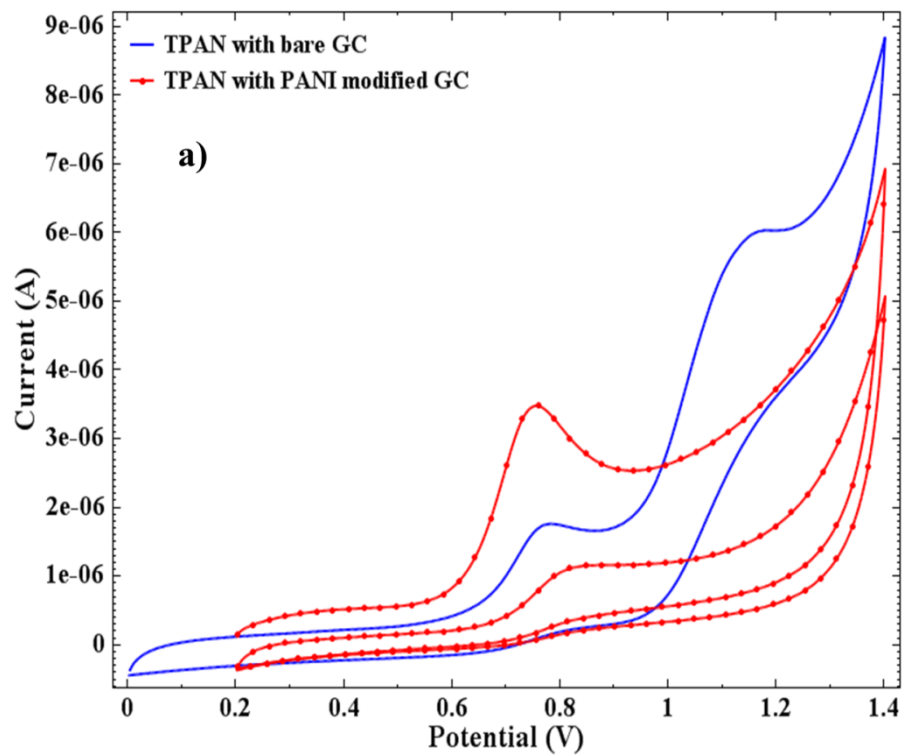


Fig 7.2.4 SEM images of a) porous morphology of polyaniline after chronopotentiometric treatment b) ionophore coated polyaniline



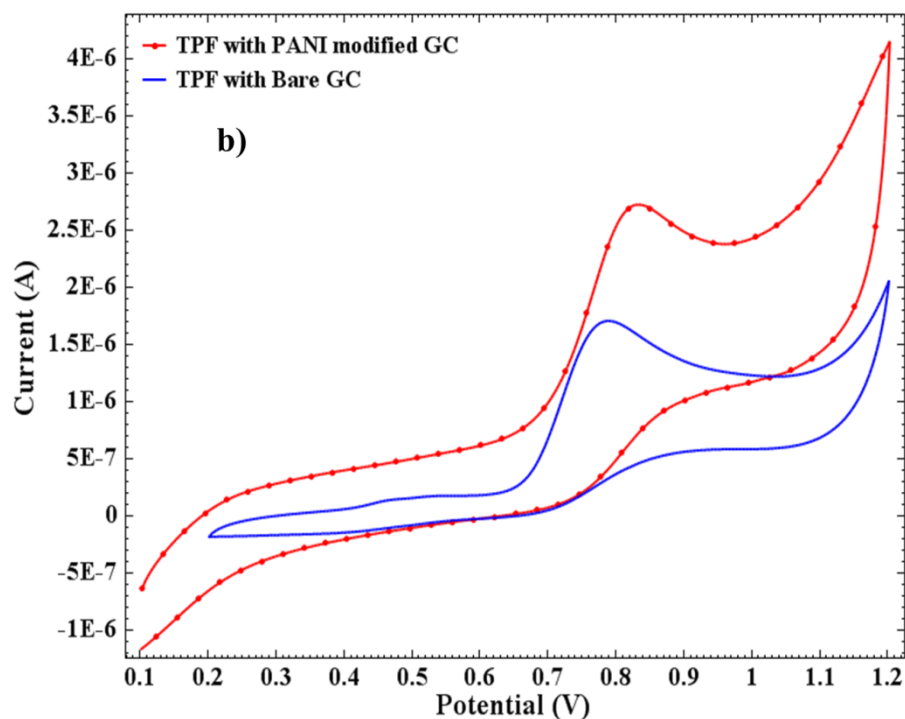


Fig. 7.2.5 Cyclic voltammogram of a) TPAN/PANI coated glassy carbon electrode, b) TPF/PANI coated glassy carbon electrode, in acetonitrile containing 0.1M TBAP as supporting electrolyte, scan rate 0.02Vs^{-1} , E vs Ag/Ag^+

Fig. 7.2.5a shows the comparison of CV of TPAN with modified and unmodified glassy carbon electrodes. Two oxidation peaks were obtained for TPAN with unmodified GC electrode but only one oxidation peak was observed after modification and with increased current magnitude. The absence of second oxidation can be explained on the basis of probability of 2nd oxidation process getting quenched by polyaniline which exists as a conductive polymer in emeraldine form having equal number of oxidisable and reducible sites. For TPF only a cathodic shift of 40mV was observed in peak potential of oxidation peak and with increase in current (Fig. 7.2.5b). Reproducibility of the modified system was limited only to second scan as the peak current decreased after the second CV scans (Fig. 7.2.5a). So fresh coating was done every time for the studies.

7.2.5 Real samples

The real samples were drawn from soil samples collected from the dumping site of compact fluorescent lamps (CFL). The soil samples were extracted using acid digestion

and diluted with distilled water to carry out the studies. Differential pulse voltammetry (DPV) study of the real samples was done using ionophore/PANI/GC modified electrode for mercury detection in aqueous system at acidic pH. Both the ionophores showed similar DPV behavior in water system. So PANI modification of electrode increased the detection limit from $1\mu\text{M}$ to 10nM (3-sigma method) for Hg^{2+} and Cu^{2+} ions.

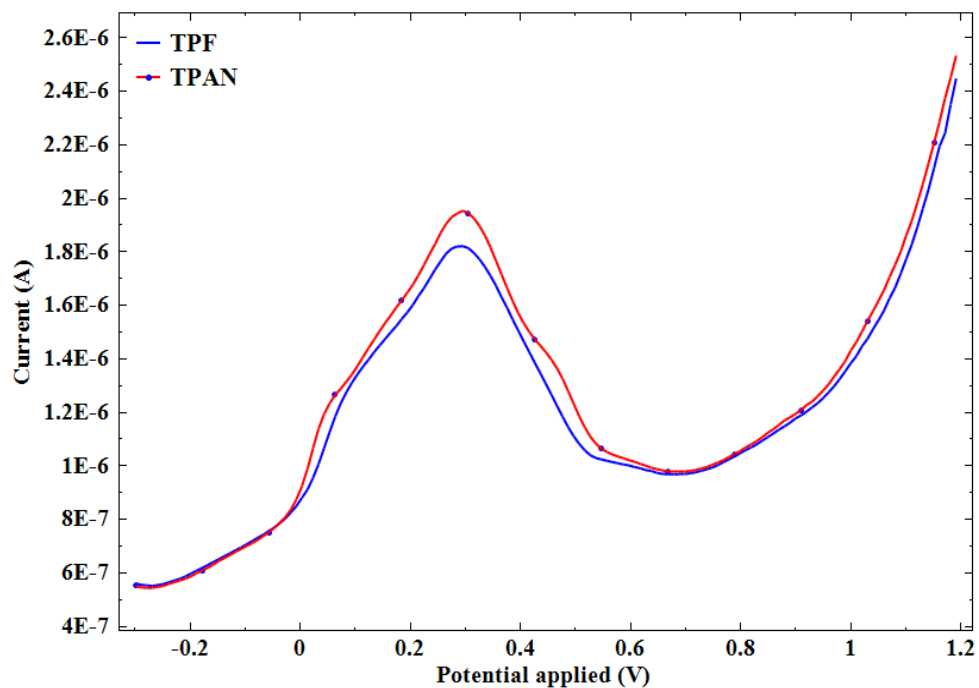


Fig. 7.2.6 DPVs of TPAN and TPF coated PANI/GC modified electrode in 0.2M HNO_3 aqueous solution, conditioning potential -0.3 V for 60 s at amplitude 25 mV .

Fig. 7.2.7 and 7.2.8 show differential pulse voltammograms of soil sample collected from main dump site and at some distance from it, respectively. Peaks obtained after spiking the samples with standard solutions of mercury and copper ions clearly shows that the peaks obtained from samples belonged to copper and mercury ions. While samples collected from nearby park did not show any peak for mercury ion. Peak intensity of mercury is higher than copper though amount of copper is higher in soil samples because on deposition at the electrode mercury forms an amalgam which increases its conductivity and resulted in higher peak intensity. Calibrations plots were drawn for both copper and mercury ions using DPV with modified electrode. Table 7.2.1 shows the data obtained for soil samples from atomic absorption spectrophotometry and differential pulse voltammetry.

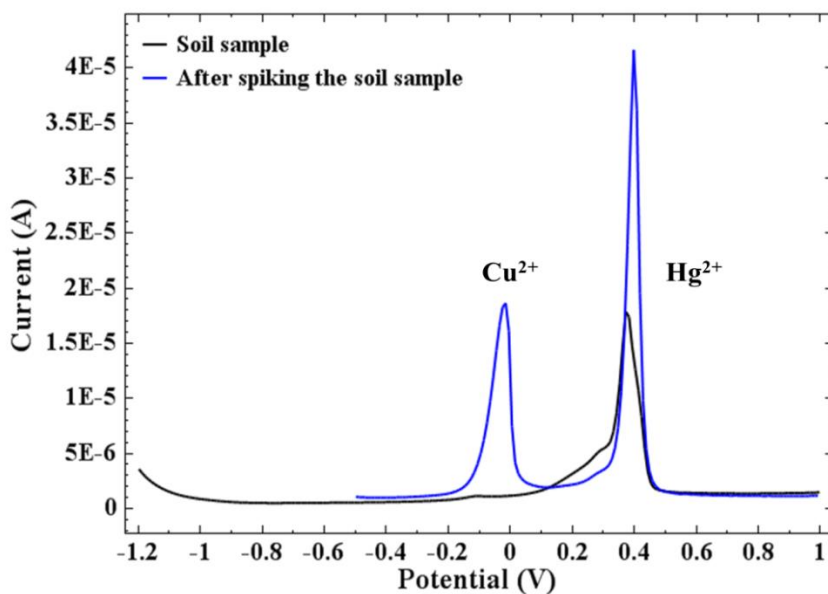


Fig. 7.2.7 Differential pulse voltammograms of soil sample with ionophore/PANI/GC electrode from main dump site and after spiking the sample with Cu^{2+} and Hg^{2+} solution(0.01M) at pH 3, scan rate 0.02Vs^{-1} , E vs Ag/AgCl)

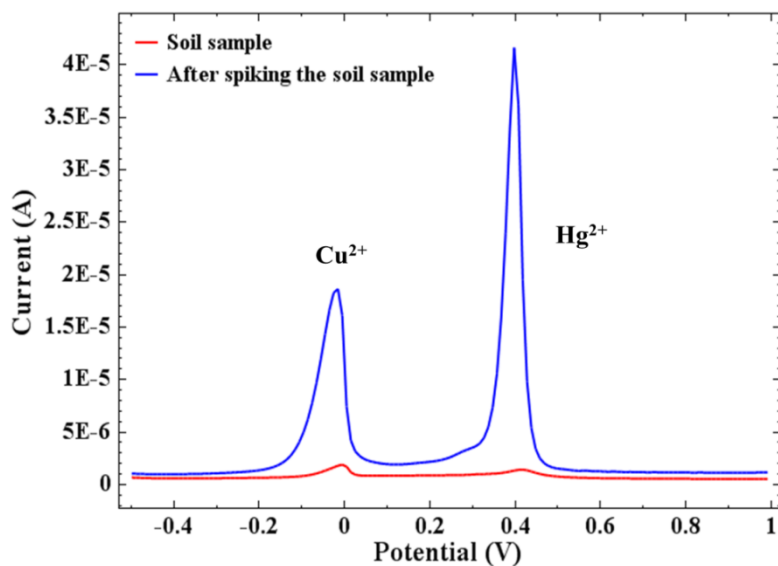


Fig. 7.2.8 Differential pulse voltammograms of soil sample with ionophore/PANI/GC electrode collected from some distance from main dump site and after spiking the sample with Cu^{2+} and Hg^{2+} solution(0.01M) at pH 3, scan rate 0.02Vs^{-1} , E vs Ag/AgCl)

Table 7.2.1 Real time sample analysis of soil samples from CFL dump site and their verification with atomic absorption spectroscopy for Hg^{2+} and Cu^{2+} ions.

Sample Sites	AAS(μM)		Voltammetry (μM)	
	Hg^{2+}	Cu^{2+}	Hg^{2+}	Cu^{2+}
CFL dump site	0.03 \pm 0.01	6.3 \pm 0.1	0.027 \pm 0.01	5.9 \pm 0.1
At some distance from the CFL dump site	0.01 \pm 0.02	2.5 \pm 0.3	0.01 \pm 0.005	2.23 \pm 0.3
From the nearby park	0.005 \pm 0.001	2.3 \pm 0.1	Not detected	1.97 \pm 0.3

7.3 Conclusions

Anthrone³ modified screen printed electrodes as well as GC electrode has been used as voltammetric sensors for heavy metal ions. Based on the shift in potential, in presence of different heavy metal ions have been put in decreasing order of selectivity, being more for Hg^{2+} and least for Co^{2+} ions. On comparison of anthrone³ modified SPE with glassy carbon electrode, the former is far better in performance with regard to reproducibility and sensitivity. Amongst different compositions of solvents, water-acetonitrile in 1:1 ratio gives the best performance. SPEs are reported for the first time as reproducible voltammetric sensors after treatment with EDTA.

Polyaniline modified gave better results than unmodified GC electrode. As tested with ferrocene it was found to be highly permeable. Results obtained after modifying the electrode with ionophores TPAN and TPF were better than bare GC electrode results in terms of peak current intensity. On the basis of selectivity shown by TPAN and TPF toward ions Hg^{2+} and Cu^{2+} ions, ionophore/PANI/GC modified electrode was also used to sense these ions and for their determination in soil sample of CFL dump site.

7.4 References

- Bernalte**, E., Marín Sánchez, C., Gil, E. P., 2011, Determination of mercury in ambient water samples by anodic stripping voltammetry on screen-printed gold electrodes, *Analytica Chimica Acta*, , 689, 60-64.
- Dhand**, C., Dasa, M., Datta, M., Malhotra, B.D., 2011, Recent advances in polyaniline based biosensors, *Biosensors and Bioelectronics*, 26, 2811–2821.
- Emanuel**, C.E.J., Ellison, B., Banks, C.E., 2010, Spice up your life: screening the illegal components of ‘Spice’ herbal products, *Analytical Methods*, 2, 614-616.
- Evtugyn**, G.A., Stoikov, I.I., Beljyakova, S.V., Shamagsumova, R.V., Stoikova, E.E., Zhukov, Yu., A., Antipin, I.S., Budnikov, H.C., 2007, Ag selective electrode based on glassy carbon electrode covered with polyaniline and thiacalix[4]arene as neutral carrier, *Talanta*, 71, 1720–1727.
- Grennan**, K., Killard, A.J., Smyth, M.R., 2001, Physical characterizations of a screen-printed electrode for use in an amperometric biosensor system, *Electroanalysis*, 13, 745-750.
- Hallam**, P.M., Kampouris D.K., Kadara, R.O., Banks, C.E., Graphite screen printed electrodes for the electrochemical sensing of chromium(VI), 2010, *Analyst*, 135, 1947-1952.
- Heitzmann**, M., Basaez, L., Brovelli, F., Bucher, C., Limosin, D., Pereira, E., Rivas, B.L., Royal, G., Saint-Aman, E., Moutet, J., 2005, Voltammetric Sensing of Trace Metals at a Poly(pyrrole-malonic acid) Film Modified Carbon Electrode, *Electroanalysis*, 21, 1970-1976.
- Kampouris**, D.K., Kadara, R.O., Jenkinson, N., Banks, C.E., 2009, Screen printed electrochemical platforms for pH sensing, *Analytical Methods*, 1, 25-28.
- Manigandan**, S., Jain, A., Majumder, S., Gangulya, S., Kargupta, K., 2008, Formation of nanorods and nanoparticles of polyaniline using Langmuir Blodgett technique: Performance study for ammonia sensor, *Sensors and Actuators B*, 133, 187–194.
- Montesinos**, T., Pérez-Munguia, S., Valdez, F., Marty, J., 2001, Disposable cholinesterase biosensor for the detection of pesticides in water miscible organic solvents, *Analytica Chimica Acta*, 431, 231-237.
- Muthukumar**, C., Kesarkar, S.D., Srivastava, D.N., 2007, Conductometric mercury [II] sensor based on polyaniline–cryptand-222 hybrid, *Journal of Electroanalytical Chemistry*, 602, 172–180.
- Sahin**, Y., Percin, S., Sahin, M., Ozkan, G., 2003, Electrochemical Preparation of Poly(2-bromoaniline) and Poly(aniline-co-2-bromoaniline) in Acetonitrile, *Journal of Applied Polymer Science*, 90, 2460–2468.
- Sljukic**, B.R., Kadara, R.O., Banks, C.E., 2011, Disposable manganese oxide screen printed electrodes for electroanalytical sensing, *Analytical Methods*, 3, 105-109.

Somerset, V., Leaner, J., Mason, R., Iwuoha, E., Morrin, A., 2010, Development and application of a poly(2,2'-dithiodianiline) (PDTDA)-coated screen-printed carbon electrode in inorganic mercury determination, *Electrochimica Acta*, 55, 4240-4246.

Tahir, Z. M., Alocilja, E.C., Grooms D.L., 2005, Polyaniline synthesis and its biosensor application, *Biosensors and Bioelectronics*, 20, 1690–1695.

Xu, K., Zhu, L., Zhang, A., Jiang, G., Tang, H., 2007, A peculiar cyclic voltammetric behavior of polyaniline in acetonitrile and its application in ammonia vapor sensor, *Journal of Electroanalytical Chemistry*, 608, 141–147.

Zhang L., Zhang, J., Zhang, C., 2009, Electrochemical synthesis of polyaniline nano-network on alanine functionalized glassy carbon electrode and its application for the direct electrochemistry of horse heart cytochrome *c*, *Biosensors and Bioelectronics*, 24, 2085–2090.

7.5 List of Publications

Accepted Papers

1. Susheel K Mittal, **Karamjeet Kaur**, Ashok Kumar SK, Subodh Kumar and Ashwani Kumar, Anthrone derivatives as voltammetric sensors for applications in metal ion detection, **Sensor Letters**, 11, 223-236 (2013) (**Impact Factor = 0.85**)
2. **Karamjeet Kaur**, Susheel K Mittal, Ashok Kumar SK, Ashwani Kumar and Subodh Kumar, Cyclic Voltammetric Study of Viologen Substituted Anthrone Derivatives and Selective Detection of Cyanide Ions (**Accepted - Analytical Methods**) AY-ART-05-2013-040912.R1. (**Impact Factor = 1.855**)
3. **Karamjeet Kaur**, Susheel K Mittal, Ashok Kumar SK, Ashwani Kumar, Subodh Kumar, Jonathan P. Metters and Craig E. Banks, Disposable Voltammetric Sensor for Mercury Ions, (**Accepted- International Journal Of Electrochemical Science**)

Under process

4. **Karamjeet Kaur**, Susheel K Mittal, Ashok Kumar SK, Sandeep Kumar and Subodh Kumar, Ionophore/Polyaniline Modified Electrode for Voltammetric Cation Sensing.

Conference publications

1. Susheel K Mittal, Subodh Kumar, **Karamjeet Kaur** and Ashwani Kumar, Voltammetric Sensing of Hg^{2+} and Cu^{2+} Ions by Anthrone Derivatives, IT-11, pp 81-94, **Fourth ISEAC International Discussion Meet on Electrochemistry and its Applications, DM-ISEAC-2011**
2. **Karamjeet Kaur**, Susheel K Mittal, Ashok Kumar SK, Ashwani Kumar, Subodh Kumar, Jonathan P. Metters and Craig E Banks, Voltammetric Sensors for Some Anions and Cations, **Fifth ISEAC Triennial International Conference on Advances and Recent Trends in Electrochemistry (ELAC-2013)**